

The copyright of this thesis vests in the author. No quotation from it or information derived from it is to be published without full acknowledgement of the source. The thesis is to be used for private study or non-commercial research purposes only.

Published by the University of Cape Town (UCT) in terms of the non-exclusive license granted to UCT by the author.

UNIVERSITY OF CAPE TOWN

DEPARTMENT OF HUMAN BIOLOGY:

BIOMEDICAL ENGINEERING



**Exploring the range of motion between the
acetabular component and the femoral component
in hip resurfacing**

Richard William Mudd

Submitted to the University of Cape Town in partial fulfilment of
the requirements for the degree of

MSc (Med) in Biomedical Engineering

February 2012

Supervisor: Dr. George Vicatos

Co-supervisor: Dr. Sudesh Sivasu

Abstract

Accurate placement of the femoral and acetabular components is crucial to retain the natural hip Range of Motion (RoM) in hip resurfacing, as well as prevent accelerated wear and subsequent premature component failure. Currently, magnetic resonance images and anterior-posterior radiographs are commonly used to diagnose and assess pathological conditions of the hip that may require a hip resurfacing arthroplasty. However, these techniques provide a two-dimensional image of the patient's morphology and may limit the surgeon's ability to fully diagnose the problem, visualise and plan the surgery, as well as select the best suited prosthetic component sizes.

The main objective of this study was to investigate the use of an existing computer-aided design (CAD) software package to generate a three-dimensional (3D) computer model of the pelvis and upper femur, for use by a surgeon in pre-surgical planning. This was in order to identify the ideal prosthesis size and position, based on hip RoM analysis, and specify the optimal operative angles in which to place the components during hip resurfacing surgery. Further, this study had the purpose of providing groundwork for future development of a user-friendly software program for pre-surgical planning of hip resurfacing.

Based on input data, the CAD program SolidWorks was successfully used to generate an artificial femur to be representative of the new patient's femur for hip RoM analysis. The prosthetic femoral head and acetabular cup positions could then be fully defined within the 3D hip joint. Their respective positions within the bones were compared to the attainable hip RoM through a visual on-screen inspection and the use of a 3D vector spreadsheet which calculated the angles of inclination and anteversion. SolidWorks was able to import new patient computed tomography (CT) scans and superimpose them over the 3D model for hip RoM analysis.

Having a 3D view of the patient's anatomy and the ability to investigate different positioning scenarios for the prosthetic components may improve the pre-surgical planning process as well as reduce the risks and complications associated with this procedure. Should this software tool be further developed it has the potential to be integrated into a comprehensive hip resurfacing pre-surgical planning procedure and contribute to preventing surgical malpositioning and thus ultimately improve the life cycle of a hip resurfacing prosthesis.

University of Cape Town

Declaration

I, Richard William Mudd, hereby declare that the work on which this dissertation/thesis is based is my original work (except where acknowledgements indicate otherwise) and that neither the whole work nor any part of it has been, is being, or is to be submitted for another degree in this or any other university.

I empower the university to reproduce for the purpose of research either the whole or any portion of the contents in any manner whatsoever.

Signature:

Date:

University of Cape Town

Acknowledgements

I would like to thank the following people for their invaluable contribution of time, advice and effort throughout the duration of my thesis.

Dr. George Vicatos, who supervised the project, for his encouragement, and patience in guiding and helping me to understand and complete this work.

Dr. Sudesh Sivarasu, who co-supervised the project, for his technical advice and general support in making the project a success.

Smith & Nephew, for the opportunity and funding to undertake this investigation.

Dr. Brendan Dower and Dr. Garth Grobler, for the initial concept of the project and their valuable input throughout, as well as assistance in securing funding.

Andries Koorzen, from MECAD Systems, for his valuable support on the SolidWorks side.

Robert Honiball, from Physical 3D Modelling, for his high-quality work on 3D rendering and image processing.

Table of contents

ABSTRACT	i
DECLARATION	iii
ACKNOWLEDGEMENTS	iv
TABLE OF CONTENTS	v
LIST OF FIGURES	viii
LIST OF TABLES	xii
1. INTRODUCTION	1
1.1. Description of the problem	1
1.2. Importance of the problem.....	1
1.3. Objectives of study.....	3
1.4. Overview of the research methodology.....	3
2. LITERATURE REVIEW	4
2.1. The hip joint.....	4
2.2. Basic biomechanics of the hip joint.....	5
2.3. Hip Range of Motion	6
2.4. Measurement of the anatomy of the hip joint.....	7
2.4.1. Anatomical reference frames.....	7
2.4.2. Anatomical femoral angles	10
2.4.3. Anatomical acetabulum angles.....	12
2.5. Hip replacement arthroplasties	17
2.5.1. Indications for hip replacements	17
2.5.2. THR vs hip resurfacing	18
2.5.3. Hip resurfacing components.....	19
2.5.4. Component positioning in hip resurfacing.....	19
2.5.5. Hip RoM and component positioning and size.....	21
2.5.6. The effects of malpositioning	24
2.5.7. Computer models used to investigate hip RoM for hip resurfacing.....	26
2.5.8. Computer assisted hip resurfacing	28

3. MATERIALS, EQUIPMENT AND METHODOLOGY.....	30
3.1. Initial testing and pre-processing.....	30
3.2. Creating the solid 3D models in SolidWorks.....	34
3.3. Setting up the anatomical reference planes.....	34
3.4. Importing the BHR component files into SolidWorks.....	35
3.5. Designing the artificial femur.....	38
3.6. Setting up the left acetabular socket for prosthetic placement.....	44
3.7. Measuring acetabular inclination and anteversion angles.....	52
3.8. Converting inclination and anteversion angles between the different spatial reference systems	58
3.9. Converting pelvic tilt in AP radiographs.....	59
3.10. Constructing the combined assembly in SolidWorks	59
3.11. Performing hip RoM analysis in SolidWorks.....	62
4. RESULTS	65
4.1. The artificial femur.....	65
4.2. The 3D vector spreadsheet.....	66
4.3. Converting inclination and anteversion angles between the different spatial reference systems	71
4.4. Converting pelvic tilt	72
4.5. Placement of the acetabular cup.....	73
4.6. Superimposing patient-specific STLs into the model.....	77
4.7. Hip RoM analysis	79
5. DISCUSSION.....	80
5.1. Artificial femur.....	80
5.2. The 3D vector spreadsheet and position of the acetabular cup.....	82
5.3. Spatial reference systems.....	84
5.4. Importing patient-specific CT scans	85
5.5. Hip RoM analysis	85
5.6. Limitations.....	86

6. CONCLUSIONS AND RECOMMENDATIONS	89
6.1. Major conclusions drawn from this study	89
6.2. Recommendations	90
7. REFERENCES.....	91
8. APPENDICES.....	I
8.1. Appendix A	I
8.2. Appendix B	III
8.3. Appendix C	IV

University of Cape Town

List of Figures

Figure 2.1 – Showing points of interest on the pelvis (Drake et al. 2009).	4
Figure 2.2 – Showing a sketch of the anterior side of the left femoral bone (Darling 2011).	4
Figure 2.3 – Showing a right side view of the pelvis and acetabular socket (Drake et al. 2009).	5
Figure 2.4 – A). Showing flexion/extension B). Showing abduction/adduction (Drake et al 2009).	6
Figure 2.5 – C). Showing internal rotation/external rotation D). Circumduction (Drake et al. 2009).	7
Figure 2.6 – Illustrating the whole body or ground-based reference frame and the pelvic reference frame (Yoon et al. 2008).	8
Figure 2.7 – An illustration showing the three main anatomical planes (Primal Pictures Ltd. 2011).	8
Figure 2.8 – Illustrating pelvic tilt or pelvic reclination relative to the coronal plane (angle α is negative) (Lembeck et al. 2005).	9
Figure 2.9 – Illustrating different CCD angles between the femoral neck and femoral shaft (Amini 2007).	10
Figure 2.10 – Sketch illustrating the femoral anteversion angle formed between the TCA and NA (Caillet 2003).	11
Figure 2.11 – Sketch illustrating how the Q angle is measured (Medical Arts Rehabilitation Inc. 2011).	12
Figure 2.12 – Illustrating one method of measuring acetabular inclination, adapted from (Wolf et al. 2005).	13
Figure 2.13 – This image is a section of the pelvis, showing the left acetabulum socket with the acetabular axis (black arrow) pointing perpendicular to the acetabular plane.	14
Figure 2.14 – Image showing operative anteversion (OA) and operative inclination (OI), relative to the right acetabulum socket, adapted from (Murray 1993).	15
Figure 2.15 – Image showing radiographic anteversion (RA) and radiographic inclination (RI), relative to the right acetabular socket, adapted from (Murray 1993).	15

Figure 2.16 – Image showing anatomical anteversion (AA) and anatomical inclination (AI), relative to the right acetabular socket, adapted from (Murray 1993).....	16
Figure 2.17 – An AP radiograph showing a THR prosthesis in the right hip and a hip resurfacing prosthesis in the left hip (Su 2011).	18
Figure 3.1 – Showing the section of the left acetabulum removed from the whole pelvis STL file and converted into a solid 3D model.	33
Figure 3.2 – Flow chart illustrating how different equipment and software programs are used during the initial set-up stages and pre-processing.	33
Figure 3.3 – Image of the full pelvis showing the APP represented by the green triangle and the mid-sagittal plane represented by the purple rectangle.	34
Figure 3.4 – (a) Showing the full pelvis with the APP before adjustment for pelvic tilt and (b) after.	35
Figure 3.5 – An image of a BHR femoral head and acetabular component (Daniel et al. 2004).....	36
Figure 3.6 – (a) Showing the acetabular cup before modification and (b) after.	37
Figure 3.7 - Showing the femoral component before (a) and after (b) data removal, including the new centre of rotation point, reference plane and drilling axis.	38
Figure 3.8 – Showing the femoral length set at 80 mm and the femoral diameter set at 35 mm.....	40
Figure 3.9 – Showing the CCD angle set at 135°, Q angle set at 12°, femoral neck to femoral head centre at 60 mm, femoral head diameter of 50 mm, femoral neck diameter of 35 mm and CDD to tip of greater trochanter at 30 mm.	41
Figure 3.10 – Showing the resection level set at 10 mm away from the femoral neck edge.....	42
Figure 3.11 – Showing the femoral head offset angle set to 45 °and the femoral head offset distance set to 10mm.	43
Figure 3.12 – Showing the inclination and anteversion planes, with the intersecting axis referred to as the drilling axis.	43

Figure 3.13 – Showing a side view of the left acetabular socket indicating the three vertex points on the acetabular rim, as well as the acetabular reference plane passing through them. Labels 1 to 3, indicate the vertex point numbers.	45
Figure 3.14 – Showing the acetabular rim circle drawn on the acetabular reference plane and the centre point of the circle.	46
Figure 3.15 – Showing the three reference axes passing through vertex points 1, 2 and 3.....	47
Figure 3.16 – Is a zoomed-in section of the acetabular socket showing the adjustable point, fixed point and vertex 1 point along the vertex 1 axis.	48
Figure 3.17 – Showing the new acetabular movement plane passing through the three adjustable points at vertexes 1, 2 and 3, including, the new construction circle and centre point.	49
Figure 3.18 – Illustrates the different positions of the two acetabular planes, the blue plane representing the anatomical or reference plane and the red plane representing the movement plane.	50
Figure 3.19 – Flow chart illustrating the effect of Equation 3.1 on the specified surgeon input values.	52
Figure 3.20 – A frontal view of the full pelvis, illustrating the radiographic inclination angle (RI) of the left acetabular reference plane.	53
Figure 3.21 – An inferior view of the full pelvis, illustrating the anatomical anteversion angle (AA) of the left acetabular reference plane.	53
Figure 3.22 – Showing the BHR femoral head (green) connected to the artificial femur.	60
Figure 3.23 – Illustrating the acetabular cup positioned in the centre of the socket with the edge sitting parallel with the acetabular movement plane (shaded red).	61
Figure 3.24 – Flow chart illustrating how software programs SolidWorks, DriveWorks and the 3D vector spreadsheet interact with each other.	64
Figure 4.1 – Artificial femur with varying CCD angles (a) coxa vara with CCD = 110°, (b) coxa normal with CCD = 130° and (c) coxa valga with CCD = 140°	65

Figure 4.2 – An artificial femur with the CCD angle of the femoral neck set at 135° and the inclination angle for the femoral stem set at 55°	66
Figure 4.3 – Illustrating the 3D vector spreadsheet used to calculate the inclination and anteversion angles.	69
Figure 4.4 – Illustrating the spreadsheet used to convert inclination and anteversion angles between anatomical, operative and radiographic spatial reference systems.	71
Figure 4.5 – Illustrating the pelvic tilt adjustment spreadsheet, showing radiographic inclination and anteversion angles before and after adjustment.	72
Figure 4.6 – (a) Showing the front view of the left acetabular socket with the acetabular cup rim parallel with the acetabular reference plane and (b) showing a side view of the cup in the same position.	73
Figure 4.7 – (a) Showing the front view of the left acetabular socket with the acetabular cup rim parallel with the acetabular movement plane (b) showing a side view of the same cup.	74
Figure 4.8 – Illustrating the complete assembly file, with the acetabular cup in its new position according to the offsets: vertex 1 = -2 mm, Vertex 2 = -4 mm and Vertex 3 = +4 mm.	76
Figure 4.9 – Illustrating the new patient's STL (purple) superimposed over the test patient's STL (green), with (a) a frontal view and (b) a side view of the pelvis.	78

List of Tables

Table 3.1 – Table showing properties of the original STL after 3D rendering.....	31
Table 3.2 – Showing BHR component characteristics.....	36
Table 3.3 – Default values used in the DriveWorks input form to create the artificial femur.....	39
Table 3.4 – Table showing the parameters used for the input for for DriveWorks.	50
Table 3.5 – Showing the inputs for vertex point locations on the acetabular reference plane.	54
Table 3.6 – Showing the formulae used to calculate the unit normal vector n	55
Table 3.7 – Showing the formulae used to calculate the angle θ between the unit vector n and the respective projection vectors c , d and e	55
Table 3.8 – Showing the formulae used to project the unit vector n onto the respective planes.	55
Table 3.9 – Showing the formulae used to calculate the angles α , β & γ of the projected vector, in the respective anatomical reference planes.....	56
Table 4.1 – Displaying the results calculated by the 3D vector spreadsheet for the acetabular reference plane.....	67
Table 4.2 – Illustrating the results calculated by the 3D vector spreadsheet for the new acetabular movement plane.....	68
Table 4.3 – Illustrating the results calculated by the 3D vector spreadsheet for cup inclination and anteversion angles, in terms of the three different spatial reference systems.....	70
Table 4.4 – Illustrating the effect on inclination and anteversion angles associated with an acetabular cup offset of -2, -4 and +4 mm.	71
Table 4.5 – Displaying the results measured in SolidWorks for cup inclination and anteversion angles, in terms of the respective spatial reference systems.....	75

List of Acronyms

3D – three dimensional
AA – Anatomical Anteversion
AI – Anatomical Inclination
AP – anterior-posterior
APP – anterior pelvic plane
ASIS – anterior superior iliac spines
CAD – computer aided design
CAS – computer assisted surgery
CCD – caput-collum-diaphyseal
CoCr – cobalt-chromium
CT – computed tomography
DICOM – Digital Imaging and Communications in Medicine
FAI – femoroacetabular impingement
IGES – Initial Graphics Exchange Specification
MoM – Metal-on-Metal
MRI – magnetic resonance images
NURBS – Non-Uniform Rational B-spline Surfaces
OA – Operative Anteversion
OI – Operative Inclination
Q angle – quadriceps femoris angle
RA – Radiographic Anteversion
RI – Radiographic Inclination
RoM – Range of Motion
STL – stereolithography
THR – total hip replacements

1. Introduction

1.1. Description of the problem

Hip resurfacing, or partial hip replacement, is a procedure in which a metal cup is placed inside the acetabular socket and a spherical metal cap inserted over the femoral head, thus replacing the articulating surfaces of the hip joint. The procedure involves removing less bone compared to that of a total hip replacement (THR) and may be beneficial to younger, more active patients. The primary aim of the procedure is to alleviate joint pain and to restore normal joint function as far as possible.

Conditions that may necessitate hip resurfacing include osteoarthritis, osteonecrosis, degenerative conditions secondary to developmental hip dysplasia, injury and bone tumours (Shimmin et al. 2005a).

Currently, magnetic resonance images (MRIs) and anterior-posterior (AP) radiographs are commonly used to diagnose and assess pathological conditions of the hip, however these techniques provide a two-dimensional image of the patient's morphology. This may limit the surgeon's ability to fully diagnose the problem, visualise and plan the surgery, as well as select the best suited prosthetic component sizes.

Malpositioning of the resurfacing components can lead to premature failure of the prosthesis, decreased post-surgical hip Range of Motion (RoM) and increased wear rates which can lead to other pathological conditions in patients.

1.2. Importance of the problem

Preventing surgical malpositioning through comprehensive pre-surgical planning can improve the life cycle of a hip resurfacing prosthesis. Incorrect femoral component orientation can lead to impingement between the edge of

the acetabular component and the bony femoral neck. This is referred to as notching and can lead to femoral neck fracture (De Haan et al. 2008b). This mode of failure usually occurs relatively early in the life cycle of the prosthesis, in some cases as early as one month after the initial surgery (De Haan et al. 2008b) and is one of the most common reasons for early failure (United Kingdom. The National Health Service, National Joint Registry for England and Wales. 2007).

The foremost reason for undergoing hip resurfacing is to alleviate joint pain and to improve or restore natural hip RoM. Yet, if these hip resurfacing components are inserted incorrectly, the patient may be worse off after the surgery. This can have serious quality of life implications and may have a long-term effect on the ability of the individual to live a productive life.

Finally, incorrect orientation of the components in hip resurfacing can lead to generation of wear debris and metal ions (Langton et al. 2008). The articulating surfaces of most hip resurfacing components on the market are manufactured from a cobalt-chromium (CoCr) alloy. High CoCr metal ion levels, both locally in the joint capsule or in circulation, are associated with a range of negative effects. In some cases the release of metal ions has been linked to aseptic loosening of the prosthesis and subsequent failure, formation of pseudo-tumours and renal complications (De Haan et al. 2008b; Pandit et al. 2008). There is also a possibility that chronic exposure to these metal ions may have a carcinogenic effect, cause hypersensitivity (Willert et al. 2005), and in the case of pregnant women may affect the unborn foetus (Ziaee et al. 2007).

Correct positioning of the prosthetic components is essential to reduce complications after surgery. If surgeons were able to view the patient's hip in a three-dimensional (3D) computer model, as well as virtually insert the hip resurfacing components they may be in a better position to select the optimal component location and size, and analyse the predicted hip RoM. This may further serve to reduce surgical time.

1.3. Objectives of study

The main objective of this study was to investigate the use of an existing CAD software package to generate a 3D computer model of the pelvis and upper femur, for use by a surgeon in pre-surgical planning. This was in order to identify the ideal prosthesis size and position, based on hip RoM analysis, and specify the optimal operative angles in which to place the components during hip resurfacing surgery. Further, this study had the purpose of providing groundwork for future development of a user-friendly software program for pre-surgical planning of hip resurfacing.

The secondary objectives of the study were to investigate incorporating various surgeon requirements; and to investigate the possibility of incorporating new patient computed tomography (CT) scans, and manipulate certain anatomical variables to test different placement scenarios.

1.4. Overview of the research methodology

High definition CT scans of a healthy patient, showing the full pelvis and upper region of the femur, were rendered into stereolithography (STL) files. Subsequently, these files were imported into the CAD software package to generate solid 3D models. Anatomical reference planes were set-up and location points inserted into the model to facilitate accurate location and orientation of the electronic prosthetic components. A platform was created, using an add-on software package, to allow the surgeon to specify femoral dimensions and acetabular cup positions, then test those against the on-screen attainable hip RoM. This can aid in the pre-surgical planning of the arthroplasty as well as the selection of the ideal component sizes and positions.

2. Literature Review

2.1. The hip joint

The hip joint or acetabulofemoral joint, is the joint between the acetabulum of the pelvis (Figure 2.1) and femur (Figure 2.2), forming a classical ball-and-socket joint. The acetabulum is concave shaped and is the junction of the three pelvic bones the ilium, ischium and the pubis (Figure 2.3). The femoral head is convex and nearly circular in shape, which permits rotation about a fixed axis (Caillet 2003). The acetabulum encircles the anterior, superior and posterior aspects of the spherical femoral head (Figure 2.3)

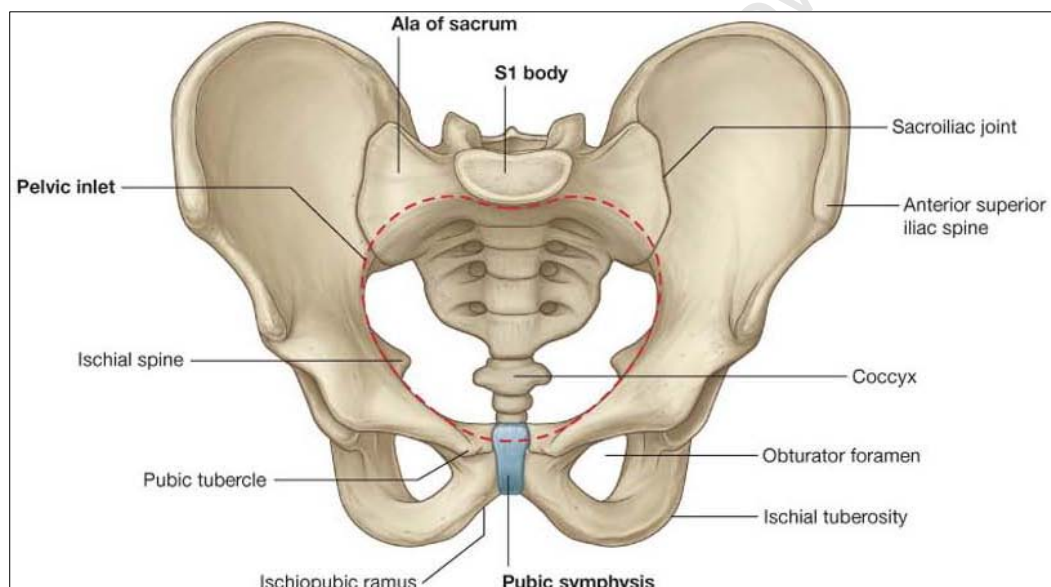


Figure 2.1 – Showing points of interest on the pelvis (Drake et al. 2009).

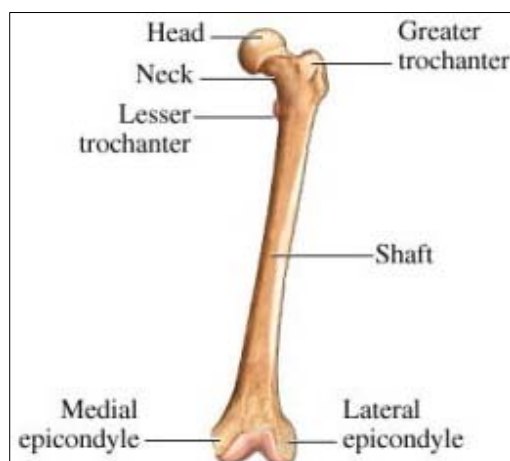


Figure 2.2 – Showing a sketch of the anterior side of the left femoral bone (Darling 2011).

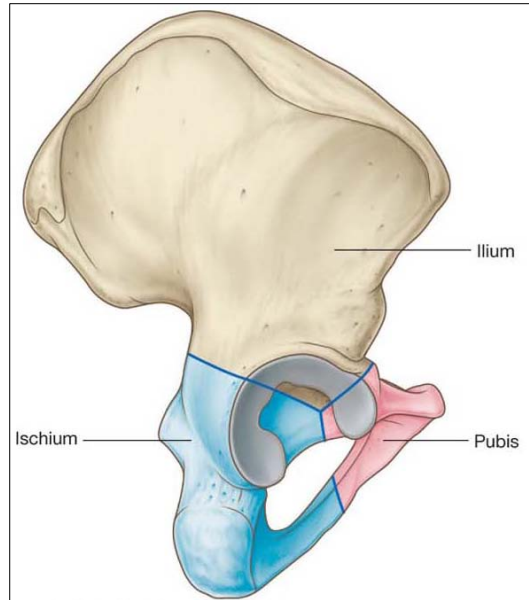


Figure 2.3 – Showing a right side view of the pelvis and acetabular socket (Drake et al. 2009).

2.2. Basic biomechanics of the hip joint

Understanding the biomechanics of the hip joint is important for the planning of procedures such as hip resurfacing, as well as the design and development of the prosthetic components (Byrne 2010).

The hip joint comprises of 22 muscles which provide the forces necessary for movement as well as stability. The principal function of the hip joint is load bearing and retaining balance, whilst allowing rotational motion in all directions. In the standing position, with the body weight supported by both legs, the centre of gravity is located centrally between the two hips and the force is distributed equally. In this scenario the weight of the upper body minus the weight of both legs is supported equally on the femoral heads. This generates compressive forces approximately equal to one third of body weight acting on each femoral head (Pauwels 1980). During walking, the single leg stance phase of the gait cycle can produce compressive forces as high as four times the body weight. Additionally during some athletic activities the hip joint may be exposed to much higher than normal axial and torsional loading (Byrne 2010). Three contributing factors to the magnitude and

direction of the compressive forces acting on the femoral head include: the position of the centre of gravity; the abductor lever arm length (which is a function of the neck-shaft angle, discussed later in Section 2.4.2 and the magnitude of body weight (Johns Hopkins 2012).

2.3. Hip Range of Motion

Range of Motion (RoM) refers to the distance and direction a joint can move to its full potential. Each specific joint has a normal RoM that is expressed in degrees and can be measured using a device called a goniometer. In order to understand hip RoM it is necessary to introduce the movements described below and seen in (Figure 2.4 and Figure 2.5).

- Flexion / extension (A)
- Adduction / abduction (B)
- Internal / external rotation (C)
- Circumduction (D)

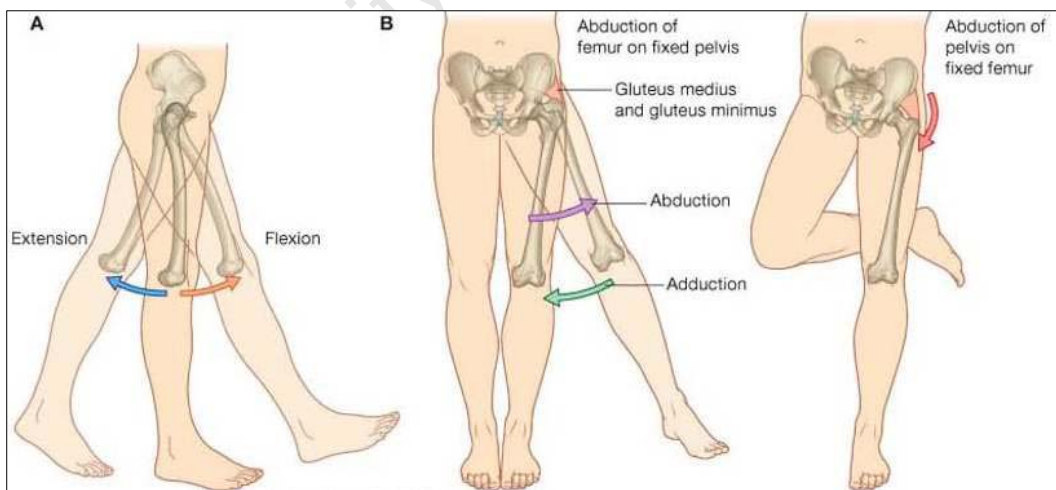


Figure 2.4 – A). Showing flexion/extension B). Showing abduction/adduction (Drake et al 2009).

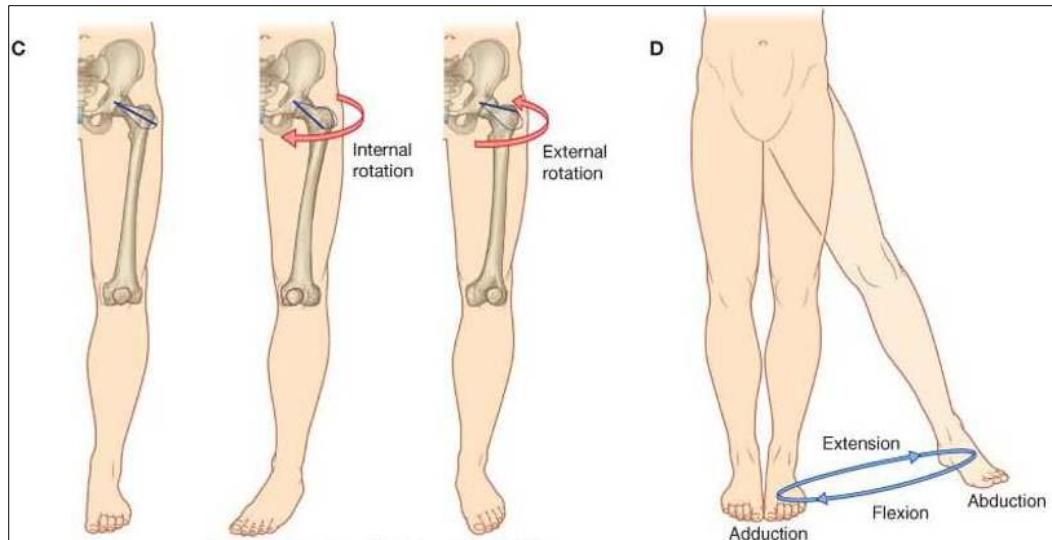


Figure 2.5 – C). Showing internal rotation/external rotation D). Circumduction (Drake et al. 2009).

Using these basic movements, hip RoM can be analysed by measuring the following four movement arcs:

- Flexion /extension in neutral abduction and rotation
- Adduction /abduction in 0° flexion and neutral rotation
- Internal /external rotation in 0° flexion
- Internal / external rotation in 90° flexion

2.4. Measurement of the anatomy of the hip joint

The outcome of hip resurfacing arthroplasties significantly depends on the correct anatomical placement of the components during the surgical procedure. Accurate measurement and pre-surgical planning rely on the techniques discussed below.

2.4.1. Anatomical reference frames

The first parameter to consider when measuring any anatomical angles of the body is the type of reference frame to use. Defining the anatomical reference frame in 3D space will set-up the orientation of the x, y, and z axes from

which angular measurements can be made. These axes are superior/inferior (SI), anteroposterior (AP) and mediolateral (ML). The anatomical reference planes are defined by pairs of these axes: mid-sagittal (SI and AP axes), transverse, horizontal or axial (AP and ML axes) and coronal or frontal (ML and SI axes) (Yoon et al. 2008) (Figure 2.6 and Figure 2.7).

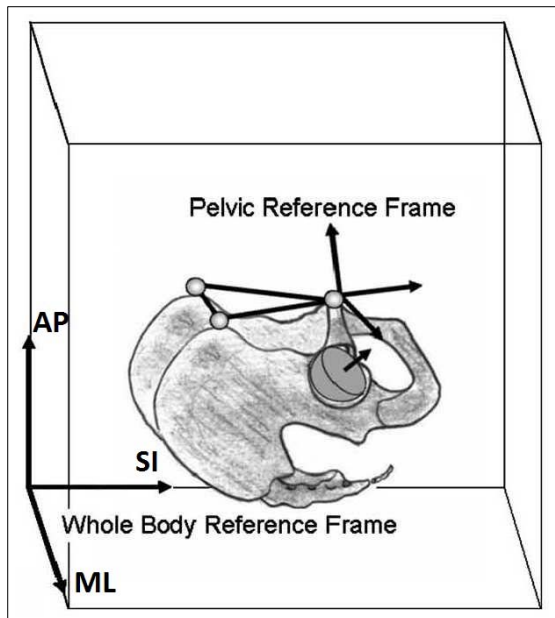


Figure 2.6 – Illustrating the whole body or ground-based reference frame and the pelvic reference frame (Yoon et al. 2008).

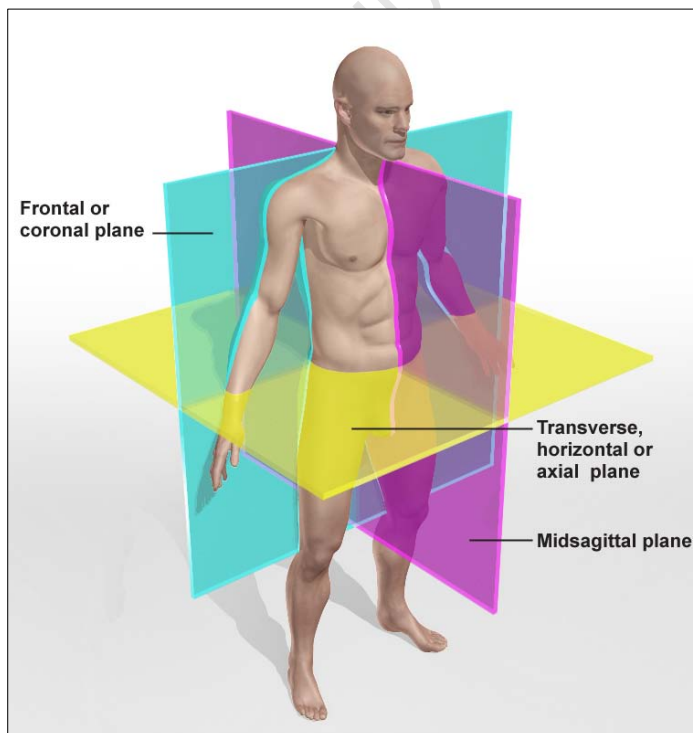


Figure 2.7 – An illustration showing the three main anatomical planes (Primal Pictures Ltd. 2011).

The ground-based axis system or whole body reference frame is compared to the pelvic reference frame in Figure 2.6. Pelvic orientation is not fixed in the ground-based reference system and it does not take into consideration the degree of pelvic tilt, which depends on posture and activity (Yoon et al. 2008). This is illustrated as the angle $-\alpha$ in Figure 2.8. The average pelvic tilt or reclination measured in 30 healthy subjects was found to be -8° in the standing position and -4° in the lying position (Lembeck et al. 2005), these values were comparable to those described by Yoon et al. (2008).

The most common reference system in use today is thus defined relative to the pelvic reference frame or anterior pelvic plane (APP) (Figure 2.6). The APP is defined by the left and right anterior superior iliac spines (ASIS) and the centre of the anterosuperior surface of the pubic spines (Figure 2.1) (Lewinnek et al. 1978; Lembeck et al. 2005; Murtha et al. 2008; Nagao 2008; Yoon et al. 2008; Hart et al. 2009; Köhnlein et al. 2009; Lubovsky et al. 2010; Perreira et al. 2010). By using an anatomical reference frame based on the APP, acetabular orientations can be measured that are independent of the patient relative to the ground (Yoon et al. 2008).

The orientation of the APP relative to the frontal plane can differ significantly depending on whether the subject is in the standing or lying position (Lembeck et al. 2005). If pelvic tilt is not taken into consideration it can cause false values when evaluating anatomical angles based on AP radiographs.

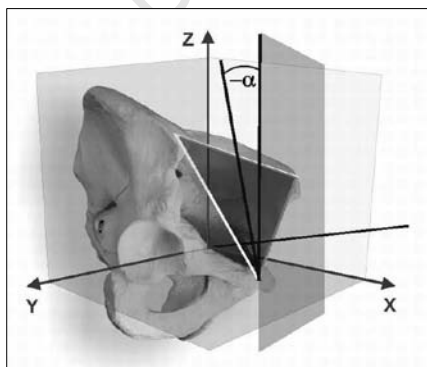


Figure 2.8 – Illustrating pelvic tilt or pelvic reclination relative to the coronal plane (angle α is negative) (Lembeck et al. 2005).

2.4.2. Anatomical femoral angles

Certain anatomical angles of the femur are relevant for location and orientation of the femoral component in hip resurfacing. These angles are defined below.

The caput-collum-diaphyseal (CCD) angle or neck-shaft angle is the oblique angle formed between the central axis of the femoral neck and the central axis of the femoral shaft, when viewed in the frontal plane (Figure 2.9). The majority of healthy adults have a CCD angle of 120° to 135° , which is referred to as coxa normal. As can also be seen in Figure 2.9, coxa vara is the condition when the CCD angle is less than 120° and coxa valga is the condition when the angle is greater than 135° . These are both abnormal physiological conditions that are either congenital, developmental, or acquired. Coxa valga or excessive femoral inclination will cause a decrease in the abductor lever arm length which will result in an increased abductor muscle demand and therefore increased joint loading.

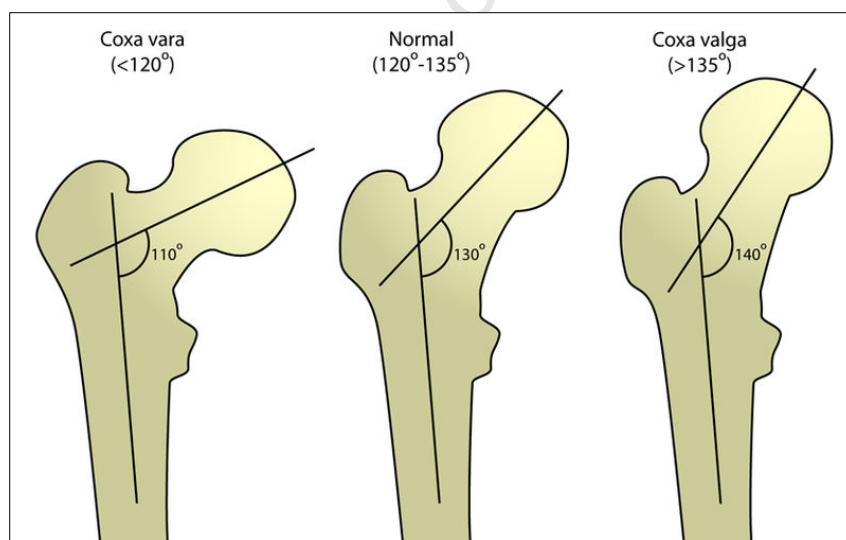


Figure 2.9 – Illustrating different CCD angles between the femoral neck and femoral shaft (Amini 2007).

In sketch B in Figure 2.10, the femoral head and neck are rotated anteriorly and viewed in the transverse plane. The angle of femoral anteversion is measured between a transverse axis passing through the femoral condyles known as the transverse condyle axis (TCA) and the central axis of the

femoral neck (NA). An anteversion angle of between 15° and 25° is considered normal for a healthy patient (Murphy et al. 1987; Maruyama et al. 2001; Bråten M. et al. 2009). A high degree of femoral anteversion will cause the knee and foot to internally rotate towards the midline of the body, whilst abnormal femoral retroversion is associated with an external rotation of the knee and foot (Johns Hopkins 2012).

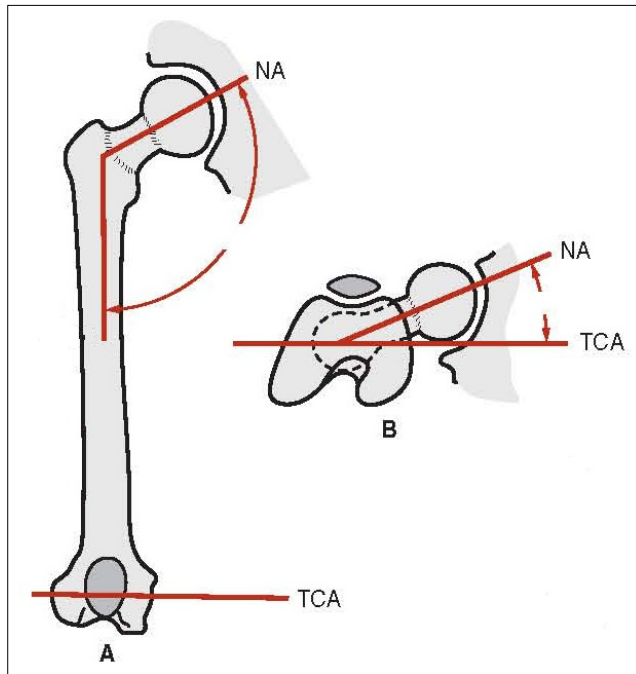


Figure 2.10 – Sketch illustrating the femoral anteversion angle formed between the TCA and NA (Caillet 2003).

The quadriceps femoris angle (Q angle) is formed by a line drawn from the anterior superior iliac spine through the midpoint of the patella and a line drawn from the midpoint of the patella to the centre of the tibial tuberosity (Figure 2.11).

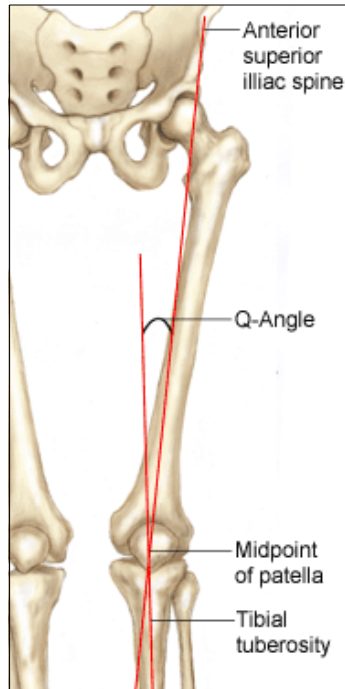


Figure 2.11 – Sketch illustrating how the Q angle is measured (Medical Arts Rehabilitation Inc. 2011).

Horton and Hall (1989) found that the mean Q angle for healthy women was $15.8^{\circ} \pm 4.5^{\circ}$ and $11.2^{\circ} \pm 3.0^{\circ}$ for healthy men; Wheeless (2011) found similar results in his investigation. The Q angle, along with the vector for the combined pull of the quadriceps femoris muscle and the patellar tendon, determine the magnitude of the lateral pull on the patella. Hypothetically, an increase in the Q angle will cause an increase in the lateral pull on the patella and can lead to subluxation (partial dislocation) and damage to the cartilage at the back of the patella (Horton and Hall 1989; Mizuno et al. 2001; Herrington and Nester 2004).

2.4.3. Anatomical acetabulum angles

Along with the angles described in Section 2.4.2 above, the anatomical acetabular angles play an important role in locating and orientating the acetabular cup in hip resurfacing arthroplasties. These angles are defined below.

Acetabular inclination or opening angle is the angle between the transverse plane and the rim of the acetabulum, when viewed in the frontal plane. This is also referred to as prosthetic cup inclination angle in hip replacement surgery (Figure 2.12).

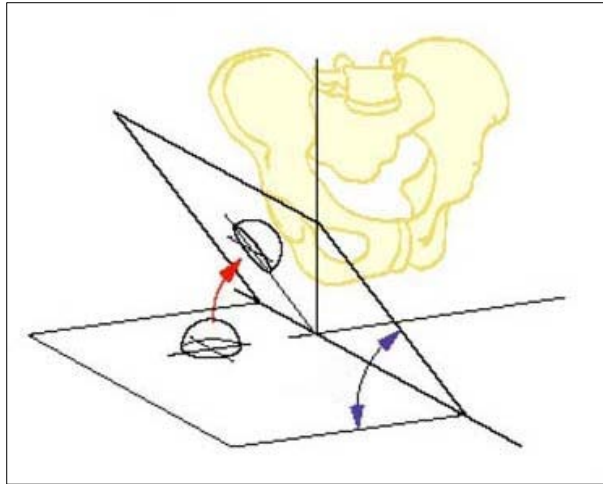


Figure 2.12 – Illustrating one method of measuring acetabular inclination, adapted from (Wolf et al. 2005).

The geometry of the acetabulum (as well as the orientation of the prosthetic cup in hip resurfacing) can be defined by inclination and anteversion angles (Murray 1993; Yoon et al. 2008; Grammatopoulos et al. 2010; Köhnlein et al. 2009; Lubovsky et al. 2010). Inclination can additionally be referred to as the abduction or opening angle. In some cases variability in acetabular inclination and anteversion angles between patients was found to be as high as 24° (Lubovsky et al. 2010). In addition to inter-patient variability, there is also angular variability between the left and right sides, sometimes as much as 17° (Lubovsky et al. 2010) which strengthens the case for patient-specific component placement in hip resurfacing arthroplasties. Acetabular angles can be described or assessed anatomically, radiographically and through direct observation during an operation (Murray 1993).

The definitions described below are crucial when defining acetabular orientation, in terms of the different spatial reference systems.

- **Acetabular axis** – This can be described by a vector perpendicular to the acetabular plane, passing through the centre of the socket (Figure 2.13).

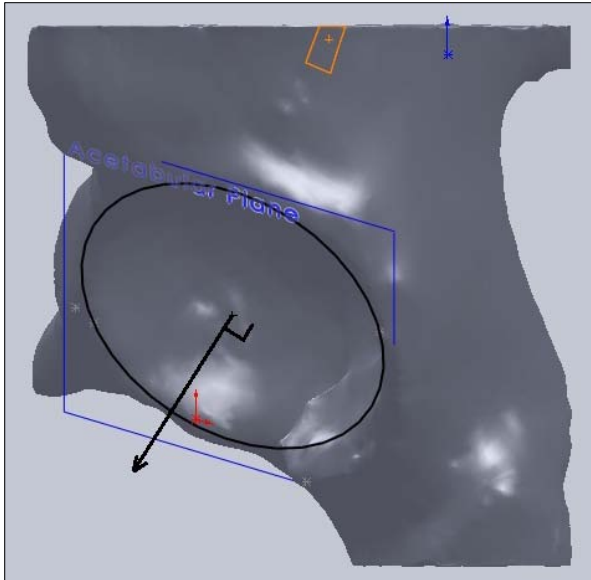


Figure 2.13 – This image is a section of the pelvis, showing the left acetabulum socket with the acetabular axis (black arrow) pointing perpendicular to the acetabular plane.

- **Operative anteversion (OA)** – is the angle between the sagittal axis of the patient and the projection of the acetabular axis onto the sagittal plane (Murray 1993) (Figure 2.14).
- **Operative inclination (OI)** – is the angle between the acetabular axis and the sagittal plane. It is the angle of inclination of the acetabular axis (Murray 1993) (Figure 2.14).

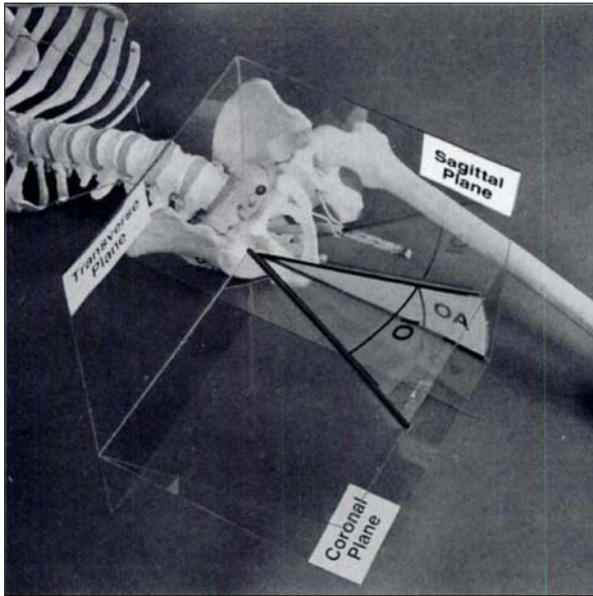


Figure 2.14 – Image showing operative anteversion (OA) and operative inclination (OI), relative to the right acetabulum socket, adapted from (Murray 1993).

- **Radiographic anteversion (RA)** – is defined as the angle between the acetabular axis and the coronal plane (Murray 1993) (Figure 2.15).
- **Radiographic inclination (RI)** – is defined as the angle between the sagittal axis and the projection of the acetabular axis onto the coronal plane (Murray 1993) (Figure 2.15).

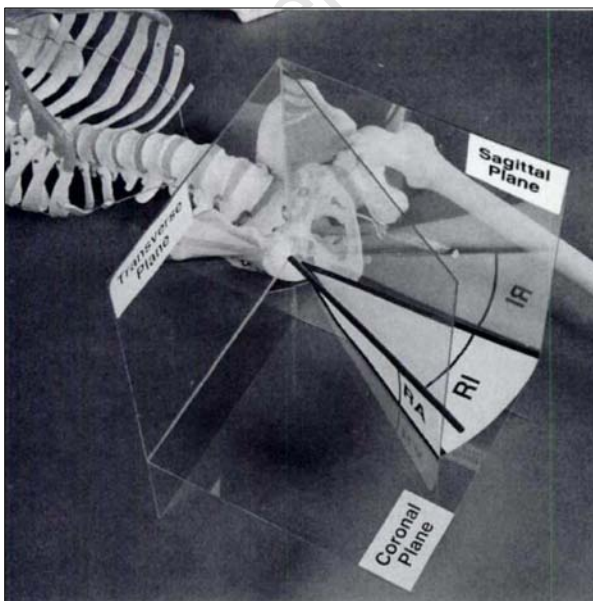


Figure 2.15 – Image showing radiographic anteversion (RA) and radiographic inclination (RI), relative to the right acetabulum socket, adapted from (Murray 1993).

- **Anatomical anteversion (AA)** – is defined as the angle between the transverse axis and the projection of the acetabular axis onto the transverse plane (Murray 1993) (Figure 2.16).
- **Anatomical inclination (AI)** – is defined as the angle between the sagittal axis and the acetabular axis (Murray 1993) (Figure 2.16).

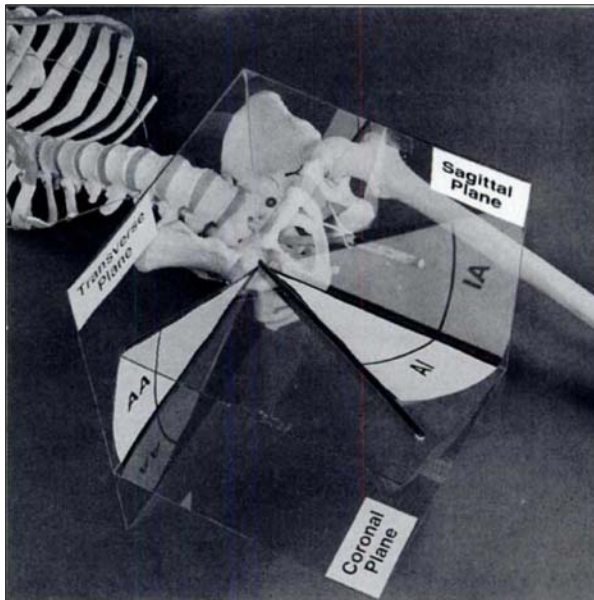


Figure 2.16 – Image showing anatomical anteversion (AA) and anatomical inclination (AI), relative to the right acetabular socket, adapted from (Murray 1993).

The main difference between the operative, radiographic and anatomical definitions above relates to how the anteversion angle is measured. OA is measured around the transverse axis, AA around the sagittal axis and RA around an oblique axis. (Murray 1993; Wolf et al. 2005; Yoon et al. 2008; Grammatopoulos et al. 2010) recommend using operative angles to describe inclination and anteversion for hip replacement surgeries. The OI angle can be thought of as inclination of the prosthetic component and OA as hip flexion, whilst RI and RA are projected angles (Grammatopoulos et al. 2010).

Post-operative AP radiographs can be used to assess the outcome of the surgery in terms of acetabular cup orientation, by converting the radiographic angles back to either operative or anatomical angles. Using certain

trigonometric functions it is possible to convert the inclination and anteversion angles between the different spatial reference systems (Appendix A). AP radiographs do not account for pelvic tilt as mentioned in Section 2.4.1, therefore when using them to assess the outcome of hip arthroplasties a correction algorithm needs to be applied (See Appendix B). Approximately 1° of pelvic inclination requires a correction of RA of 0.7° (Lembeck et al. 2005). Therefore, if the subject is in the standing position, with pelvic tilt at -8° , this will result in 5.6° more anteversion than originally measured. Thus, surgeons need to consider the need to make these corrections for AA when making use of AP radiographs for pre-surgical planning. The effect of pelvic tilt on RI is considered minimal and therefore does not require correction (Lembeck et al. 2005).

2.5. Hip replacement arthroplasties

There are two main hip replacement arthroplasties available, total hip replacements (THR) and hip resurfacing or partial hip replacements. THR involves the removal and replacement of both the femoral head (including most of the femoral neck) and acetabulum. Hip resurfacing is a procedure in which only the articulating surfaces of femoral head and the acetabulum are replaced. The primary aim for receiving a hip replacement is to alleviate joint pain and to restore normal joint function as far as possible.

2.5.1. Indications for hip replacements

Hip replacements are most commonly required as a result of end-stage osteoarthritis. Osteoarthritis is a common joint disease which is associated with many structural and morphological abnormalities of the acetabulum. The disease causes articular cartilage to break down and the bone surfaces to rub against each other. This causes damage to both tissue and bone and is associated with joint pain, stiffness and decreased RoM (United Kingdom. The National Health Service, National Collaborating Centre for Chronic Conditions. 2008). Other conditions which may warrant a hip replacement include structural abnormalities, osteonecrosis or avascular necrosis (death

of bone caused by insufficient blood supply), rheumatoid arthritis, injury, fracture and bone tumours.

2.5.2. THR vs hip resurfacing

During THR surgery the femoral head and neck are excised to make way for a long stemmed femoral component (Figure 2.17) (Vendittoli et al. 2007). The diameter of the prosthetic femoral head used is smaller than that of the original femoral head. The prosthetic femoral head is attached to the femoral component and inserted into the prosthetic acetabular cup. The cup is made up of a titanium outer shell and a CoCr, polyethylene or ceramic inner lining.



Figure 2.17 – An AP radiograph showing a THR prosthesis in the right hip and a hip resurfacing prosthesis in the left hip (Su 2011).

High failure rates with THR in younger and more active patients, in the form of dislocations, has seen a move to hip resurfacing as a viable alternative. One of the major advantages of hip resurfacing is the preservation of bone stock on the femoral side, thereby helping to restore the original anatomy. The femoral neck is preserved and the head is resurfaced (Figure 2.17). This equates to a more natural physiological loading of the joint and may help to reduce the degree of bone resorption post-operatively (Barrett et al. 2007). Beaulé et al. (2004b) propose that patients of 40 years or younger should be considered for hip resurfacing as they have the most to gain from this conservative prosthetic solution.

Hip resurfacing arthroplasties can be technically more challenging compared to THR, since retaining the femoral head obscures the exposure of the acetabular socket and may affect correct positioning of the cup (De Haan et al. 2008b). The skin incision is generally larger compared to THR, as access to the lateral cortex of the femur is required (Barrett et al. 2007). This usually means that there is increased short-term morbidity and longer hospital stays. Although mid-term results of hip resurfacing are positive, the long term results are unknown. Not all patients are suitable candidates for hip resurfacing arthroplasties and careful patient selection is critical to the success of the operation (Amstutz et al. 2004).

2.5.3. Hip resurfacing components

Hip resurfacing components consist of an acetabular cup and a short-stemmed femoral head. The use of CoCr Metal-on-Metal (MoM) bearing surfaces in hip resurfacing began in the UK in 1991. After investigating various fixation methods, McMinn introduced a hybrid cementless hydroxylapatite (HA) coated acetabulum (McMinn et al. 1996). Subsequently, many other hip resurfacing products have been introduced to the market, but most employ the same MoM design principles.

2.5.4. Component positioning in hip resurfacing

For THR arthroplasties a longstanding “safe zone” has been identified for positioning of the acetabular cup based on radiographic measurements, which is $40^{\circ} \pm 10^{\circ}$ inclination and $20^{\circ} \pm 10^{\circ}$ anteversion to minimise the risk of dislocation (Lewinnek et al. 1978). In contrast, although there is a large knowledge base on the MoM bearing engineering and tribology, there is little concrete data available on the optimum hip resurfacing component position and size (Williams et al. 2009).

Valgus placement, or a greater angle of inclination, of the femoral component may help reduce stresses in the narrow femoral head-neck region (Beaule et al. 2004a) and optimise the load bearing capacity of the femoral neck

(Shimmin and Back 2005b). This is consistent with Amstutz et al. (2001) who recommend placing the femoral component at a valgus angle of approximately 140° and anatomically anteverted to minimise lateral neck and head interfacial stress. De Haan et al. (2008b) propose a desired CCD angle for the femoral component of between 135° and 145° , with a 10° limit on anteversion or retroversion from the neutral position. By increasing the valgus angle of the femoral component the femoral offset is reduced (Beaule et al. 2004a; Shimmin and Back 2005b). Femoral offset is defined as the perpendicular distance from the long axis of the femur to the centre of rotation of the femoral head (McGrory et al. 1995). Patients with a higher femoral offset have increased RoM before bony impingement occurs (Kluess et al. 2008).

A number of different recommendations for the placement of the acetabular component have been made. During revision surgery of failed or malpositioned hip resurfacing prostheses the acetabular component was placed in a position of 40° of inclination and 20° of anteversion (De Haan et al. 2008b). Similarly, $15 - 20^\circ$ of anteversion and $40 - 45^\circ$ of inclination is recommended for the BHR resurfacing system in the BHR FDA Surgical Technique document (Smith & Nephew 2007). Both De Haan et al. (2008b) and the BHR FDA Surgical Technique document (Smith & Nephew 2007) do not specify whether the angles are operative, radiographic or anatomical. Grammatopoulos et al. (2010) recommend that surgeons implant the acetabular component with $45^\circ \pm 10^\circ$ inclination and $20^\circ \pm 10^\circ$ anteversion based on post-operative radiographs. Taking into the account the differences in radiographic and operative angles, this recommendation was revised to specify an OI of 40° and an OA of 25° (Grammatopoulos et al. 2010). A number of other manufacturers and designers of hip resurfacing prostheses recommend placing the acetabular component at 40° of inclination and 20° of anteversion, but do not specify whether these are operative, anatomical or radiographic angles.

2.5.5. Hip RoM and component positioning and size

Hip RoM analysis based on 3D anatomical models revealed that RoM before impingement was significantly lower for a hip resurfacing prosthesis compared to that of a THR prosthesis (Klues et al. 2008). The attainable RoM to a large degree is dependent on the angular distance or angle between the inner rim of the acetabular cup and the point of contact on the femoral neck bone (Vendittoli et al. 2007). This angle increases as the femoral head-neck ratio increases. The femoral head-neck ratio is defined as the diameter of the femoral head divided by the diameter of the femoral neck. In THR prostheses, the head-neck ratio is significantly larger, as the original femoral neck has been excised and replaced with a thin stemmed neck, therefore reducing the chance of impingement. The large femoral head diameter in hip resurfacing, compared to THR, provides greater mobility without compromising on the stability of the hip joint, but the small head-neck ratio may have a negative effect on the range of flexion (Malviya et al. 2010).

After hip resurfacing, extreme flexion movements cause the anterior border of the acetabular cup to impinge against the neck relatively earlier than expected, as the head-neck ratio is decreased. During these extreme movements in a natural healthy hip, the large diameter of the femoral neck does not limit the RoM, as the rim of the acetabulum is partially cut out to provide more movement before impingement (Klues et al. 2008).

The transverse section of the bony femoral neck is not circular in shape, but more of an ovoid with the larger diameter located postero-superiorly. This can cause the natural head-neck offset distance (which is the perpendicular distance between the outer surface of the femoral head and outer surface of the femoral neck) to be irregular around the head-neck circumference (Vendittoli et al. 2007). Therefore, a generalised head-neck offset ratio cannot be applied in hip resurfacing as it is in THR arthroplasty. To overcome this difficulty the anterior femoral head-neck offset ratio can be used as a technique for predicting the probability of impingement (Beaule et al. 2007b). The head-neck offset ratio is calculated by measuring the anterior head-neck

offset distance divided by the diameter of the femoral head, using a cross-table radiograph (Beaule et al. 2007b). Femoral head-neck offset ratios ≤ 0.15 may present a considerable risk for femoroacetabular impingement (FAI) (Beaule et al. 2007b; Malviya et al. 2010). This offset ratio is dictated by the patient's natural anatomy and the aim of most hip resurfacing arthroplasties is to restore this natural hip RoM. Therefore, if the patient is at risk of FAI prior to surgery the surgeon needs to decide whether the underlying deformity is correctable, or whether it is necessary to investigate a different method of corrective surgery. Any anterior rim osteophytes (bone spurs) in patients with osteoarthritic hips should be removed to correct a deficient femoral head-neck offset ratio during a hip resurfacing arthroplasty (Beaule et al. 2007b). This procedure will not cause an increased risk to femoral neck fracture after surgery (Mardones et al. 2005).

Another factor that can affect the femoral head-neck offset is the metallic femoral component offset, which is defined as the perpendicular distance between the outer surface and the neck opening (where the femoral neck is inserted), plus the bone cement mantle thickness. This is termed the minimal head-neck offset of the prosthesis (Vendittoli et al. 2007). Depending on the manufacturer, component offset values can range from 3 – 4 mm, and cement mantle thicknesses from ~ 0 – 1.25 mm, therefore prosthetic femoral head-neck offset can vary from 3 – 5 mm. This factor needs to be taken into consideration when the surgeon is aiming to reproduce the patient's natural femoral head-neck ratio.

Translation involves offsetting the prosthetic femoral stem relative to the central neck axis (also known as the CCD). It has been suggested that translation of the femoral component relative to the central femoral neck axis during surgery may also affect the head-neck offset in certain directions, which could have adverse effects on the hip RoM (Vendittoli et al. 2007). Hip RoM in the direction of translation improves, but at the same time is reduced in the opposite direction (Vendittoli et al. 2007). Translation of the femoral component could thus be used to rectify a deficient head-neck offset present in one quadrant, or to provide more or less RoM in a particular direction

depending on the patient. The amount of translation possible is limited so as not to compromise the integrity of the femoral neck bone.

Natural hip range of flexion is dependent on anatomical femoral neck anteversion, and so this femoral anteversion angle is retained in hip resurfacing (Malviya et al. 2010). The centre of rotation of the femoral component does not change when modifying its orientation with respect to varus-valgus and anteversion-retroversion (Vendittoli et al. 2007). Combined with the fact that the femoral head is an extended hemisphere, the impingement zone between the acetabular rim and the femoral neck is not affected by a change in femoral head orientation and therefore has little effect on hip RoM.

Hip RoM is affected by femoral component orientation when the femoral neck is reamed, thereby removing natural bone and increasing the angular distance between the inner rim of the acetabular cup and the point of contact on the femoral neck. Research has indicated that femoral neck reaming should be avoided as this may be detrimental to life of the prosthesis and can lead to premature femoral neck fracture (Shimmin and Back 2005b; Beaulé et al. 2007a).

Analysis conducted using 3D computer models indicates a small to significant gain in hip RoM can be achieved with a femoral implant of one size larger (2 mm) than the ideal size (Vendittoli et al. 2007; Klues et al. 2008). By increasing the femoral component by two sizes (4 mm) RoM improvement was not as pronounced (Vendittoli et al. 2007). This increase in RoM can be attributed to circumferentially increasing the femoral head-neck offset and lateralising the femoral head centre of rotation, while at the same time not increasing the femoral neck diameter. The drawbacks to this approach are that the size of the femoral component is limited by the outer diameter of the femoral neck, and an increase in femoral component size equates to a larger acetabular cup and therefore more acetabular bone resection. The surgeon must assess whether it is beneficial to use a larger femoral component and therefore attain a better RoM with less risk of

impingement, at the expense of resecting more acetabular bone stock. In most cases the patient's anatomy dictates the component size options available to the surgeon.

The hip RoM attainable is also dependent on the cup position, with reference to cup inclination and anteversion angles (Williams et al. 2009; Malviya et al. 2010). Post-operative patient surveys reveal that the degree of hip flexion attainable increases as cup anteversion increases for hip resurfacing prostheses (Malviya et al. 2010). Increasing the cup inclination angle from 30° to 50°, as well as increasing the cup anteversion from 0° to 25° gives a more physiologic hip RoM (Williams et al. 2009). Studies have shown that steeply inclined cups greater than 50° inclination and anteversion angles greater than 25° have been associated with higher wear rates and raised metal ion levels (Williams et al. 2009; Hart et al. 2009b; Malviya et al. 2010). On the other hand, if the inclination angle is too low this may lead to antero-superior overhang of the acetabular cup and lead to subluxation in flexion and internal rotation movements (Kluge 2009).

Increasing the seating depth of the acetabular cup, whilst leaving a bony acetabular rim has a negligible effect on hip RoM (Vendittoli et al. 2007). Findings suggest that if there is over-deepening of the acetabular component, acetabular rim trimming should be considered especially in the antero-superior section (Vendittoli et al. 2007).

2.5.6. The effects of malpositioning

In addition to restricting hip RoM, malpositioning of the resurfacing components can lead to premature failure of the prosthesis, and increased wear rates which can lead to other pathological conditions in patients.

Incorrect femoral component orientation can lead to impingement between the edge of the acetabular component and the bony femoral neck. This is referred to as notching and can lead to femoral neck fracture (De Haan et al. 2008b). This mode of failure usually occurs relatively early in the life cycle of

the prosthesis, in some cases as early as one month after the initial surgery (De Haan et al. 2008b) and is one of the most common reasons for early failure (United Kingdom. The National Health Service, National Joint Registry for England and Wales. 2007). A biomechanical investigation relating orientation of the femoral component to the maximum stresses in the femoral head and neck, revealed that early failure was 6.1 times greater in patients with a stem-shaft angle of $\leq 130^\circ$ (Beaule et al. 2004a). Another patient study also revealed that premature failure of the femoral component is six times more likely if CCD angle is less than 130° , meaning that a more valgus CCD angle is preferable (Williams et al. 2009).

If the inclination angle of the acetabular cup is too small, superior impingement and medial edge loading may occur, whilst if the angle is too large this may lead to superior edge loading (Grammatopoulos et al. 2010). If the cup anteversion angle is too small this may lead to anterior impingement and posterior edge loading in flexion, whilst if the angle is too large posterior impingement or anterior edge loading may occur during extension (Grammatopoulos et al. 2010).

Component misalignment can lead to increased wear and metal ion release through rim contact, impingement, acetabular component deformation, point loading and reduced thickness of the lubricating film (Langton et al. 2008). The articulating surfaces of most hip resurfacing components on the market are manufactured from a CoCr alloy. High CoCr metal ion levels, both locally in the joint capsule or in circulation, are associated with a range of negative effects. In some cases the release of metal ions has been linked to aseptic loosening of the prosthesis and subsequent failure, formation of pseudo-tumours and renal complications (De Haan et al. 2008b; Pandit et al. 2008). The incidence of pseudo-tumours is four times lower when acetabular cups are placed within the limits of $45^\circ \pm 10^\circ$ inclination and $20^\circ \pm 10^\circ$ anteversion on post-operative radiographs, compared to outside these limits (Grammatopoulos et al. 2010). There is also a possibility that chronic exposure to these metal ions may have a carcinogenic effect, cause hypersensitivity (Willert et al. 2005), and in the case of pregnant women may

affect the unborn foetus (Ziaee et al. 2007). Amstutz et al. (2004) report unusual lymphocytic aggregates found in the tissues surrounding a third of failed hip resurfacing components. It has been suggested that unexplained hip pain in patients with hip resurfacing prostheses can furthermore be linked to high levels of CoCr metal ions in the blood (Hart et al. 2009b).

It is thus imperative to keep the rate of metal ion release as low as possible, to improve the life cycle of the prosthesis and prevent pathological conditions developing in the patient. Langton et al. (2008) suggest focussing on optimising acetabular orientation to reduce metal ion release. If surgeons were able to insert the prosthesis in the ideal position with the help of a pre-surgical software tool, this may reduce the chance of misalignment and subsequent excessive wear and failure.

2.5.7. Computer models used to investigate hip RoM for hip resurfacing

There are numerous ways to investigate hip RoM using 3D computer models based on CT scans of the upper femur and pelvis. The accuracy of 3D surface model generation using CT scans has been shown to be within 1 mm, whilst ± 2 mm is generally accepted as adequate for surgical purposes (Barrett et al. 2007).

The key difference between these investigations however and this study is that the objective of this project was to investigate the use of an existing CAD software package to generate a 3D computer model of the pelvis and upper femur, for use by a surgeon in pre-surgical planning, rather than investigating precise angular measurements of hip RoM.

However, several of these studies validate the methods employed in this project. For example, the research conducted by Vendittoli et al. (2007) and Kluess et al. (2008) are two investigations that employ similar principles to analyse hip RoM to those described in this study.

Kluess et al. (2008) investigated hip RoM using a 3D CAD model, based on CT scans of the pelvis and upper femur from three healthy patients. The CT scans were reconstructed to produce stereolithography (STL) files using AMIRA¹ software. Following this, these files were converted to NURBS (non-uniform rational B-spline surfaces) using the software Geomagic Studio². Hip RoM analysis and virtual insertion of the prosthetic components were performed using Pro/Engineer³. The femoral component was positioned according to the resection level, which was defined as the distance between the centre of rotation of the femoral component and the distal opening edge. The following three different leg movements were analysed:

- maximum flexion
- maximum internal rotation at 90° flexion
- maximum external rotation at 15° adduction and 10° extension

Vendittoli et al. (2007) made use of pre-operative pelvic and upper femoral CT scans from a patient presenting with end stage osteoarthritis of the left hip. A hybrid Durom⁴ hip resurfacing system was used for the arthroplasty. CT scans were produced using multi-slice CT acquisition with a GE LightSpeed VCT⁵ at 120 Kvp. The images were encoded in Digital Imaging and Communications in Medicine (DICOM) format with a slice thickness of 1.25 mm, with no overlap. CAD Catia software, v5⁶ was used to create the 3D computer model as well as conduct hip RoM analysis. Simulations between the femur and pelvis were performed with only one degree of freedom. The following four movement arcs were investigated:

- flexion/extension in neutral abduction and rotation
- adduction/abduction in 0° flexion and neutral rotation
- internal/external rotation in 0° flexion
- internal/external rotation in 90° flexion

¹ AMIRA – Mercury Computer Systems, Chelmsford, MA

² Geomagic Studio – Raindrop Geomagic, Research Triangle Park, NC

³ Pro/ENGINEER – Parametric Technology Corporation, Needham, MA

⁴ Durom Hip Resurfacing – Zimmer, Warsaw, IL, USA

⁵ General Electric – GE Health Care Technologies, Waukesha, Wisconsin USA

⁶ Catia – Dassault Systems, Suresnes Cedex, France

Various femoral component variables were investigated in relation to RoM, these included:

- femoral component size
- varus/valgus orientation
- anteversion/retroversion
- anterior/posterior translation (perpendicular to the axis of the femoral component stem)

The two acetabular component variables analysed were seating depth and anteversion/retroversion of the component.

2.5.8. Computer assisted hip resurfacing

Recent studies suggest that computer assisted surgery (CAS) can help to improve the accuracy of implant positioning and therefore reduce the revision rate for hip resurfacing (Kluge 2009) and occurrence of pathological conditions. CAS may also help to reduce the incision size, therefore making the procedure less invasive (Krüger et al. 2007).

There are two main technologies available on the market, image-guided (CT and fluoroscopy) and imageless navigation systems. CT guided systems make use of pre-operative 3D CT scans to generate a 3D surface model based on the patient's upper femur and pelvis, which facilitates a clear understanding of the patient's bony anatomy. Some of these systems allow the surgeon to virtually insert the prosthetic components, to help select the ideal component size and orientation, based on RoM analysis (Barrett et al. 2007). During the surgery, 3D surface model registration is achieved via a selection of points on the exposed surfaces of the bone. The navigation system then assists in performing the surgery according to the pre-operative plan. Post-operative CT scans can be used to evaluate the outcome of the arthroplasty, in terms of implant position, by superimposing the image over the original pre-operative model (Barrett et al. 2007). The fluoroscopy guided system makes use of pre-operative AP radiographs to generate an image of

the patient's anatomy, which is then used during the surgery to assist in orientating the components, precluding the need for further exposure to x-rays.

The imageless navigation system is based on accurate mechanical registration through use of point to surface acquisition by the surgeon during the operation to generate an animated bone model, which is then used to guide the surgeon in placing the prosthetic components. The imageless CAS system requires a more extensive surgical approach compared to that of the limited access procedures used in fluoroscopy or CT based systems (Kluge 2009).

Some CAS systems are adaptable to be used with a range of hip resurfacing components, whilst other CAS systems are specifically designed to handle only one manufacturer's products.

The outcome of one study showed that patients who were operated on using CAS presented with better acetabular cup position, especially for cup anteversion, compared to those who underwent a standard hip resurfacing procedure (Krüger et al. 2007). Other studies have revealed that CAS is accurate and reliable for component placement in hip resurfacing arthroplasties (Barrett et al. 2007), even independent of surgeon experience (Romanowski and Swank 2008; Seyler et al. 2008). With the aid of CAS surgeons become familiar with hip resurfacing procedures more quickly, and it improves the surgeon's ability to perform the procedure safely (Seyler et al. 2008).

3. Materials, Equipment and Methodology

The main objective of this study was to investigate the use of an existing CAD software package to generate a 3D computer model of the pelvis and upper femur, for use by a surgeon in pre-surgical planning. This was in order to identify the ideal prosthesis size and position, based on hip RoM analysis, and specify the optimal operative angles in which to place the components during hip resurfacing surgery. Further, this study had the purpose of providing groundwork for future development of a user-friendly software program for pre-surgical planning of hip resurfacing.

The secondary objectives of the study were to investigate incorporating various surgeon requirements; and to investigate the possibility of incorporating new patient CT scans, and manipulate certain anatomical variables to test different placement scenarios.

The 3D CAD program SolidWorks¹ was used as a platform in this investigation to design and build the 3D anatomical model. This software is currently utilized by many sectors within the engineering industry, as well as tertiary institutions, but does not have any medical implant applications.

In this chapter the process of how the individual components were designed is laid out, as well as the intended use of each of the components.

3.1. Initial testing and pre-processing

The initial investigation was based on using MRI images to create a 3D model of the hip, these images are commonly used by surgeons to assess and diagnose hip abnormalities. This method would have been favourable due to the fact that patient would not require a CT scan, thus reducing costs in addition to preventing further exposure to x-rays. The process of 3D

¹ SolidWorks – Dassault Systems SolidWorks Corp., Concord, USA

rendering of the MRI images into STL files, however, proved to be subjective (as the bone to soft tissue interface was not clearly defined) and especially time-consuming. Therefore, it was decided not to pursue this method and adopt the use of CT images instead for 3D model generation.

High definition 3D axial CT scans of a healthy patient, showing the full pelvis and upper region of the femur, were obtained from radiologists¹. The CT images were produced from a multi-slice CT acquisition with a Siemens Sensation Cardiac 64² at 120 Kvp. The images were encoded in DICOM format with a slice thickness of 1 mm and no overlap.

The 3D rendering process of converting the CT scans to STL files was performed at Physical 3D Modelling³, using Mimics⁴ software. The files were divided into separate components, namely left and right upper femur and the pelvis (Table 3.1).

Table 3.1 – Table showing properties of the original STL after 3D rendering.

Part	No. of triangulated surfaces	File size (MB)
Left femur	108110	5.3
Right femur	111059	5.4
Pelvis	847322	41.4

Due to the complex anatomy of the pelvis the STL file of the entire pelvis produced during rendering from the CT scan was especially large (approximately 45 MB). This was due to the vast number of triangulated surfaces contained within the surface image. This file simply contained too much data to convert directly to a solid 3D model with the CAD program SolidWorks using a regular desktop personal computer. Initial runs conducted by MECAD⁵ took many hours and were unsuccessful.

¹Morton & Partners Radiologists – St Georges Mall, Cape Town, South Africa

²Siemens – Global Siemens Healthcare Headquarters, Henkestrasse, Erlangen, Germany

³Physical 3D Modelling CC – Stellenbosch, South Africa

⁴Mimics – Materialise, Leuven, Belgium

⁵MECAD Systems Pty. Ltd – Cape Town, South Africa

For this reason, only the acetabular section of the pelvis was converted to a solid model that could be manipulated. In terms of hip arthroplasties this portion of the pelvis is of greatest concern to surgeons.

STL manipulation was performed by MECAD using Blender¹ software with an STL add-on enabled. The pelvic STL file was imported into Blender and the section around the acetabulum selected and copied to create a new file. Following this, the gaps were filled along the cutting planes and where any holes had appeared on the outer surface. Foreign data passed down through the rendering stage in Mimics was removed from the STL image. This foreign data included free standing edges, but mainly consisted of surfaces contained within the core of the image (surfaces representing the inside of the bone). This data was deemed irrelevant as the solid 3D model was to be based on the outer most surface of the bone. By removing this data the size of the STL file was significantly reduced. Additionally, the STL files of the left and right femur were imported into Blender to fill any holes on the outer surface and to reduce the file size before exporting into SolidWorks.

The section of acetabulum removed from the full STL image of the pelvis was sliced horizontally along the ilium and the ischium bones, approximately 30 mm above and below the rim of the left acetabular socket, as well as vertically through the pubis (Figure 3.1).

Figure 3.2 gives a general overview of the equipment and software programs utilized in the initial set-up and pre-processing of the CT scans before being imported into SolidWorks.

¹ Blender Institute BV – Amsterdam, the Netherlands

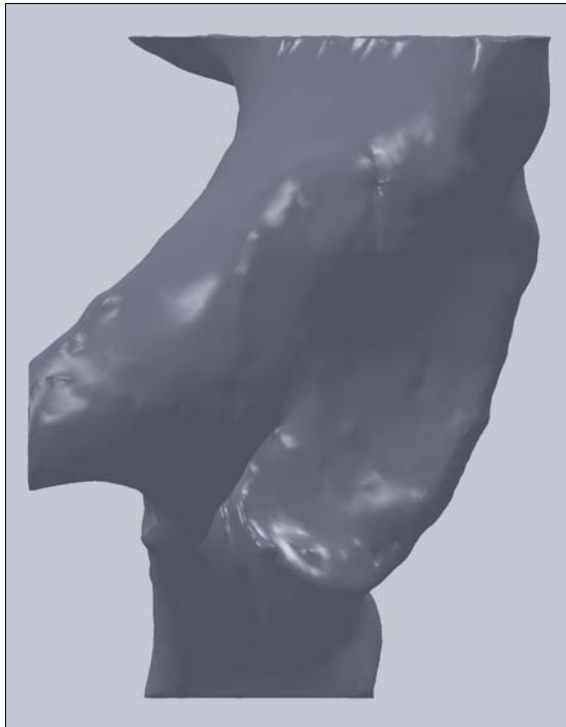


Figure 3.1 – Showing the section of the left acetabulum removed from the whole pelvis STL file and converted into a solid 3D model.

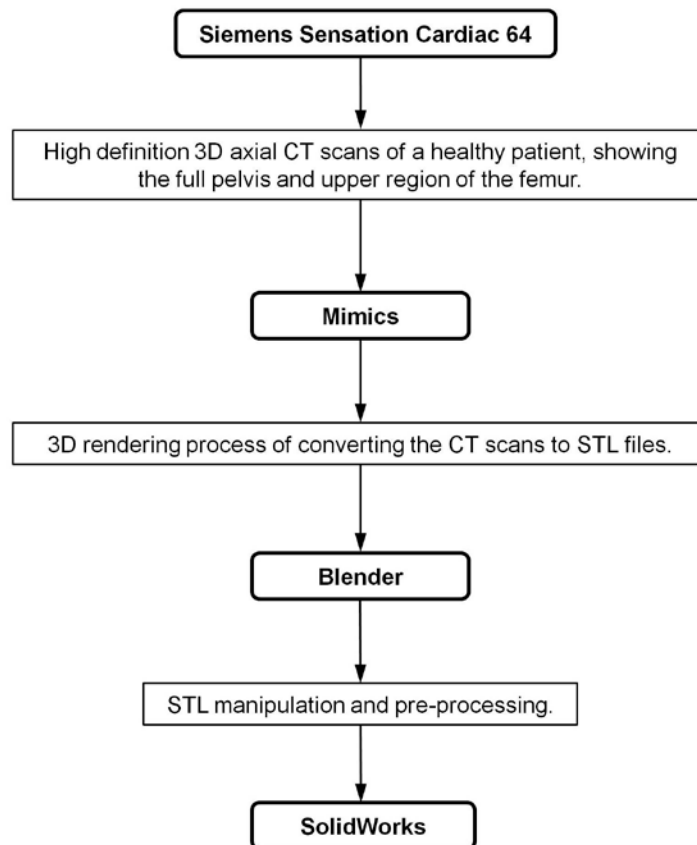


Figure 3.2 – Flow chart illustrating how different equipment and software programs are used during the initial set-up stages and pre-processing.

3.2. Creating the solid 3D models in SolidWorks

Following the pre-processing, the STLs were imported into SolidWorks and solid 3D models were created using the mesh surface wizard set to auto-creation. The scan to 3D tool was enabled and the file was opened as a mesh type, as opposed to opening it as an STL. This process was repeated for the pelvis and both femurs.

3.3. Setting up the anatomical reference planes

Although it was decided to convert only a section of the pelvis (Figure 3.1) to a solid 3D model, the full pelvis was still required in order to set up and define the anatomical reference planes. The STL file of the full pelvis was imported into SolidWorks as a mesh file.

The first and most critical anatomical reference plane defined on the 3D pelvic image was the APP. The APP was defined as a plane passing through the left and right ASIS points, and the centre of the antero-superior surface of the pubic spines (Figure 3.3). The mid-sagittal plane was defined as a vertical plane passing through the centre of the pubic symphysis and the tip of the coccyx (Figure 3.3). Subsequently the transverse plane was defined as a plane perpendicular to the mid-sagittal plane.

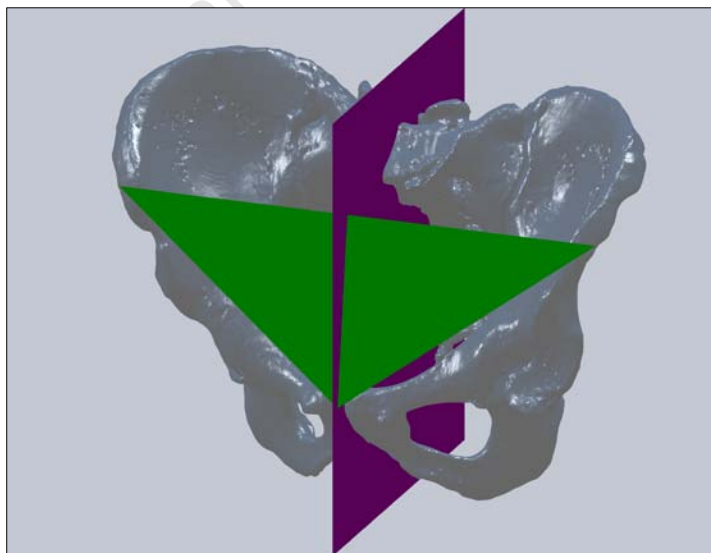


Figure 3.3 – Image of the full pelvis showing the APP represented by the green triangle and the mid-sagittal plane represented by the purple rectangle.

When viewed in the mid-sagittal plane, it was possible to identify and measure the degree of pelvic tilt. The pelvic image generated from the test subject required an anti-clockwise rotation of approximately 8° to bring the APP into the vertical position (Figure 3.4).

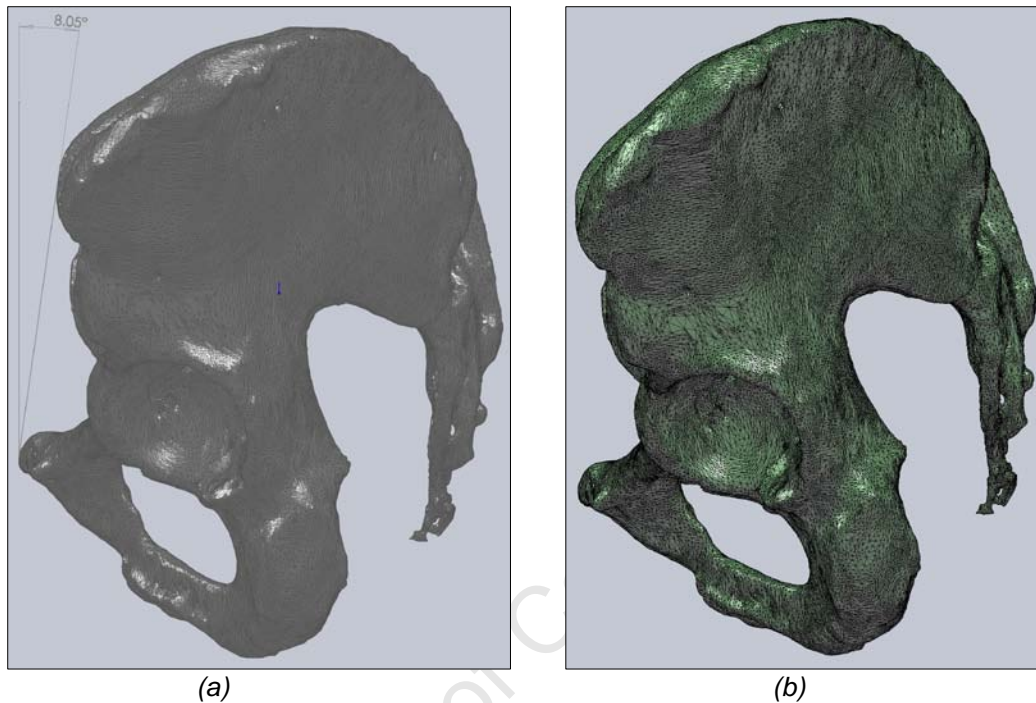


Figure 3.4 – (a) Showing the full pelvis with the APP before adjustment for pelvic tilt and (b) after.

3.4. Importing the BHR component files into SolidWorks

The hip resurfacing components used in this investigation (Figure 3.5) were from the BHR¹ system and the component properties are listed in (Table 3.2) below (Campbell et al. 2006):

¹ BHR System – Smith & Nephew Orthopaedics Ltd, Warwick, UK

Table 3.2 – Showing BHR component characteristics.

Bearing Material	CoCr Alloy (as cast)
Acetabular Component Shape	Hemisphere
Shell Surface	Co-Cr beads (0.9–1.3 mm) cast-in + HA
Shell Thickness (mm)	Rim=3, Dome=6
Femoral Size Increments (mm)	4
Desired Cement Mantle (mm)	0
Femoral Stem	Tapered



Figure 3.5 – An image of a BHR femoral head and acetabular component (Daniel et al. 2004).

The BHR hip resurfacing component files were supplied in an Initial Graphics Exchange Specification (IGES) format from the manufacturer and were divided into standard sizes and non-standard sizes for both the acetabular cups and femoral heads. The IGES files were compatible with SolidWorks, therefore the conversion process was uncomplicated. By converting the BHR components into SolidWorks part files, virtual insertion into the 3D model was possible. Certain reference points and planes were created in the acetabular cup and femoral head files to facilitate how these components would be located and orientated within the 3D model.

During the conversion of the acetabular cups into SolidWorks files, some additional curves and surfaces were generated. These were deemed unnecessary for this investigation and therefore deleted. A reference point

was created at the centre of the cup circle, located in a plane parallel with the cup edge or rim (Figure 3.6b). No further reference points or planes were necessary.

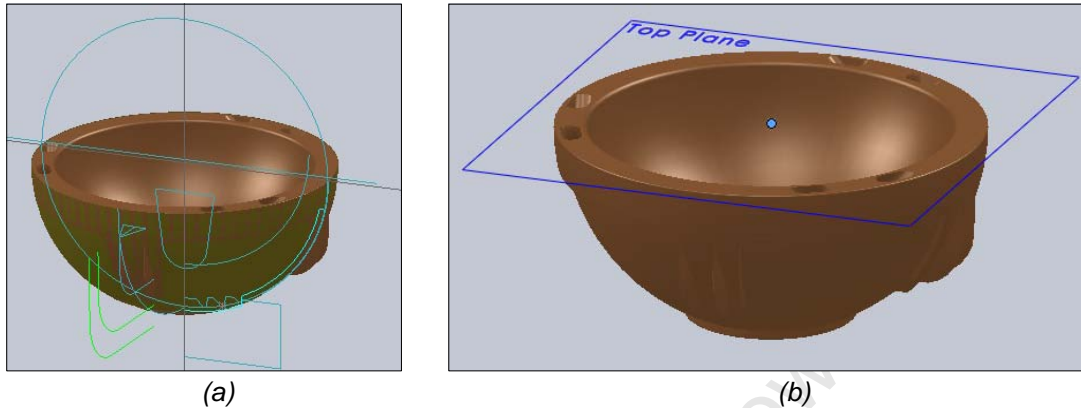


Figure 3.6 – (a) Showing the acetabular cup before modification and (b) after.

During the conversion of the femoral head components, similar additional curves and surfaces were generated; these were also removed. The central axis (drilling axis) of the femoral stem was defined as an axis of intersection between two planes equally and perpendicularly bisecting the component. This drilling axis was used to locate and orientate the femoral stem within the femoral neck. The centre of rotation was defined as an intersecting point between the centre of a circle constructed around the circumference of the femoral head and the drilling axis (Figure 3.7b). This point was used to specify where along the drilling axis the component was placed, i.e. the resection depth into the bone along the femoral neck. Additionally a reference plane was created passing through the centre of rotation and perpendicular to the drilling axis, to further facilitate accurate placement and orientation within the femoral neck bone.

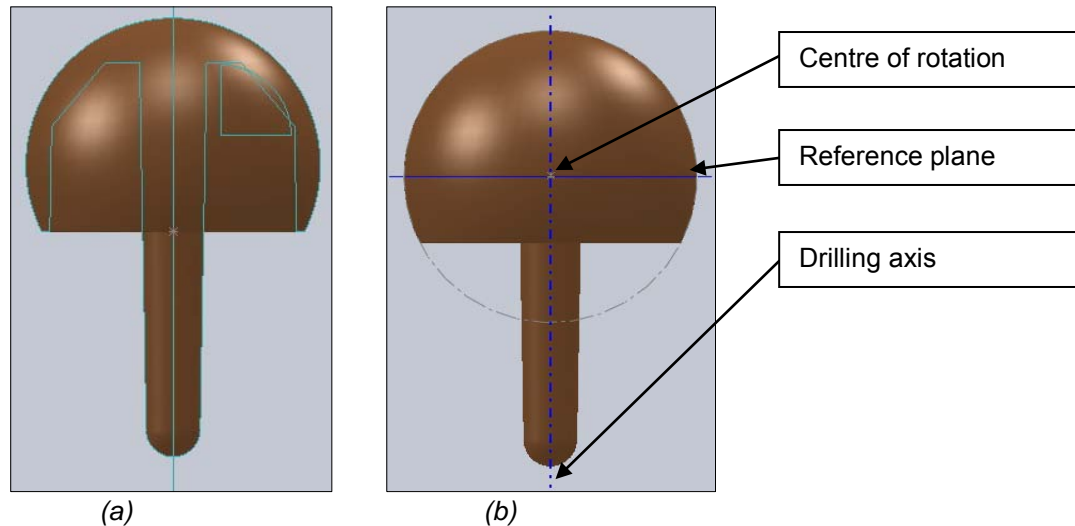


Figure 3.7 - Showing the femoral component before (a) and after (b) data removal, including the new centre of rotation point, reference plane and drilling axis.

3.5. Designing the artificial femur

The STL files produced from 3D rendering using Mimics software are merely 3D images, and the data contained in the file cannot be manipulated in any way. In order to make the hip model patient-specific the surgeon would need to be able to modify certain anatomical variables. Additionally, to assist virtual insertion of the prosthetic components, reference points and planes need to be specified. This facilitates accurate placement of the components for each individual patient. This task cannot be achieved using STL files. Therefore, an artificial femur was designed in SolidWorks using standard CAD drawing techniques. In specifying key anatomical dimensions, the artificial femur was manipulated to be representative of a patient's anatomy and accurate hip RoM analysis was performed. A list of these dimensions and variables can be seen in Table 3.3.

Using an add-on package within SolidWorks called DriveWorks¹, input forms were created to allow the surgeon to specify all the critical dimensions in order to generate a representative artificial femur. Based on the specified dimensions, this rapidly generates a new component file for each completed

¹ DriveWorks – DriveWorks Ltd, Cheshire, United Kingdom

input form. This permits the surgeon to effortlessly test various anatomical configurations. Following this exercise, the STL of the actual patient's upper femur can be imported into the program and superimposed over the artificial femur to ensure it is as accurate as possible.

The artificial femur consists of two cylinders representing the femoral shaft and femoral neck, with a sphere representing the femoral head. In order to make the design as close a representation as possible of the natural anatomy of the upper femur, numerous dimensions, reference planes and points were constructed. An example of the input form created to generate the artificial femur can be seen in Appendix C and the input variables used are listed in Table 3.3.

The default values listed in Table 3.3 were measured directly from the test patient and are representative of a healthy adult male. Default values were used in the input form to reduce the number of inputs required by the surgeon and therefore save time, as he or she may not wish to change or adjust each variable. The input values needed to complete this form can be measured or estimated from an AP radiograph, or measured directly in the CAD program. Dimension inputs are in millimetres and angular inputs are in degrees.

Table 3.3 – Default values used in the DriveWorks input form to create the artificial femur.

Patient Name	Default
Femoral Length	80
Femoral Diameter	35
CCD Angle	135
Q Angle	12
Femoral neck to femoral head centre	60
Femoral neck diameter	35
Femoral head diameter	50
Resection level	0.0001
CCD to tip of greater trochanter	30
Femoral head offset angle	0
Femoral head offset distance	0.0001
Inclination angle	45
Anteversion angle	0

The input form for the artificial femur requires the following entries (Table 3.3):

- **Patient Name** – The surgeon is required to input the patient's name. This information is also used as part of the file name.
- **Femoral Length** – This dimension specifies the length of the patient's upper femur, from the lower extremity in the CT scan to the tip of the greater trochanter (Figure 3.8).
- **Femoral diameter** – This is the diameter of the femoral shaft (Figure 3.8).

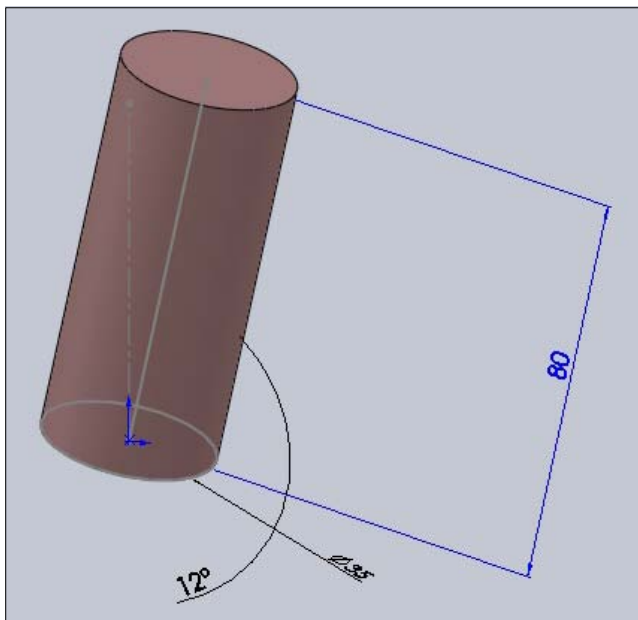


Figure 3.8 – Showing the femoral length set at 80 mm and the femoral diameter set at 35 mm.

- **CCD angle** – This obtuse angle is measured between the centre of the femoral shaft and the centre of the femoral neck axis (Figure 3.9).

- **Q angle** – This angle is formed by a line drawn from the ASIS to the centre of the patella and a second line drawn from centre of the patella to the tibial tuberosity (Figure 3.9).
- **Femoral neck to femoral head centre** – This dimension specifies the length of the femoral neck, the measurement is taken from the centre of the femoral shaft to the centre of the femoral head (Figure 3.9).
- **Femoral neck diameter** – This specifies the diameter of the femoral neck.
- **Femoral head diameter** – This is the diameter of the spherical femoral head.

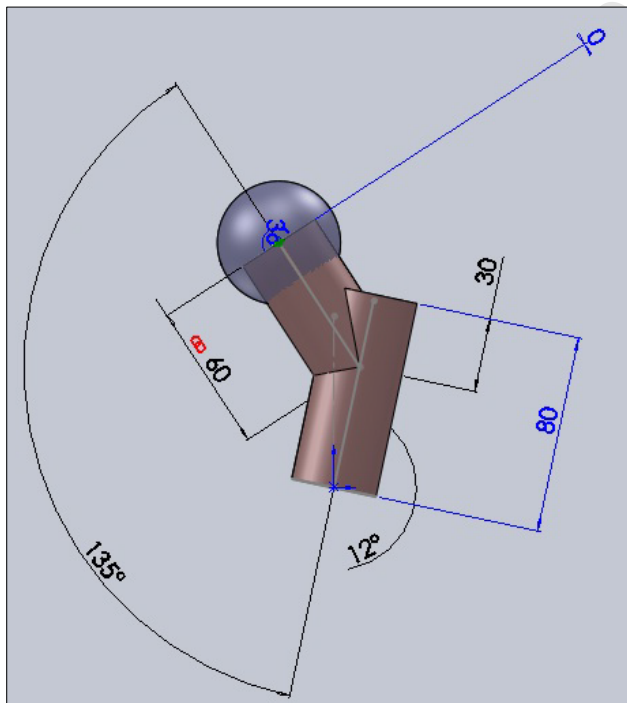


Figure 3.9 – Showing the CCD angle set at 135°, Q angle set at 12°, femoral neck to femoral head centre at 60 mm, femoral head diameter of 50 mm, femoral neck diameter of 35 mm and CDD to tip of greater trochanter at 30 mm.

- **Resection level** – This dimension allows the surgeon to set the depth into the femoral neck bone at which the femoral component will be

located. The minimum value was set at 0.0001 mm, as DriveWorks cannot recognise a zero dimension. For illustrative purposes, in Figure 3.10 it was set to 10 mm.

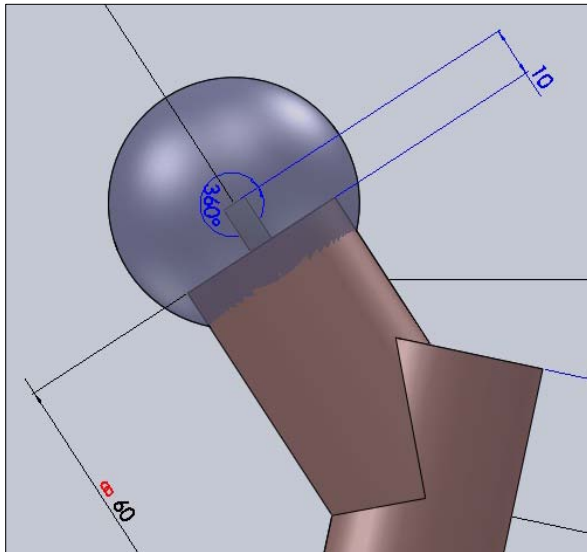


Figure 3.10 – Showing the resection level set at 10 mm away from the femoral neck edge.

- **CCD to tip of greater trochanter** – This dimensional input is used to set the height of the greater trochanter. It is measured from the point where the CCD intersects the centre of the femoral shaft, with a default value of 30 mm (Figure 3.9).
- **Femoral head offset angle and Femoral head offset distance** – These two dimensions are used in conjunction with one another to locate the femoral component inside the femoral neck. This location point is specified relative central axis of the femoral neck and is referred to as the centre of rotation. The femoral head offset angle specifies in which quadrant of the transverse femoral neck cross section the point is located. In Figure 3.11, the femoral head centre point is located in the first quadrant, the angular input being 45° measured anti-clockwise from the horizontal. The femoral head offset distance is the distance away from the central axis of the femoral neck cross-section. In Figure 3.11, the femoral head centre point is located 10 mm away from the central axis of the neck. The femoral head offset distance is specified using a circle, therefore this dimension is represented as a diameter; 20 mm in Figure

3.11. A rule was created in the input form to take this into account, and the surgeon therefore only needs to specify the distance.

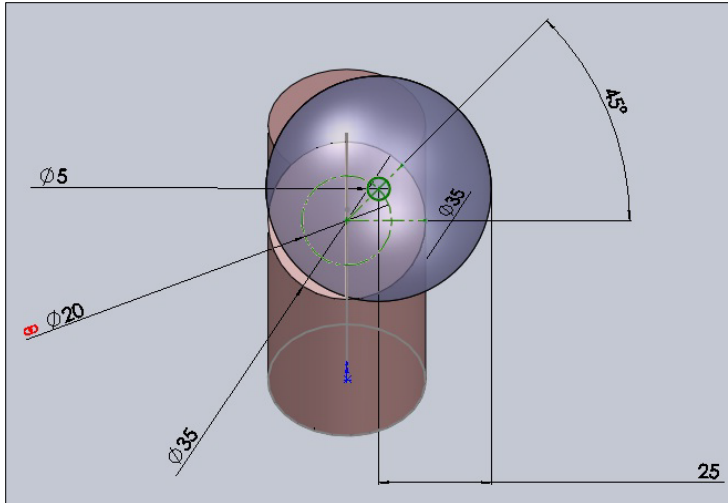


Figure 3.11 – Showing the femoral head offset angle set to 45 °and the femoral head offset distance set to 10mm.

- **Stem inclination angle and stem anteversion angle** – these two angles specify the orientation of the prosthetic femoral stem inside the femoral neck. As can be seen in Figure 3.12, these two angular definitions specify two planes, the inclination and anteversion planes. The intersection of these two planes forms an axis, which is referred to as the drilling axis. By aligning this drilling axis with the one specified for the prosthetic femoral head, it ensures accurate location and orientation.

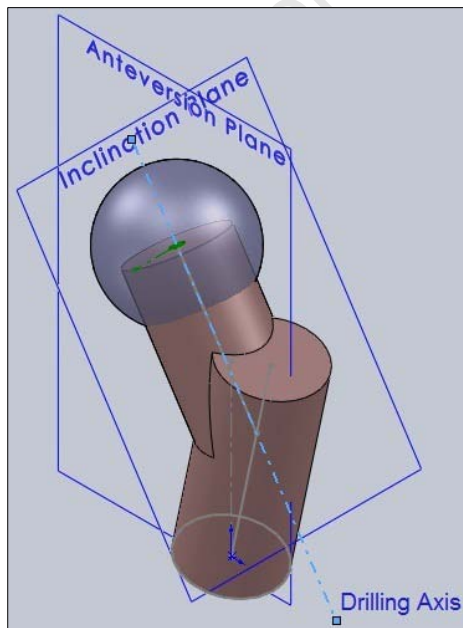


Figure 3.12 – Showing the inclination and anteversion planes, with the intersecting axis referred to as the drilling axis.

Rules were created for the DriveWorks input forms to manipulate how the data affected the output file. Designing the left artificial femur required four rules (i to iv), which were used to correctly produce the desired output file. These rules can be tailored to suit the surgeon's requirements. An example of how these rules were incorporated into the input forms can be seen in Appendix C.

- (i) **File name** – this rule specified the output file name and contained the patient's name, as well as the diameter of the femoral head for ease of reference.
- (ii) **Femoral head diameter** – this rule divided the surgeon input value by two, converting it into a radius. This was necessary as the femoral head was specified as a radius in the design file.
- (iii) **Femoral head offset distance** – this dimension was specified in the design file by the diameter of a circle, therefore the surgeon input value is multiplied by a factor of two. The input requires the surgeon to specify a distance away from the centre of the femoral neck (See above and Figure 3.11).
- (iv) **Inclination angle** – the Q angle needs to be considered when specifying the stem inclination angle; therefore this rule automatically added the Q angle to the input value for the inclination angle to give the correct value.

3.6. Setting up the left acetabular socket for prosthetic placement

This process involved utilising the section of the left acetabulum that was converted from a STL file to a solid 3D model (Figure 3.1). Reference planes and points were created in order to facilitate the placement of the prosthetic acetabular cup. Following this, DriveWorks was used to create an input form that allows the surgeon to specify the cup location and orientation within the

acetabular socket for accurate hip RoM analysis. These are the steps that were taken:

Step 1 – The acetabular plane was defined by selecting three points on the rim of the socket, on the outer-most bony prominences. The first point was located anteriorly, the second posteriorly, and the third superiorly. These were named vertex 1, 2 & 3 respectively (Figure 3.13). This plane is referred to as the acetabular reference plane, as it is the anatomical acetabular plane for our test patient.

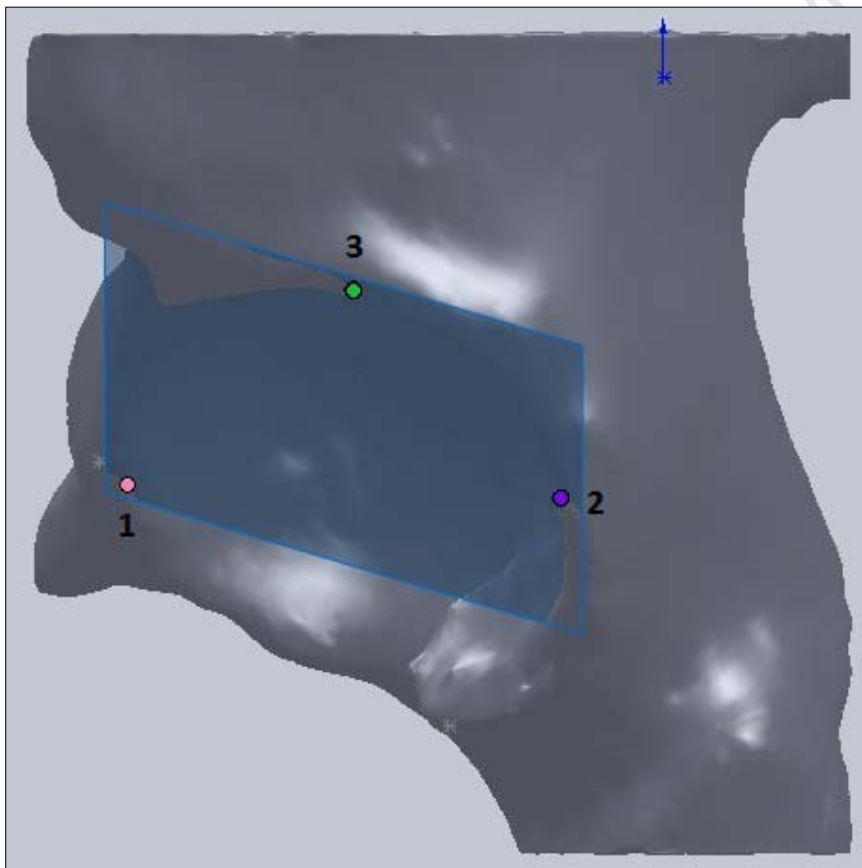


Figure 3.13 – Showing a side view of the left acetabular socket indicating the three vertex points on the acetabular rim, as well as the acetabular reference plane passing through them. Labels 1 to 3, indicate the vertex point numbers.

Step 2 – To locate the centre point of the acetabulum on the acetabular reference plane, a circle was constructed through the three vertex points (Figure 3.14). Connecting the centre point of this rim circle to the centre of the prosthetic cup permitted the depth of the cup to be set inside the acetabular socket. Subsequently, by aligning the acetabular reference plane with a plane parallel to the rim of the acetabular cup, the cup orientation was fixed.

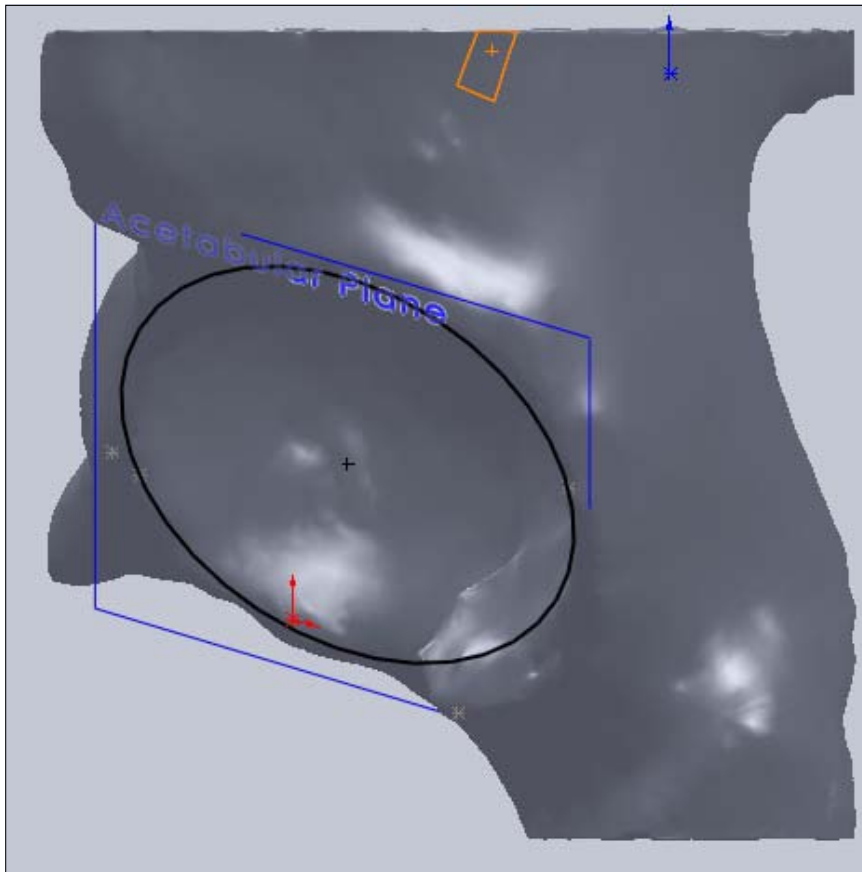


Figure 3.14 – Showing the acetabular rim circle drawn on the acetabular reference plane and the centre point of the circle.

Step 3 – The next step in the process was to set up and define a new plane that would permit the surgeon to specify the location and orientation of the acetabular cup. This was accomplished by creating reference axes normal to the acetabular reference plane at each vertex point. These reference axes were named according to the associated vertex point (Figure 3.15).

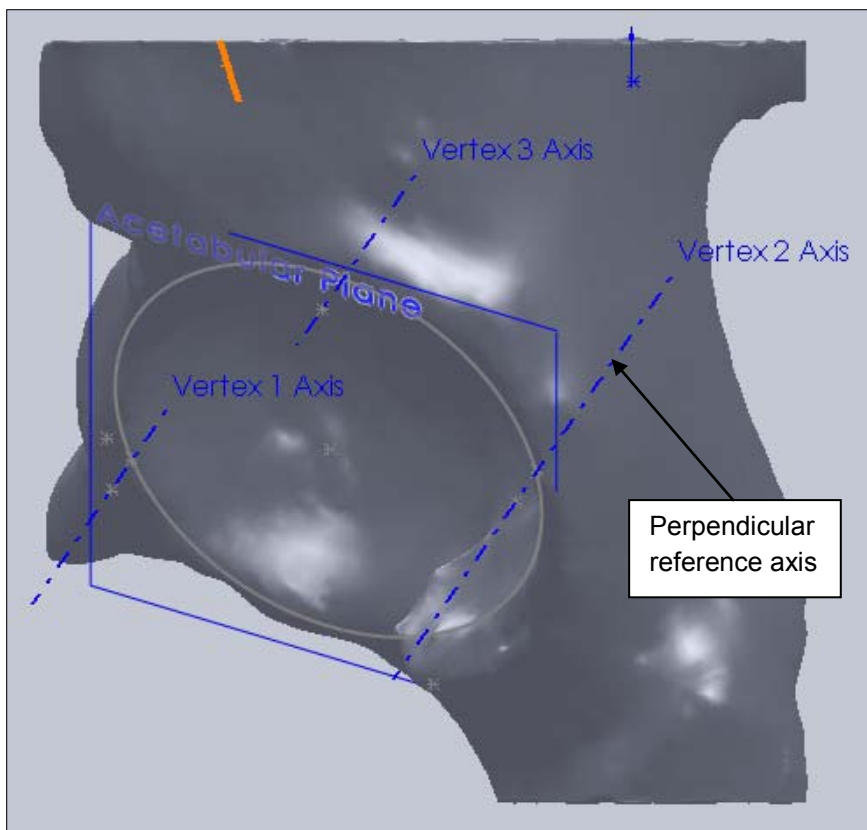


Figure 3.15 – Showing the three reference axes passing through vertex points 1, 2 and 3.

Step 4 – Along these reference axes, two reference points were placed at specified distances away from each vertex point. One point was inserted 6 mm away from the vertex point in a direction moving away from the bone; this point was set to be fixed in that position. For this investigation it was decided to set the maximum distance away from the acetabular rim at 6 mm (Figure 3.16). Another point was placed 10 mm away from the vertex point, but in a direction going into the bone. The maximum distance into the bone was set at 10 mm. This point is referred to as the adjustable point (Figure 3.16). The dimension between the fixed point and the adjustable point was specified using the input forms.

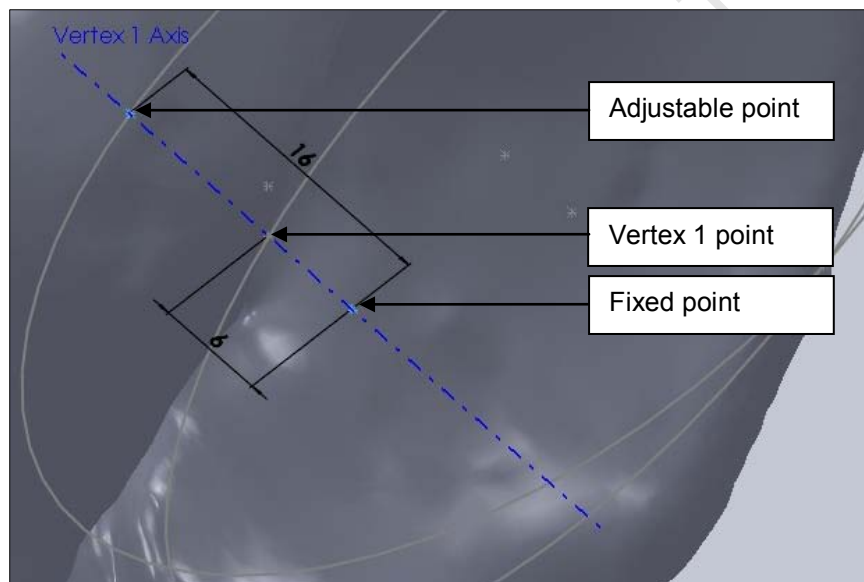


Figure 3.16 – Is a zoomed-in section of the acetabular socket showing the adjustable point, fixed point and vertex 1 point along the vertex 1 axis.

Step 5 – Using the three new adjustable points at the respective vertices, a new plane was created in the same way described in Step 1 above. This plane is referred to as the acetabular movement plane (Figure 3.17). Using these same three points a new circle was constructed to find the new centre point lying on the acetabular movement plane. As described in Step 2, the acetabular cup is connected to this centre point and the cup edge aligned with the new acetabular movement plane. Therefore, by adjusting the acetabular movement plane the location and orientation of the acetabular cup can be specified. Figure 3.18 illustrates the effect of a 10 mm offset of the acetabular movement plane into the bone, from vertex point no. 1, relative to the acetabular reference plane.

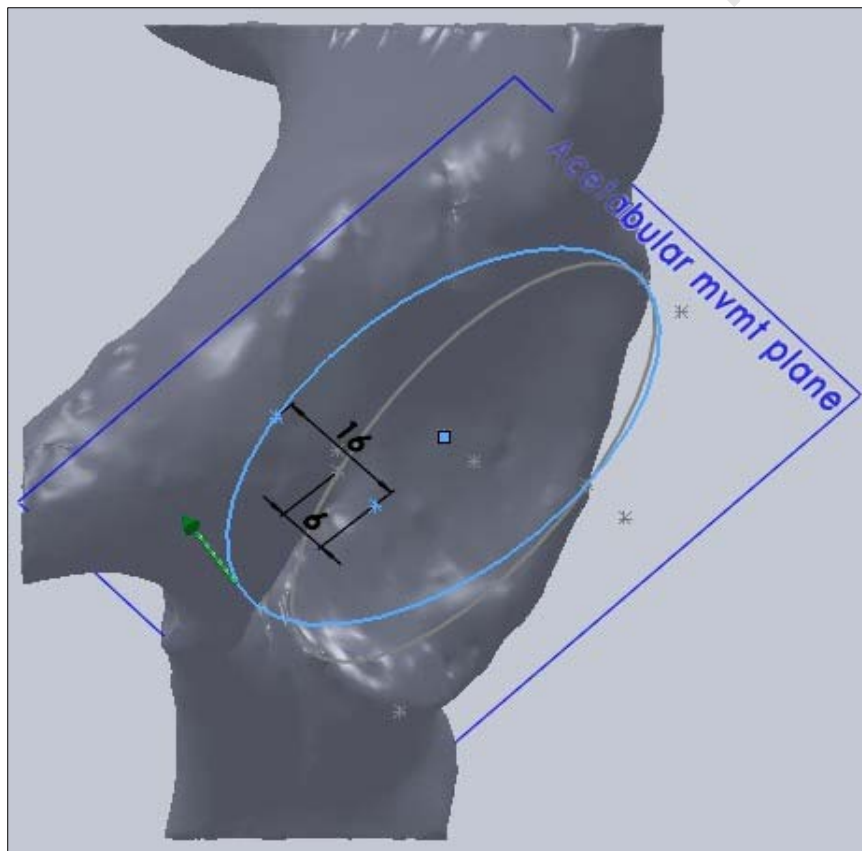


Figure 3.17 – Showing the new acetabular movement plane passing through the three adjustable points at vertices 1, 2 and 3, including, the new construction circle and centre point.

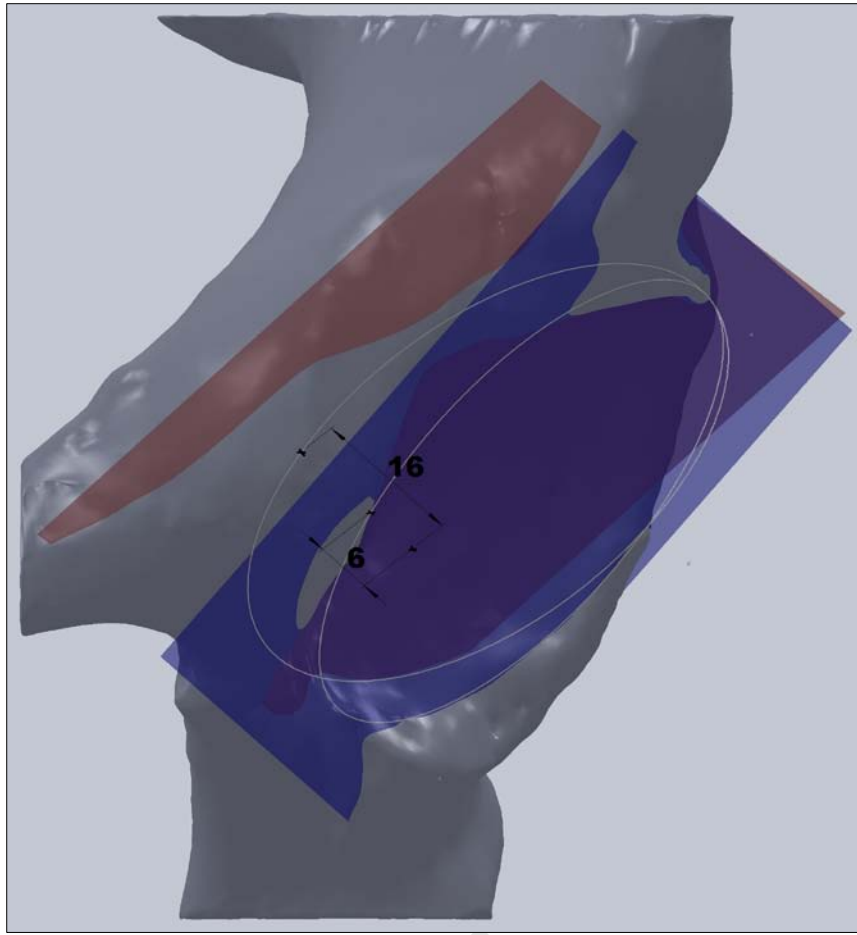


Figure 3.18 – Illustrates the different positions of the two acetabular planes, the blue plane representing the anatomical or reference plane and the red plane representing the movement plane.

To enable the surgeon to specify the location and orientation of the acetabular cup, an input form was created with variables specified in Table 3.4 below.

Table 3.4 – Table showing the parameters used for the input for for DriveWorks.

Patient Name	
Anterior Offset (Vertex 1)	-10 to + 6 (in 2 mm increments)
Posterior Offset (Vertex 2)	-10 to + 6 (in 2 mm increments)
Superior Offset (Vertex 3)	-10 to + 6 (in 2 mm increments)

The input form was set up in such a way that the input variables can be selected from drop-down lists. Anterior offset is used to specify the location of the acetabular cup relative to vertex 1. Posterior offset is used for vertex 2 and superior offset for vertex 3. Negative values move the cup into the bone

and positive values move it away. As with the artificial femur, a separate file is produced containing the patient's name and the offset value at each vertex location.

Using this input form, the dimension from the fixed point to the adjustable point is specified, this in turn modifies the location and orientation of the acetabular movement plane and cup centre point. A rule was designed so that for an input value of (0, 0, 0) the movement plane is parallel with the acetabular reference plane, thus allowing the surgeon to place the acetabular cup at this anatomical position. An image of the input form used to locate and orientate the acetabular cup can be seen in Appendix C.

The rules within DriveWorks do not allow for negative values to be associated with dimensions; therefore a series of "if" statements were created for each offset location that would allow for negative inputs. Refer to Equation 3.1 below for the Posterior Offset rule. As a default, a zero offset is assigned when +6 mm is selected in the input form.

=IF(PosteriorOffset = -10 , 16 , IF(PosteriorOffset = -8 , 14 , IF(PosteriorOffset = -6 , 12 , IF(PosteriorOffset = -4 , 10 , IF(PosteriorOffset = -2 , 8 , IF(PosteriorOffset = 0 , 6 , IF(PosteriorOffset = 2 , 4 , IF(PosteriorOffset = 4 , 2 ,))))))))

Equation 3.1 – Showing the "if" statement used in DriveWorks to specify the offset location of the movement plane at the Posterior Offset point or vertex point number 2.

As noted above, the fixed points at all 3 vertices lie 6 mm away from the bony acetabular rim and the acetabular reference plane (Figure 3.16). Therefore, Equation 3.1 converts an input of (0, 0, 0) to (6, 6, 6) and the movement plane now lies parallel to the acetabular reference plane. Similarly an input value of (-2, -4, +4) is converted to (8, 10, 2), thereby specifying the respective dimension from each fixed point and subsequently the location and orientation of the acetabular movement plane. An overview of how Equation 3.1 was applied in DriveWorks can be seen in Figure 3.19.

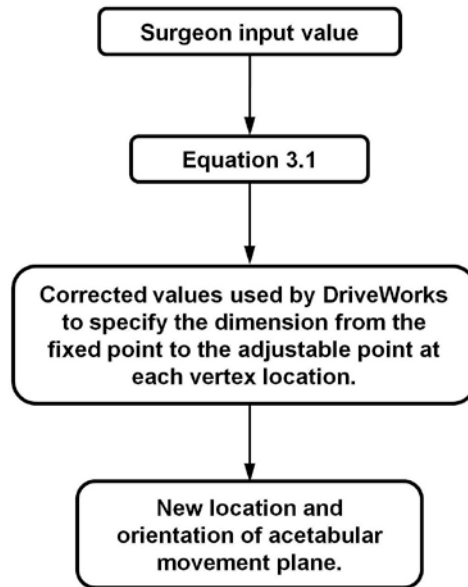


Figure 3.19 – Flow chart illustrating the effect of Equation 3.1 on the specified surgeon input values.

3.7. Measuring acetabular inclination and anteversion angles

The inclination and anteversion angles were measured directly in SolidWorks using the built-in measure tool, but certain reference geometry had to be set up first. To measure the inclination angle of the acetabular reference plane, a reference axis, which is referred to as the inclination axis was created using the intersection between the acetabular reference plane and the APP (Figure 3.20). By measuring the angle between the inclination axis and the transverse plane the inclination angle was calculated. The method in which the inclination angle was measured within SolidWorks dictates that it must be referred to as the radiographic inclination (RI) angle.

To measure the anteversion angle, an intersecting axis, that is referred to as the anteversion axis (Figure 3.21) was created using the acetabular reference plane and the transverse plane. By measuring the angle between the anteversion axis and the mid-sagittal plane the anteversion angle was calculated. This method of measurement dictates that this must be referred to as the anatomical anteversion (AA) angle.

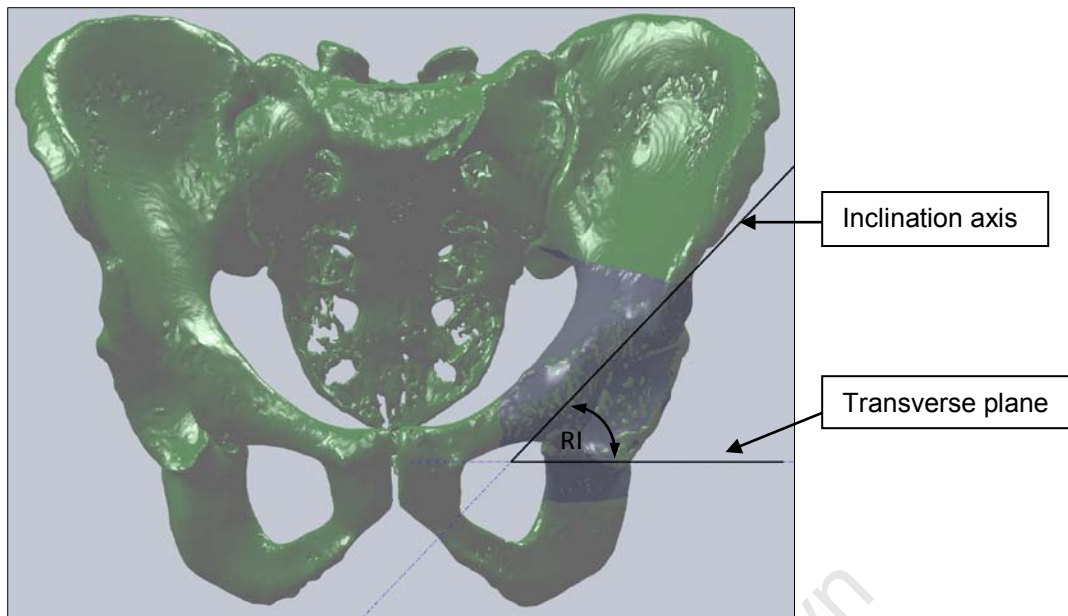


Figure 3.20 – A frontal view of the full pelvis, illustrating the radiographic inclination angle (RI) of the left acetabular reference plane.

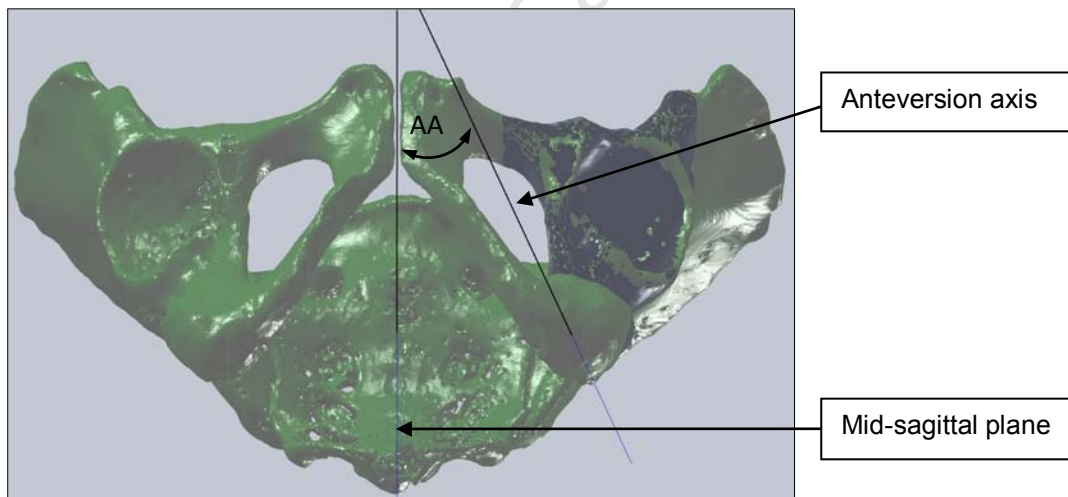


Figure 3.21 – An inferior view of the full pelvis, illustrating the anatomical anteversion angle (AA) of the left acetabular reference plane.

The default location for the placement of the acetabular cup is parallel to the acetabular reference plane. Using the input form the surgeon is able to specify an alternative location and orientation of the acetabular cup, then investigate the effect on hip RoM. The inclination and anteversion angles of the acetabular cup are two crucial variables that have a significant outcome on the post-surgical hip RoM. Therefore, it is important for the surgeon to

know the anatomical inclination and anteversion angles of the patient, as well as be able to decide what angles to place the acetabular cup during surgery. Using the input form, the surgeon is able to specify an alternative location and orientation of the acetabular cup, then investigate by simulation on the screen, the effect on hip RoM.

As demonstrated above, using the CAD program SolidWorks as a means to measure these angles required a detailed knowledge of the program and a significant amount of set-up work. This process was user-intensive and time consuming and would have to be repeated each time a DriveWorks simulation was run. Using 3D vector geometry and Microsoft Excel 2007¹ a spreadsheet was created to make this process semi-automated.

The 3D coordinates of the three vertex points were measured directly in SolidWorks and manually inserted into the spreadsheet. These three vertex points were the same three points used to define the acetabular reference plane. The tables below display the equations used to calculate acetabular inclination and anteversion angles.

Table 3.5 – Showing the inputs for vertex point locations on the acetabular reference plane.

	X	Y	Z
Vertex 1	x_1	y_1	z_1
Vertex 2	x_2	y_2	z_2
Vertex 3	x_3	y_3	z_3

Using these three points, two direction vectors \vec{a} and \vec{b} were calculated. The cross product of these two vectors generated a normal vector. This was reduced to a unit normal vector \hat{n} , which is also normal to acetabular reference plane.

¹ Microsoft Excel [2007] – Microsoft, Redmond, Washington, USA

Table 3.6 – Showing the formulae used to calculate the unit normal vector \hat{n} .

\vec{a}	$x_2 - x_1$	$y_2 - y_1$	$z_2 - z_1$
\vec{b}	$x_3 - x_1$	$y_3 - y_1$	$z_3 - z_1$
$\vec{a} \times \vec{b}$	$(a_2b_3 - a_3b_2)i$	$(a_3b_1 - a_1b_3)j$	$(a_1b_2 - a_2b_1)k$
\hat{n}	$\frac{ i }{\sqrt{ i ^2 + j ^2 + k ^2}}$	$\frac{ j }{\sqrt{ i ^2 + j ^2 + k ^2}}$	$\frac{ k }{\sqrt{ i ^2 + j ^2 + k ^2}}$

Three projection vectors in conjunction with the dot product were used to calculate the angle θ between the unit vector \hat{n} and the respective x, y and z axes.

Table 3.7 – Showing the formulae used to calculate the angle θ between the unit vector \hat{n} and the respective projection vectors \vec{c} , \vec{d} and \vec{e} .

\vec{c}	1	0	0
\vec{d}	0	1	0
\vec{e}	0	0	1
θ	$\cos^{-1} \frac{\hat{n} \cdot \vec{c}}{ \hat{n} \vec{c} }$	$\cos^{-1} \frac{\hat{n} \cdot \vec{d}}{ \hat{n} \vec{d} }$	$\cos^{-1} \frac{\hat{n} \cdot \vec{e}}{ \hat{n} \vec{e} }$

To measure the angle of the unit vector \hat{n} relative to a certain plane, the unit normal vector was projected onto that plane.

Table 3.8 – Showing the formulae used to project the unit vector \hat{n} onto the respective planes.

Projection of \hat{n} onto x-y plane (coronal plane)	
Projection length x-y	$\sqrt{\left(\frac{ i }{\sqrt{ i ^2 + j ^2 + k ^2}}\right)^2 + \left(\frac{ j }{\sqrt{ i ^2 + j ^2 + k ^2}}\right)^2}$
Projection of \hat{n} onto the y-z plane (mid-sagittal plane)	
Projection length y-z	$\sqrt{\left(\frac{ j }{\sqrt{ i ^2 + j ^2 + k ^2}}\right)^2 + \left(\frac{ k }{\sqrt{ i ^2 + j ^2 + k ^2}}\right)^2}$
Projection of \hat{n} onto the x-z plane (transverse plane)	
Projection length x-z	$\sqrt{\left(\frac{ i }{\sqrt{ i ^2 + j ^2 + k ^2}}\right)^2 + \left(\frac{ k }{\sqrt{ i ^2 + j ^2 + k ^2}}\right)^2}$

Following this step, the angle subtended by the projection vector on each of the x-y, y-z and x-z planes was calculated. These projection angles are referred to as angles α , β & γ . The angle α_x was measured from the x axis to the projected vector and the same rationale was applied to the other angular measurements.

Table 3.9 – Showing the formulae used to calculate the angles α , β & γ of the projected vector, in the respective anatomical reference planes.

Angle α in the x-y plane (coronal plane)	
α_x	$\cos^{-1} \left(\frac{\frac{ i }{\sqrt{ i ^2 + j ^2 + k ^2}}}{\sqrt{\left(\frac{ i }{\sqrt{ i ^2 + j ^2 + k ^2}}\right)^2 + \left(\frac{ j }{\sqrt{ i ^2 + j ^2 + k ^2}}\right)^2}} \right)$
α_y	$\cos^{-1} \left(\frac{\frac{ j }{\sqrt{ i ^2 + j ^2 + k ^2}}}{\sqrt{\left(\frac{ i }{\sqrt{ i ^2 + j ^2 + k ^2}}\right)^2 + \left(\frac{ j }{\sqrt{ i ^2 + j ^2 + k ^2}}\right)^2}} \right)$
Angle β in the y-z plane (mid-sagittal plane)	
β_y	$\cos^{-1} \left(\frac{\frac{ j }{\sqrt{ i ^2 + j ^2 + k ^2}}}{\sqrt{\left(\frac{ j }{\sqrt{ i ^2 + j ^2 + k ^2}}\right)^2 + \left(\frac{ k }{\sqrt{ i ^2 + j ^2 + k ^2}}\right)^2}} \right)$
β_z	$\cos^{-1} \left(\frac{\frac{ k }{\sqrt{ i ^2 + j ^2 + k ^2}}}{\sqrt{\left(\frac{ j }{\sqrt{ i ^2 + j ^2 + k ^2}}\right)^2 + \left(\frac{ k }{\sqrt{ i ^2 + j ^2 + k ^2}}\right)^2}} \right)$
Angle γ in the x-z plane (transverse plane)	
γ_x	$\cos^{-1} \left(\frac{\frac{ i }{\sqrt{ i ^2 + j ^2 + k ^2}}}{\sqrt{\left(\frac{ i }{\sqrt{ i ^2 + j ^2 + k ^2}}\right)^2 + \left(\frac{ k }{\sqrt{ i ^2 + j ^2 + k ^2}}\right)^2}} \right)$

γ_z	$\cos^{-1} \left(\frac{\frac{ k }{\sqrt{ i ^2 + j ^2 + k ^2}}}{\sqrt{\left(\frac{ i }{\sqrt{ i ^2 + j ^2 + k ^2}}\right)^2 + \left(\frac{ k }{\sqrt{ i ^2 + j ^2 + k ^2}}\right)^2}} \right)$
------------	--

Using angles $\theta, \alpha, \beta,$ & γ along with the method specified in Section 2.4.3 it was possible to calculate inclination and anteversion in terms of radiographic, anatomical or operative spatial reference systems.

Section 3.6 specifies that the vertex axes are perpendicular to the acetabular reference plane and in the direction of the normal vector \hat{n} . The offset along the vertex axis is specified by the surgeon and used to define the location and orientation of the acetabular movement plane. Using the offset value, the unit normal vector \hat{n} and the three direction vectors (1, 0, 0), (0, 1, 0) and (0, 0, 1), the coordinates of the new movement plane are calculated. From Table 3.7 the angle θ represents the angle between the unit normal vector \hat{n} and the respective Cartesian coordinates.

At Vertex 1, the following equation parameters are relevant:

- (x_1, y_1, z_1) – Acetabular reference plane coordinates at vertex 1.
- $(\theta_x, \theta_y, \theta_z)$ – Angle between the unit normal vector \hat{n} and the respective Cartesian coordinates.
- (p, q, r) – Surgeon offsets specified at each vertex point.
- (s_1, t_1, u_1) – Acetabular movement plane coordinates at vertex 1.

Applying trigonometric functions, the following were derived:

$$\text{Offset along } x \text{ axis} = (p)(\cos\theta_x)$$

$$\text{Offset along } y \text{ axis} = (p)(\cos\theta_y)$$

$$\text{Offset along } z \text{ axis} = (p)(\cos\theta_z)$$

Equation 3.2 – Relating the input offset value to offset along the respective Cartesian axis.

Expanding Equation 3.2, generates:

$$\begin{aligned}s_1 &= x_1 + (p)(\cos\theta_x) \\ t_1 &= y_1 + (p)(\cos\theta_y) \\ u_1 &= z_1 + (p)(\cos\theta_z)\end{aligned}$$

Equation 3.3 – Relating the input offset value to the new movement plane coordinates.

In the 3D vector spreadsheet there is a “surgeon input box”, that allows the surgeon to specify the offset at each vertex location. As per Table 3.4, the offset increments in the surgeon input box are set to 2 mm and the extremities -10 mm into the bone and +6 mm away from the bone.

Using Equation 3.3 and the values from the surgeon input box, the 3D coordinates of the three new vertex points were calculated, which in turn specified the location of the acetabular movement plane. Following this, utilizing the same equations listed in Table 3.5 to Table 3.9, the inclination and anteversion angles for the movement plane were calculated. This makes it possible to calculate the change in inclination and anteversion angles relative to position of the acetabular cup, as well as investigate its effect on hip RoM.

3.8. Converting inclination and anteversion angles between the different spatial reference systems

Based on the equations listed in Appendix A, an Excel spreadsheet was created to allow the surgeon to convert inclination and anteversion angles between the different spatial reference systems (anatomical, operative and radiographic), without having to calculate them as described in Section 3.7 above. This feature can be used in conjunction with post-operative AP radiographs to assess the outcome of a hip arthroplasty, in terms of inclination and anteversion angles.

3.9. Converting pelvic tilt in AP radiographs

The position of the patient during the capture of radiographic images has an influence on the degree of pelvic tilt, as well as on the radiographic inclination and anteversion angles (Section 2.4.1). A spreadsheet was designed using the equations listed in Appendix B to account for this adjustment and to simplify the process. This feature may be utilised alone or as a pre-adjustment before using the conversion spreadsheet in Section 3.8 above. The surgeon needs to be aware that when using estimated or general values (-8° for standing and -4° for lying down) for pelvic tilt, these may cause unwanted errors when converting to the other spatial reference systems. For accurate inclination and anteversion angles from radiographic images it is recommended to directly measure the pelvic tilt for each patient.

3.10. Constructing the combined assembly in SolidWorks

To conduct hip RoM analysis all the different part files need to be imported into a single assembly. To simplify the process in SolidWorks, it was decided to link the DriveWorks function for setting the acetabular cup position to run within the combined assembly file. This allows the surgeon to test different cup seating positions and the associated effect on hip RoM with all the components at their disposal. For example, the main assembly file may contain the following part files:

- **Left acetabular model** – this is the portion of the pelvis that was converted into a solid 3D model and contains the acetabular reference and movement planes.
- **BHR acetabular cup** – this is the prosthetic cup that the surgeon has selected, based on measurements taken and experience in selecting the ideal component size.
- **Whole pelvis STL** – this is the image of the full pelvis used to set up the anatomical reference planes.

- **Artificial femur** – this is the file that the surgeon has created using DriveWorks that best represents the patient’s anatomy. The file name extension will contain the patient’s name.
- **BHR femoral head** – this is the prosthetic femoral component that the surgeon has selected, based on measurements taken and experience in selecting the ideal size.

Not all parts within the assembly need to be active at one time, the surgeon can choose to suppress or unload certain parts that are not of interest at that time. This function is useful as the whole pelvis STL file is very large, and can significantly hamper the operation of the program. Once all the separate part files have been loaded into the combined assembly file, the order and method in which they are linked together needs to be specified.

Connecting the femoral head to the artificial femur – This was achieved by aligning the drilling axis of the femoral head with the drilling axis of the artificial femur. Then, the centre of rotation point of the prosthetic head was connected to the centre point of the femoral head of the artificial femur (Figure 3.22). The resection level of the femoral component can be specified by the surgeon during the set-up of the artificial femur.

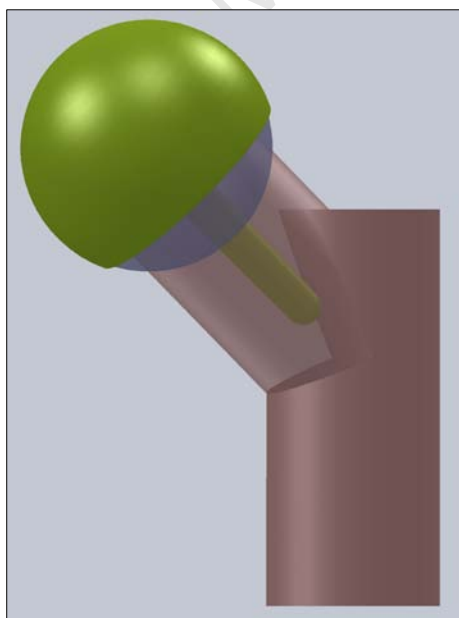


Figure 3.22 – Showing the BHR femoral head (green) connected to the artificial femur.

- **Connecting the acetabular cup to the left acetabular model** – The centre point of the acetabular cup was connected with the centre point of the acetabular construction circle on the movement plane. This fixed the location of the cup in a direction normal to the movement plane. Following this, the acetabular cup edge was aligned with the movement plane, therefore preventing it from rotating (Figure 3.23). Aligning the acetabular cup with the acetabular movement plane was necessary as the input form was set-up to adjust the orientation of this plane according to the surgeon inputs. The acetabular cup was not fixed about its third axis of freedom (the acetabular axis) as this had no effect on the type of hip RoM analysis performed in this study.

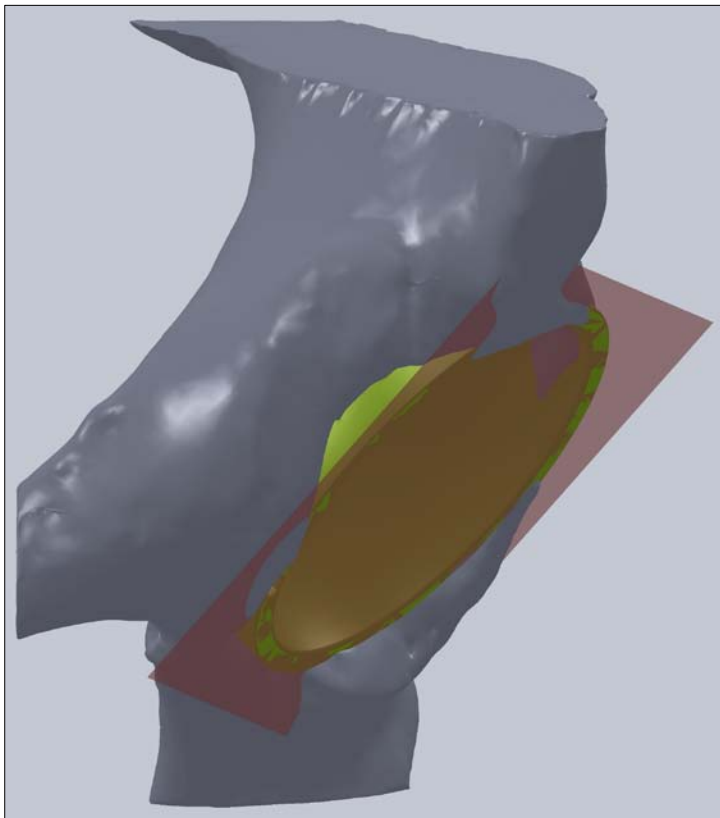


Figure 3.23 – Illustrating the acetabular cup positioned in the centre of the socket with the edge sitting parallel with the acetabular movement plane (shaded red).

- **Connecting the left acetabular model to the whole pelvis STL image** – This process proved to be uncomplicated, as the anatomical reference planes (APP, mid-sagittal and transverse planes) were identical for both files.
- **Fitting the femoral head into the acetabular cup** – This involved bringing the outer surface of the femoral head in contact with the inner surface of the acetabular cup, completing the ball-and-socket joint.
- **Importing patient-specific STLs** – A new STL requires the same anatomical reference planes to be defined prior to being imported into SolidWorks. This permits the new STL to be correctly located and superimposed over the 3D model. In order to superimpose the STL, the APP and the mid-sagittal plane of the new STL were aligned directly to the original model. The vertical position required manual positioning in order to align the acetabular sockets.

3.11. Performing hip RoM analysis in SolidWorks

After all the part files are imported into SolidWorks, the surgeon is able to use the input form to specify different positions of the acetabular cup. To rotate the artificial femur, the surgeon is required to select the component and use the move or rotate tool in SolidWorks to manually move the femur in the desired arc. No movement limitations were created in this model, therefore the surgeon is required to use his or her own judgment to decide on what movements the artificial femur can make relative to the pelvis. Some common movement arcs may include:

- **Flexion/Extension** – this occurs in a movement arc parallel to the mid-sagittal plane.
- **Abduction/Adduction** – this occurs in a movement arc parallel to the APP or coronal plane.

- **Internal rotation** – when viewed superiorly, this movement arc involves a clockwise rotation within the transverse plane.
- **External rotation** – when viewed superiorly, this movement involves an anti-clockwise rotation within the transverse plane.

Some of these movements occur in combination with others, therefore making precise angular measurements within SolidWorks challenging and outside the scope of this project. Hip RoM is not only restricted by physical anatomy, but it is also restricted by clearance between the edge of the acetabular cup and femoral neck. The surgeon should be aware of the need to avoid contact between these two surfaces.

Figure 3.24 gives a general overview of how the different software programs interact with each other.

University of Cape Town

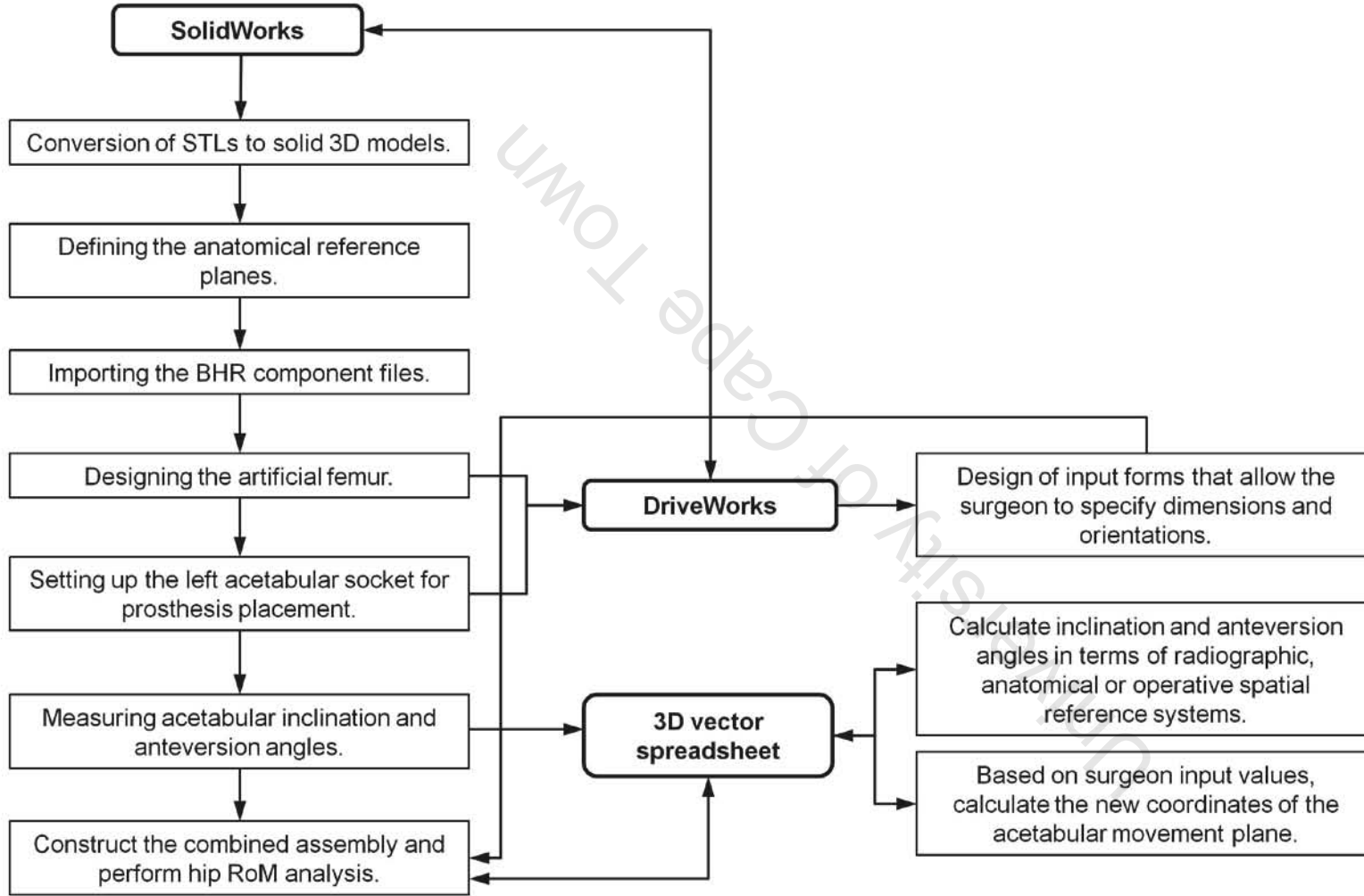


Figure 3.2.4 – Flow chart illustrating how software programs SolidWorks, DriveWorks and the 3D vector spreadsheet interact with each other.

4. Results

In this chapter various scenarios will be illustrated for the individual components, based on different specifications entered into the input forms. The 3D vector spreadsheet used for calculating the inclination and anteversion angles will be compared to direct measurements taken within SolidWorks and the results of superimposing new patient STLs will be presented.

4.1. The artificial femur

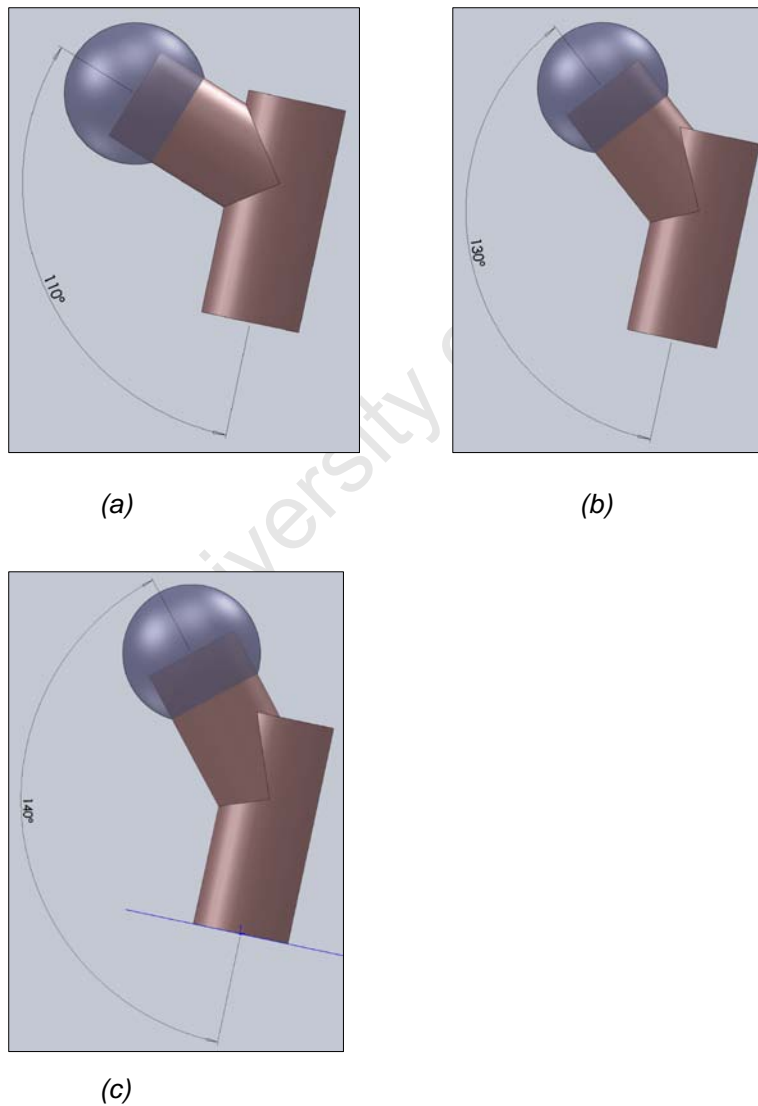


Figure 4.1 – Artificial femur with varying CCD angles (a) coxa vara with CCD = 110°, (b) coxa normal with CCD = 130° and (c) coxa valga with CCD = 140°.

Figure 4.1 illustrates different CCD angles as a result of different values inserted in the input form, demonstrating that this can be used to match the patient's anatomy.

In Figure 4.2 the CCD angle has been set to 135° , but the inclination angle of the artificial femur has been increased from 45° to 55° . This places the drilling axis into a coxa valga position, hence placing the femoral stem shaft in a valgus position. It is important for the surgeon to be able to specify this angle for the femoral component.

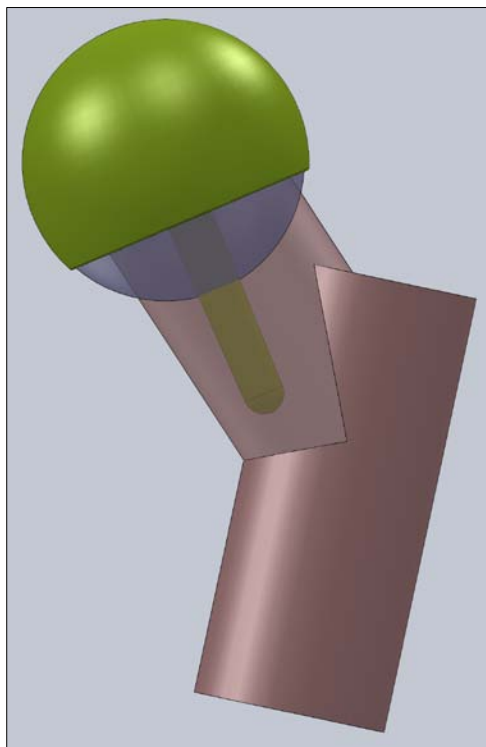


Figure 4.2 – An artificial femur with the CCD angle of the femoral neck set at 135° and the inclination angle for the femoral stem set at 55° .

4.2. The 3D vector spreadsheet

The equations in Section 3.7 and the 3D coordinates measured directly at the three vertex points for the acetabular reference plane were used to calculate the anatomical inclination and anteversion angles (Table 4.1).

Table 4.1 – Displaying the results calculated by the 3D vector spreadsheet for the acetabular reference plane.

	X	Y	Z
Vertex 1	72.2	148.3	-26.92
Vertex 2	99.54	154.07	-73.73
Vertex 3	105.64	173.02	-48.02
\vec{a}	27.34	5.77	-46.81
\vec{b}	33.44	24.72	-21.1
$\vec{a} \times \vec{b}$	1035.40	-988.45	482.89
\hat{n}	0.6854	-0.6543	0.3196
\vec{c}	1	0	0
\vec{d}	0	1	0
\vec{e}	0	0	1
θ	46.73 °	130.87 °	71.36 °
Projection of \hat{n} onto x-y plane (coronal plane)			
Projection length x-y	0.9475 mm		
Projection of \hat{n} onto the y-z plane (mid-sagittal plane)			
Projection length y-z	0.7282 mm		
Projection of \hat{n} onto the x-z plane (transverse plane)			
Projection length x-z	0.7562 mm		
Angle α in the x-y plane (coronal plane)			
α_x	43.7 °		
α_y	133.7 °		
Angle β in the y-z plane (mid-sagittal plane)			
β_y	154.0 °		
β_z	64.0 °		
Angle γ in the x-z plane (transverse plane)			
γ_x	25.0 °		
γ_z	65.0 °		

Next, the offset values were entered into the “surgeon input box” (Figure 4.3). Applying the offset values of: -2, -4, +4 mm in conjunction with Equation 3.2 and Equation 3.3, Table 4.3 displays the new coordinates for the acetabular movement plane, as well as all the other angular results derived from the equations presented in Section 3.7.

Table 4.2 – Illustrating the results calculated by the 3D vector spreadsheet for the new acetabular movement plane.

	X	Y	Z
Vertex 1	70.83	149.61	-27.56
Vertex 2	96.79	156.69	-75.01
Vertex 3	108.38	170.40	-46.74
\vec{a}	25.97	7.08	-47.45
\vec{b}	37.55	20.79	-19.18
$\vec{a} \times \vec{b}$	850.89	-1283.68	274.19
\hat{n}	0.5439	-0.8206	0.1752
\vec{c}	1	0	0
\vec{d}	0	1	0
\vec{e}	0	0	1
θ	57.05 °	145.15 °	79.90 °
Projection of \hat{n} onto x-y plane (coronal plane)			
Projection length x-y	0.9845 mm		
Projection of \hat{n} onto the y-z plane (mid-sagittal plane)			
Projection length y-z	0.8391 mm		
Projection of \hat{n} onto the x-z plane (transverse plane)			
Projection length x-z	0.5715 mm		
Angle α in the x-y plane (coronal plane)			
α_x	56.5 °		
α_y	146.5 °		
Angle β in the y-z plane (mid-sagittal plane)			
β_y	167.9 °		
β_z	77.9 °		
Angle γ in the x-z plane (transverse plane)			
γ_x	17.9 °		
γ_z	72.1 °		

Figure 4.3 is an image taken of the 3D vector spreadsheet used to calculate the inclination and anteversion angles before and after re-orientation of the acetabular movement plane. The offset values entered into the surgeon input cells matched those entered into the DriveWorks input form for vertices 1, 2 and 3, so that the correct angles are displayed in the 3D vector spreadsheet. The acetabular cup was aligned with the acetabular movement plane, therefore the spreadsheet is able to provide cup inclination and anteversion angles.

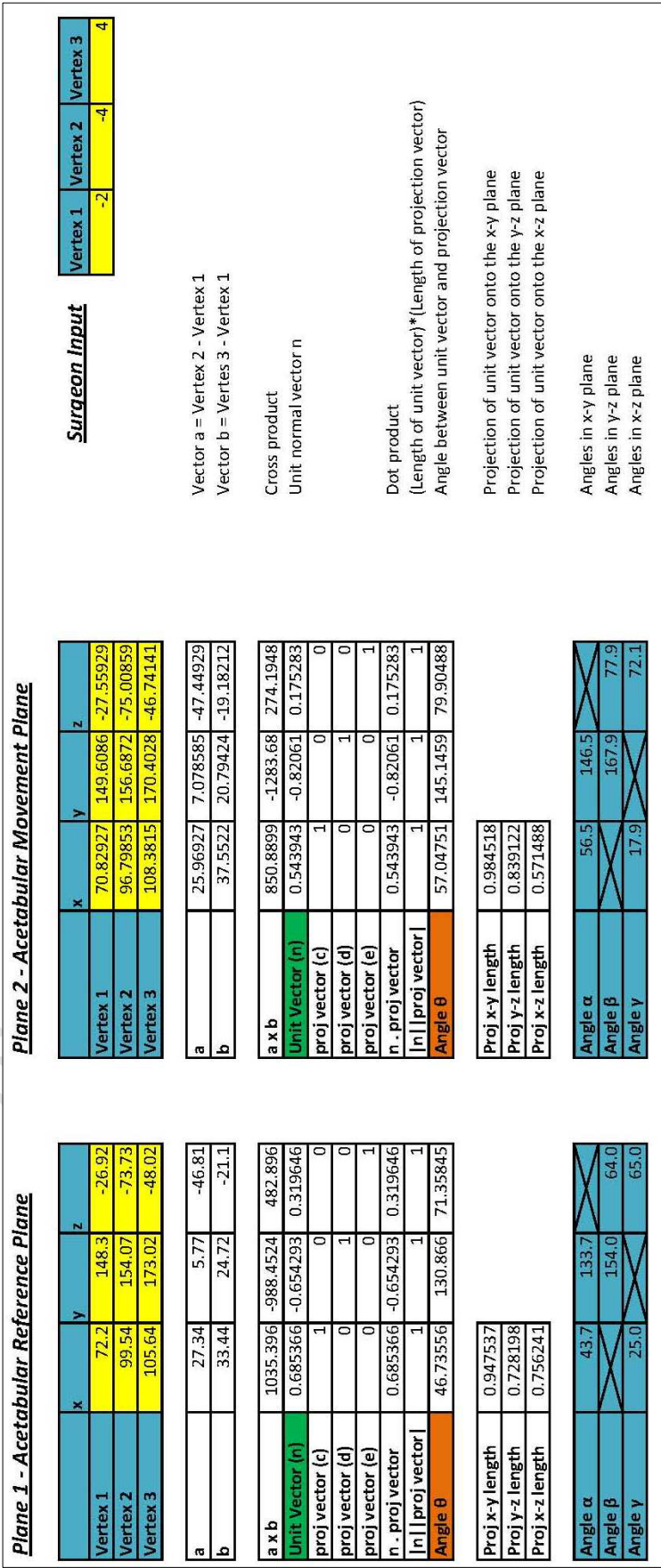


Figure 4.3 – Illustrating the 3D vector spreadsheet used to calculate the inclination and anteversion angles.

Using the methods described in Section 2.4.3 the inclination and anteversion angles are expressed in terms of anatomical, operative and radiographic spatial reference systems. These angles were calculated as follows:

- Anatomical Inclination (AI) = $180^\circ - (\text{y value of } \theta)$
- Anatomical Anteversion (AA) = $x \text{ value of Angle } \gamma \text{ or } 90^\circ - (\text{z value of Angle } \gamma)$
- Operative Inclination (OI) = Angle between projection y-z and unit normal vector
- Operative Anteversion (OA) = $(180^\circ - \text{y value of angle } \beta)$ or $(90^\circ - \text{z value of angle } \beta)$
- Radiographic Inclination (RI) = $(180^\circ - \text{y value of angle } \alpha)$ or $(90^\circ - \text{x value of angle } \alpha)$
- Radiographic Anteversion (RA) = Angle between projection x-y and unit normal vector

Using the results presented in Table 4.1 and Table 4.2 with the equations listed above, the 3D vector spreadsheet calculated acetabular cup inclination and anteversion angles according to the different spatial reference systems (Table 4.3).

Table 4.3 – Illustrating the results calculated by the 3D vector spreadsheet for cup inclination and anteversion angles, in terms of the three different spatial reference systems.

Acetabular reference plane		Acetabular movement plane	
Spatial reference	Angular value (°)	Spatial reference	Angular value (°)
AI	49.1	AI	34.9
AA	25.0	AA	17.9
OI	43.3	OI	33.0
OA	26.0	OA	12.1
RI	46.3	RI	33.5
RA	18.6	RA	10.1

An offset of -2, -4 and +4 mm of the acetabular movement plane resulted in the following changes in acetabular cup inclination and anteversion angles:

Table 4.4 – Illustrating the effect on inclination and anteversion angles associated with an acetabular cup offset of -2, -4 and +4 mm.

Change in inclination and anteversion angles	
Spatial reference	Angular value (°)
AI	14.2
AA	7.7
OI	10.3
OA	13.9
RI	12.8
RA	8.5

4.3. Converting inclination and anteversion angles between the different spatial reference systems

Using the angles calculated for the acetabular reference plane taken from Table 4.2 as inputs, this spreadsheet was used to convert the inclination and anteversion angles between anatomical, operative and radiographic spatial reference systems. This spreadsheet also served as a cross-check for the angles stated in the 3D vector spreadsheet results of Table 4.3.

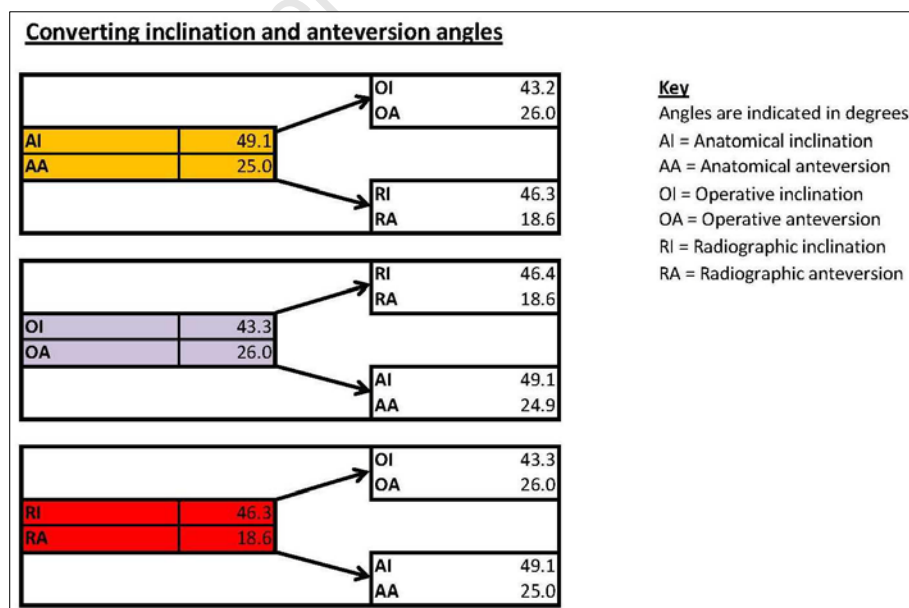


Figure 4.4 – Illustrating the spreadsheet used to convert inclination and anteversion angles between anatomical, operative and radiographic spatial reference systems.

4.4. Converting pelvic tilt

The pelvic tilt adjustment spreadsheet adjusted the radiographic inclination and anteversion angles according to the degree of pelvic tilt. Figure 4.5 illustrates this using a pelvic tilt angle of -8° .

<u>Pelvic tilt adjustment</u>	
RI =	44.7
RA =	13.0
Pelvic tilt =	-8.0
RI' =	46.3
RA' =	18.6

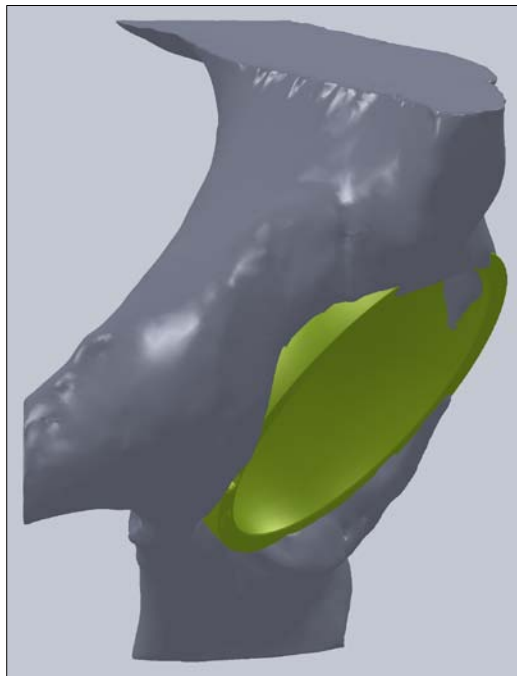
Key
All angles in degrees
RI = Radiographic inclination
RA = Radiographic anteversion
Pelvic tilt = -ve angle
RI' = Adjusted radiographic inclination
RA' = Adjusted radiographic anteversion

Figure 4.5 – Illustrating the pelvic tilt adjustment spreadsheet, showing radiographic inclination and anteversion angles before and after adjustment.

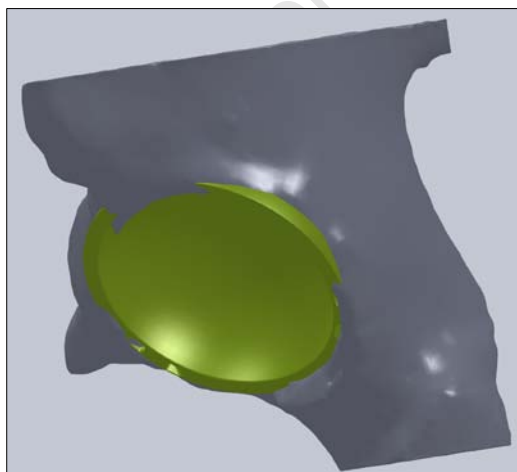
University of Cape Town

4.5.Placement of the acetabular cup

The same offset values from Section 4.2 were entered into the DriveWorks input form to illustrate how SolidWorks locates the acetabular cup within the socket. Additionally the angles of inclination and anteversion were measured directly and compared to those calculated by the 3D vector spreadsheet.



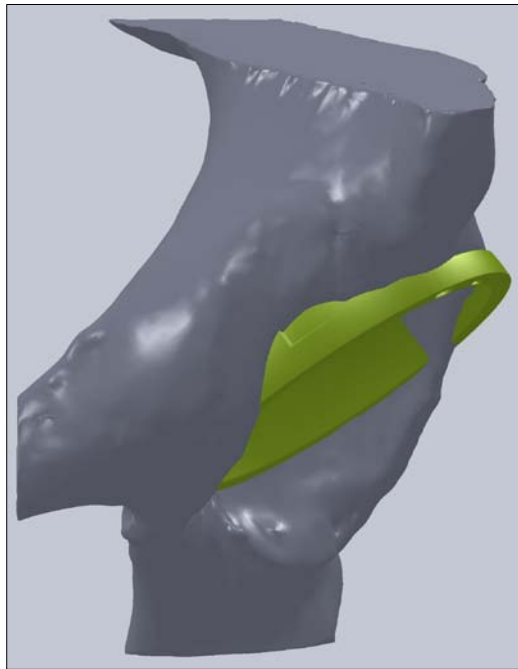
(a)



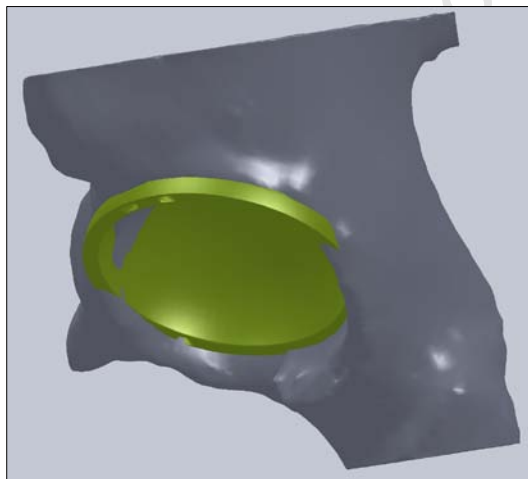
(b)

Figure 4.6 – (a) Showing the front view of the left acetabular socket with the acetabular cup rim parallel with the acetabular reference plane and (b) showing a side view of the cup in the same position.

Next, offsets of -2, -4 and +4 mm were entered into the input form, to modify the position of the acetabular cup, as seen in Figure 4.7 below.



(a)



(b)

Figure 4.7 – (a) Showing the front view of the left acetabular socket with the acetabular cup rim parallel with the acetabular movement plane (b) showing a side view of the same cup.

In Figure 4.6 it is noted that the acetabular cup edge is parallel to the acetabular reference plane. In Figure 4.7, however, it can be seen that based

on the offset values, the acetabular cup has moved into the bone at the anterior and posterior points and away from the bone at the superior point.

The radiographic inclination (RI) and anatomical anteversion (AA) angles of the position of the acetabular cup, before and after the offsets were applied, were measured using SolidWorks. The results are presented in Table 4.5.

Table 4.5 – Displaying the results measured in SolidWorks for cup inclination and anteversion angles, in terms of the respective spatial reference systems.

Acetabular reference plane		Acetabular movement plane	
Spatial reference	Angular value (°)	Spatial reference	Angular value (°)
RI	46.33	RI	33.54
AA	25.0	AA	17.86

An offset of -2, -4 and +4 mm of the acetabular cup resulted in the following changes in inclination and anteversion angles:

$$\Delta \text{RI} = 12.79^\circ$$

$$\Delta \text{AA} = 7.14^\circ$$

By comparing the values in Table 4.5 with those of Table 4.3, it is evident that there is a difference of less than 1° between the angles measured in SolidWorks and those calculated by the 3D vector spreadsheet.

In Figure 4.8 below, the combined assembly is presented illustrating the new location of the prosthetic cup according to the offsets -2, -4 and +4 mm.

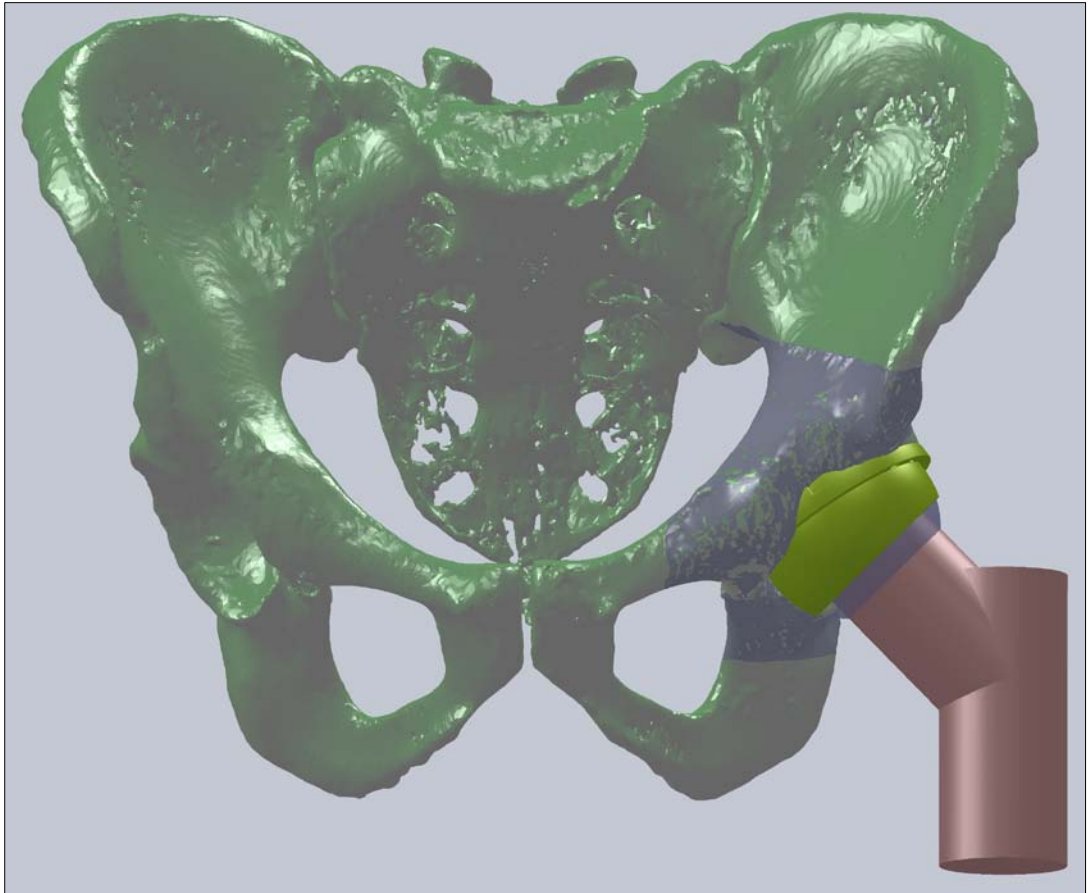
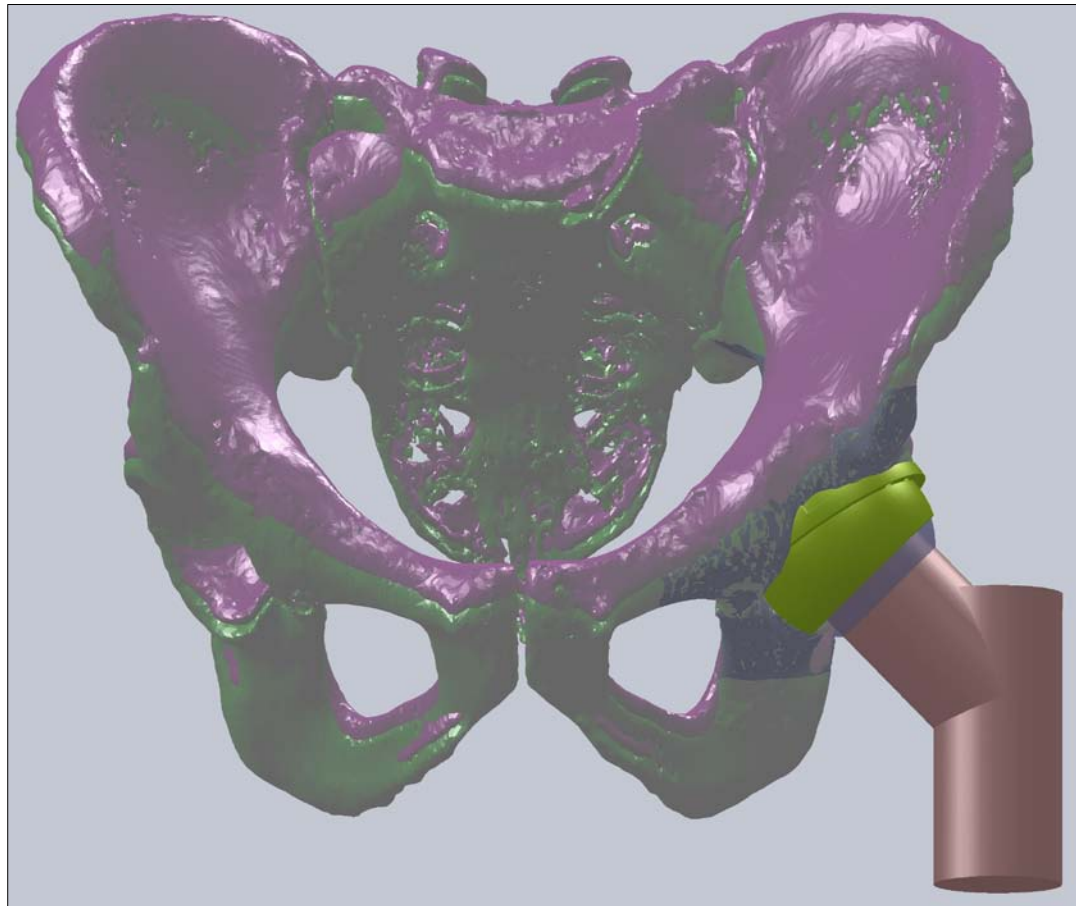


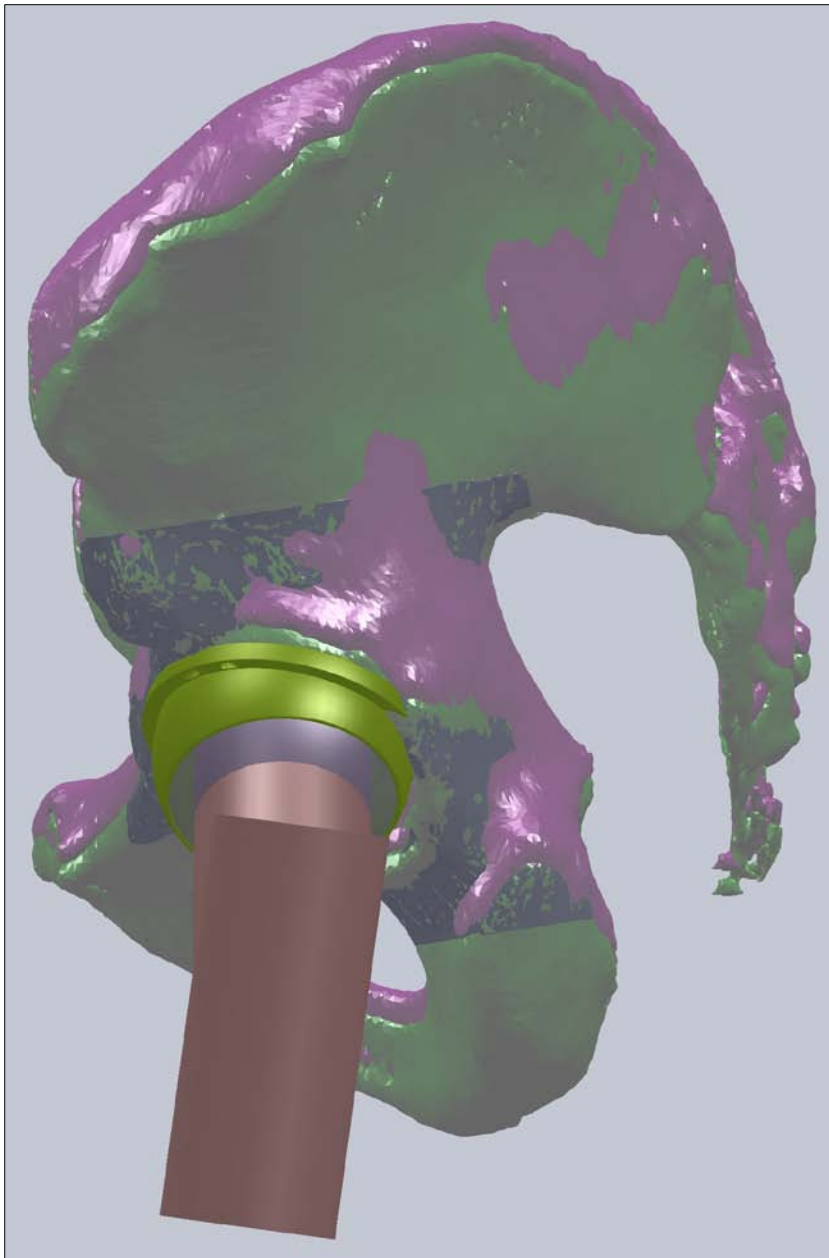
Figure 4.8 – Illustrating the complete assembly file, with the acetabular cup in its new position according to the offsets: vertex 1 = -2 mm, Vertex 2 = -4 mm and Vertex 3 = +4 mm.

4.6. Superimposing patient-specific STLs into the model

New patient STL files were successfully imported and superimposed over the 3D model. Following this, hip RoM analysis was performed. The superimposed STL (in purple) can be seen in (Figure 4.9 a & b) below.



(a)



(b)

Figure 4.9 – Illustrating the new patient's STL (purple) superimposed over the test patient's STL (green), with (a) a frontal view and (b) a side view of the pelvis.

4.7. Hip RoM analysis

During hip RoM analysis it was noted that the model was able to test any particular movement combination of the artificial femur relative to the acetabular cup and identify when impingement of the acetabular rim on the femoral neck was occurring.

There were, however, crucial parameters that could not be incorporated using SolidWorks. These included specifying the extreme limits of movement within physiological norms and displaying on-screen angular information regarding movement arcs. In addition, the user was required to have prior knowledge of the SolidWorks software package in order to move the artificial femur relative to the pelvis to test hip RoM.

This study served to identify that this type of CAD software as it stands has limitations as a tool for pre-surgical planning and is not fully surgeon user-friendly. Software modifications or the development of a specific software program could overcome these barriers, which is further discussed below.

5. Discussion

In this study, using the CAD program SolidWorks, a 3D computer model of the pelvis and upper femur was created based on CT scans. It was successfully able to virtually insert the hip resurfacing components into the 3D model and conduct hip RoM analysis. However, there were some limitations to its functionality. From the results of this study recommendations have been developed for the future design of a user-friendly software program for pre-surgical planning of hip resurfacing. This could take the form of software modifications of the current platform or the development of a specific software program.

The following chapter discusses the results presented in Chapter 4 according to each feature of the program.

5.1. Artificial femur

In this study, an artificial femur was designed to represent the patient's anatomy. It is possible to manipulate the data in the model to mimic numerous anatomical features of the upper femur, including certain pathological conditions such as coxa valga and coxa vara. Additionally, the STL of the patient's upper femur can be superimposed over the artificial femur to allow for final modifications.

DriveWorks was used to set-up the drilling axis within the artificial femoral neck, based on data entered by the surgeon for inclination and anteversion angles. It was thus possible to locate the prosthetic femoral component within the neck. This feature is essential as studies have revealed that a slight valgus orientation of the femoral component is favourable in terms of post-surgical attainable hip RoM and longevity of the prosthesis (Amstutz et al. 2001; Beaulé et al. 2004a; De Haan et al. 2008b; Klues et al. 2008; Shimmin et al. 2005a; Williams et al. 2009). Vendittoli et al. (2007) reported that the centre of rotation of the femoral component does not change when

modifying the anteversion angle, possibly due to the natural anteversion provided by the anatomical femoral neck (Malviya et al. 2010). However, this may not always be the case, as there can be a wide variance in femoral anatomy which may require the surgeon to specify custom inclination and anteversion angular placement, such as when there are abnormalities in the anatomy of the femoral neck.

The resection level variable in the DriveWorks input form permits the surgeon to adjust the seating depth of the prosthetic femoral head along the femoral neck bone. By changing this dimension the surgeon will be able to manipulate the femoral offset distance and therefore the post-surgical hip RoM. Kluess et al. (2008) report that patients with a higher femoral offset have increased RoM before bony impingement occurs. However, specifying an increased inclination angle for the femoral component reduces the femoral offset distance (Beaule et al. 2004a; Shimmin and Back 2005b). Therefore, these two variables need to be considered in conjunction with one another to find the optimal position.

The femoral head offset angle and distance can be used by the surgeon to specify the location of the centre of rotation of the femoral component, relative to the cross-section of the femoral neck. In addition, these two variables can be used to translate the femoral stem away from the central neck axis or CCD, which affects the femoral head-neck offset distance and femoral head-neck offset ratio. Hip RoM improves in the direction of translation, but at the same time is reduced in the opposite direction (Vendittoli et al. 2007). Furthermore, femoral head-neck offset ratios ≤ 0.15 may present a considerable risk for FAI (Beaule et al. 2007b; Malviya et al. 2010). This feature can therefore be used to rectify a deficient head-neck offset present in one quadrant or to provide more or less RoM in a particular direction, depending on the patient. Translation of the femoral stem, however, is limited in order to retain integrity of the femoral neck bone.

The software adjustments within SolidWorks provide the surgeon with the capability to specify the femoral stem angle in terms of inclination and

anteversion, resection depth, and femoral stem translation. These three main variables allow investigation of a wide variety of component positions in relation to attainable hip RoM simulations. This flexibility within the design of the artificial femur permits the software to be applied to a wider range of patients.

5.2. The 3D vector spreadsheet and position of the acetabular cup

The development of the 3D vector spreadsheet was necessary due to the fact that SolidWorks does not currently have the option or capability to display on-screen angular measurements based on pre-selected planes. The angles of inclination and anteversion of the acetabular cup are two crucial factors that can significantly influence the life expectancy of a hip resurfacing prosthesis (De Haan et al. 2008b; Langton et al. 2008; Williams et al. 2009; Grammatopoulos et al. 2010). These two factors also have a considerable influence on the post-surgical attainable hip RoM (Williams et al. 2009; Malviya et al. 2010). In Figure 4.3, the 3D vector spreadsheet displays the inclination and anteversion angles in terms of anatomical, operative and radiographic spatial reference systems, before and after offsetting the prosthetic cup. With the aid of the 3D vector spreadsheet the surgeon can measure the patient's acetabular anatomical angles prior to surgery, perform hip RoM analysis in the 3D computer model based on virtual insertion of the components, select the ideal prosthesis size and position, and then specify the optimal operative angles in which to place the components during hip resurfacing surgery. The spreadsheet also allows the surgeon to investigate the change in acetabular cup inclination and anteversion angles versus the on-screen effect on attainable hip RoM between different placement scenarios.

The comparison of the results presented in Table 4.3 and Table 4.5 for acetabular inclination and anteversion angles, yielded differences of less than 1°. This result serves as a validation to the accuracy of the 3D vector

spreadsheet and its function in providing key angular data to the surgeon for component positioning.

Section 4.5 illustrates how the surgeon can use the DriveWorks input forms to locate and orientate the acetabular cup. In addition to ensuring longevity of the prosthesis, the location and orientation of the acetabular cup is crucial to restoring natural hip RoM (Malviya et al. 2010), as well as prevent accelerated wear and subsequent CoCr metal ion release (Amstutz et al. 2004; Beaulé et al. 2004a; Beaulé et al. 2007b; De Haan et al. 2008a). Langton et al. (2008) suggest focussing on optimising the acetabular orientation to reduce metal ion release. The combined assembly file allows all the different prosthetic component parts and sizes, as well as the anatomical sections of the pelvis, to be displayed or hidden, depending on the surgeon's requirements. This improves usability and reduces the testing time between different placement scenarios. By using this approach, the surgeon can easily test various placement scenarios and decide which is best suited to meet the individual patient's needs.

The hip RoM attainable is dependent on the cup position, with reference to cup inclination and anteversion (Williams et al. 2009; Malviya et al. 2010). Increasing the cup inclination angle from 30° to 50°, as well as increasing the cup anteversion from 0° to 25° gave a more physiologic RoM (Williams et al. 2009). Grammatopoulos et al. (2010) recommend aiming for an operative inclination of 40° and an operative anteversion of 25°. A number of other manufacturers (including Smith & Nephew for the BHR system) and designers of hip resurfacing prostheses recommend placing the acetabular component at 40° of inclination and 20° of anteversion, but do not specify whether these are operative, anatomical or radiographic angles. In hip resurfacing there are guidelines available on the optimum component position and size, but little concrete data exists (Williams et al. 2009), therefore it is up to the surgeon to specify these based on patient-specific pre-surgical planning.

Lubovsky et al. (2010) suggest that acetabular rim plane orientation through manual landmark selection on CT datasets, as well as using the APP as a reference plane, is reliable and accurate. Hip resurfacing RoM studies conducted by Vendittoli et al. (2007) and Kluess et al. (2008) employed the same methods in setting up the anatomical reference planes as those presented in Section 3.6. Additionally, the set of tools developed in this study has very similar capabilities to other pre-surgical planning tools used in various CAS systems (Barrett et al. 2007; Krüger et al. 2007; Kluge 2009). A number of these CAS devices make use of software that generates 3D computer models based on patient CT scans (Barrett et al. 2007; Krüger et al. 2007; Kluge 2009). This data is then used for pre-surgical planning. This adds credibility to the methods and results presented in this investigation, which is specifically aimed at pre-surgical planning for hip resurfacing arthroplasties.

5.3. Spatial reference systems

To avoid errors in measurement or placement of the acetabular components, spreadsheets were designed to convert inclination and anteversion angles between the different spatial systems (Figure 4.4 and Figure 4.5), as well as take pelvic tilt into account. These two features are useful to the surgeon as a quick reference guide for an initial consultation if only AP radiographs are available for the patient. Research conducted by Yoon et al. (2008) highlighted the importance of defining and specifying the correct spatial reference systems when referring to acetabular cup angles for hip arthroplasties. Furthermore, pelvic tilt can significantly influence the measured radiographic inclination angle using AP radiographs which are regularly used by surgeons to assess and diagnose hip complications, as well as evaluate the outcome of hip resurfacing arthroplasties (Lembeck et al. 2005). With some further software programming, these two features, in addition to the 3D vector spreadsheet, can be incorporated into future program development. This will increase the user-friendliness of the software

by having angular measurement features running alongside the 3D model during on-screen hip RoM analysis.

5.4. Importing patient-specific CT scans

The results demonstrate that SolidWorks can successfully import additional pelvic STLs and superimpose them over the 3D model. This is significant, as it provides capability to be patient-specific, therefore vastly increasing the viability of its use in hip resurfacing. In order for new STLs to be incorporated into the program, the files require some initial pre-processing. This involves defining the anatomical reference planes before superimposing them over the 3D model. It is not possible at this stage to import the new STLs directly into the model, and users will still require the STL pre-processing work to be outsourced. This can be completed during the stage of 3D rendering of the CT scans to STL files, which falls outside the scope of this project. Studies conducted by Vendittoli et al. (2007) and Kluess et al. (2008) have successfully demonstrated the possibility of using 3D computer models, based on CT scans of the hip, to measure RoM angles associated with hip resurfacing using Catia v5 and Pro/ENGINEER software programs. This investigation was able to illustrate that SolidWorks has similar, if not better capability with regard to program development for pre-surgical planning as well as hip RoM analysis for resurfacing arthroplasties.

5.5. Hip RoM analysis

The results indicate that all physiological movements of the hip joint can be simulated within the combined assembly file. This feature is vital for component size selection as well as specifying the location and orientation of the prosthetic components.

The 3D model can successfully identify where impingement between the acetabular cup rim and the femoral neck is occurring. This type of impingement can lead to femoral neck notching and subsequent premature

failure of the prosthesis (Shimmin and Back 2005b; Beaule et al. 2007a; United Kingdom. The National Health Service, National Joint Registry for England and Wales. 2007 ; De Haan et al. 2008b; Williams et al. 2009; Grammatopoulos et al. 2010). This acetabular rim to femoral neck impingement is one of the main limiting factors to post-surgical hip RoM, and being able to identify it during pre-surgical RoM analysis may prove to be extremely valuable. With the aid of the 3D vector spreadsheet it is possible to demonstrate how the change in the inclination and anteversion angles of the acetabular cup affect hip RoM. Other studies have sought to specify and measure the attainable hip RoM angles after insertion of the hip resurfacing prosthesis (Vendittoli et al. 2007; Kluess et al. 2008), whereas this study aimed to investigate the potential use of a software program as an aid for pre-surgical planning to be used by the surgeon. Therefore, precise angular measurement during hip RoM analysis was not the major goal. Without having predefined movement arcs and set physiological limits, the manual movement function proved to be user-intensive and time consuming. Future development of the software would vastly improve this function.

This investigation demonstrated that it is possible to use a standard CAD design software package (SolidWorks) to design a program able to produce a 3D computer model of the pelvis and upper femur for pre-surgical planning and hip RoM analysis, specifically aimed at hip resurfacing arthroplasties.

5.6. Limitations

The initial set-up process and generation of the 3D computer model was both complex and time consuming. Due to this, it was decided to base the model on a healthy subject to use as a reference thus allowing the surgeon to use it to be patient-specific through superimposing new STLs over the 3D model. In this way, the need to create individual 3D models for each patient is eliminated. However, in some cases it may be problematic comparing certain pathological conditions to the healthy 3D hip model.

The use of 3D reconstructed surface models also has certain limitations, as it is based on subjective labelling prior to reconstruction. This process may also lead to the smoothing of the surfaces, which leads to displacement of edge nodes (Lubovsky et al. 2010). Kang et al. (2002) demonstrated that hip RoM based on 3D surface models are particularly sensitive to the specified location of the hip joint centre which is based on anatomical features of the acetabulum. This would be of particular concern if this product is used as a basis for the further development of a fully automated CAS system.

The use of an artificial femur to represent the patient's natural anatomy could be viewed as a limitation, however refinement through superimposing the STL over the artificial femur, as well as drawing on surgeon experience will limit the impact of this factor.

This study made use of a single healthy patient's STL file in order to test the capability of SolidWorks to import and superimpose patient-specific STLs into the model. This investigation was therefore limited and not able to test for gender-specific criteria or certain pathological conditions which can be present in the hip joint. However, there is no reason the principle employed during importing and superimposing the STL file cannot be applied to other femur and pelvic STL files.

As SolidWorks does not have the capability to fully measure or display the acetabular inclination and anteversion angles, it was necessary to develop a separate Excel spreadsheet. This set-up requires the surgeon to use two systems when conducting hip RoM analysis. Additionally, not having angular on-screen measurements available during manual movement of the artificial femur restricts the ability of the surgeon to investigate movement arcs within physiological limits. This study made use of the standard SolidWorks package, therefore modifying the program was outside the scope of work. Future development of the software would vastly improve this function.

The further development, implementation and commercialisation of the product fell outside the scope of work. This restriction was justified due to the

time constraints and resources available to the project. These details do not in any way undermine the relevance of the study, which has the potential to help many patients that require this complicated surgery.

University of Cape Town

6. Conclusions and recommendations

The main objective of this study was to investigate the use of an existing CAD software package (SolidWorks) to generate 3D computer models of the pelvis and upper femur, for use by a surgeon in pre-surgical planning. Further, this study had the purpose of providing groundwork for future development of a user-friendly software program for pre-surgical planning of hip resurfacing.

Hip resurfacing may be a viable alternative to THR for younger more active patients, however the associated risks and complications need to be evaluated on an individual basis. From the literature it is evident that the outcome of a hip resurfacing arthroplasty is largely based on the correct positioning of the components. Having a 3D view of the patient's anatomy and the ability to investigate different positioning scenarios for the prosthetic components may improve the pre-surgical planning process as well as reduce the risks and complications associated with this procedure.

6.1. Major conclusions drawn from this study

Engineering CAD software such as SolidWorks has the potential to be used in the field of orthopaedic surgery, specifically for hip replacement arthroplasties. This has both clinical and commercial implications.

- It is possible to import medical STL files, generated from CT scans, into SolidWorks and create solid 3D models based on the patient's anatomy.
- Subsequent to defining the anatomical reference planes, DriveWorks can be used to specify the location and orientation of both the acetabular and femoral prosthetic components in SolidWorks.
- With the aid of an Excel spreadsheet the surgeon can determine the acetabular inclination and anteversion angles before and after virtual

insertion of the prosthetic cup, in terms of either the anatomical, operative or radiographic spatial reference systems.

- Ultimately, the surgeon will be able to investigate the effect of component location and orientation, in terms of inclination and anteversion angles, on hip RoM.
- This software is not manufacturer or component-specific and has the ability to be adapted for use with other hip resurfacing products as well as THR systems.

6.2. Recommendations

Other aspects of future development, which lie outside the scope of this project may include:

- Further development of SolidWorks to incorporating the 3D vector spreadsheet, so that on-screen display of the inclination and anteversion angles is possible, to predefine hip movement arcs within physiological limits and provide on-screen angular display which may be beneficial.
- Incorporating other types of hip prostheses, such as THRs, and performance of hip RoM analysis accordingly.
- Follow-up study evaluating the outcomes of surgeries which use computer-assisted pre-surgical planning.
- Commercial development and implementation of the software in hospitals.
- It would also be possible to develop an alternative standalone CAD based software program specifically for use as a pre-surgical planning tool for hip resurfacing.

7. References

- Amini, B. (2011). *Femur Angles*. [Online]. Available from: http://wikidoc.org/index.php/Coxa_vara [Accessed on: 6 October 2011].
- Amstutz, H.C., Beaulé, P.E., Dorey, F.J., Le Duff, M.J., Campbell, P.A., Gruen, T.A. (2004). Metal-on-Metal Hybrid Surface Arthroplasty: Two to Six-Year Follow-up Study. *The Journal of Bone and Joint Surgery, American Volume*, 86(1), pp.28-39.
- Amstutz, H.C., Beaulé, P.E., Le Duff, M.J. (2001). Hybrid metal-on-metal surface arthroplasty of the hip. *Operative Techniques in Orthopaedics*, 11(4), pp.253-262.
- Barrett, A.R.W., Davies B.L., Gomes, M.P.S.F., Harris, S.J., Henckel, J., Jacopek, M., Kannan, V., Rodriguez y Baena, F.M., Cobb, J.P. (2007). Computer-assisted hip resurfacing surgery using the Acrobot® Navigation System. *Proceedings of the Institution of Mechanical Engineers, Part H: Journal of Engineering in Medicine*, 221(7), pp.773-785.
- Beaulé, P.E., Lee, J.L., Le Duff, M.J., Amstutz, H.C., Ebramzadeh, E. (2004a). Orientation of the femoral component in surface arthroplasty of the hip. A biomechanical and clinical analysis. *The Journal of Bone and Joint Surgery, American Volume*, 86(9), p.2015.
- Beaulé, P.E., Dorey, F.J., Le Duff, M.J., Gruen, T., Amstutz, H.C. (2004b). Risk factors affecting outcome of metal-on-metal surface arthroplasty of the hip. *Clinical Orthopaedics and Related Research*, (418), pp.87-93.
- Beaulé, P.E., Campbell, P., Shim, P. (2007a). Femoral head blood flow during hip resurfacing. *Clinical Orthopaedics and Related Research*, 456, pp.148-152.
- Beaulé, P.E., Harvey, N., Zaragoza, E., Le Duff, M.J., Dorey, F.J. (2007b). The femoral head/neck offset and hip resurfacing. *The Journal of Bone and Joint Surgery, British Volume*, 89(1), p.9.
- Bråten, M., Terjesen, T., Rossvoll, I. (2009). Femoral anteversion in normal adults. *Acta Orthopaedica, Scandinavica*, 1992; 63 (1): 29-32.
- Byrne, D.P. (2010). Anatomy & Biomechanics of the Hip. *The Open Sports Medicine Journal*, 4, p.51.
- Caillet, R. (2003). *The Illustrated Guide to Functional Anatomy of the Musculoskeletal System*. Chicago: American Medical Association.

- Campbell, P., Beaulé, P.E., Ebrahimpour, E., Le Duff, M.J., De Smet, K.A., Lu, Z., Amstutz, H.C. (2006). The John Charnley Award. *Clinical Orthopaedics and Related Research*, 453, pp.35-46.
- Daniel, J., Pynsent, P.B., McMinn, D.J. (2004). Metal-on-metal resurfacing of the hip in patients under the age of 55 years with osteoarthritis. *The Journal of Bone and Joint Surgery, British volume*, 86(2), p.177-184.
- Darling, D. (2011). *The Encyclopaedia of Science*. [Online]. Available from: www.daviddarling.info/encyclopedia. [Accessed on: 5 October 2011].
- De Haan, R., Pattyn, C., Gill, H.S., Murray, D.W., Campbell, P.A., De Smet, K.A. (2008a). Correlation between inclination of the acetabular component and metal ion levels in metal-on-metal hip resurfacing replacement. *The Journal of Bone and Joint Surgery, British volume*, 90(10), p.1291.
- De Haan, R., Campbell, P.A., Su, P.E., De Smet, K.A. (2008b). Revision of metal-on-metal resurfacing arthroplasty of the hip: the influence of malpositioning of the components. *The Journal of Bone and Joint Surgery, British volume*, 90(9), p.1158.
- Drake, R., Vogl, A.W., Mitchell, A.W.M (2009). *Gray's Anatomy for Students*. Second revised edition. Churchill Livingstone.
- Grammatopoulos, G., Pandit, H., Glyn-Jones, S., McLardy-Smith, P., Gundle, R., Whitwell, D., Gill, H.S., Murray, D.W. (2010). Optimal acetabular orientation for hip resurfacing. *The Journal of Bone and Joint Surgery, British Volume*, 92-B(8), pp.1072-1078.
- Hart, A.J., Sabah, S., Henckel, A., Lewis, J., Cobb, J., Sampson, B., Mitchell, A., Skinner, J.A. (2009). The painful metal-on-metal hip resurfacing. *The Journal of Bone and Joint Surgery, British volume*, 91-B(6), pp.738-744.
- Herrington, L. and Nester, C. (2004). Q-angle undervalued? The relationship between Q-angle and medio-lateral position of the patella. *Clinical Biomechanics*, 19(10), pp.1070-1073.
- Horton, M.G. and Hall, T.L. (1989). Quadriceps Femoris Muscle Angle: Normal Values and Relationships with Gender and Selected Skeletal Measures. *Physical Therapy*, 69(11), pp.897 -901.
- Johns Hopkins University School of Medicine , Department of Orthopaedic Surgery (2012) [Online]. Available from: <http://www.hopkinsortho.org> [Accessed on: January 15, 2012].
- Kang, M., Sadri, H., Mocozet, L., Magnenat-Thalmann, N., Hoffmeyer, P. (2002). Accurate Simulation of Hip Joint Range of Motion. *In Proceedings of Computer Animation*. Geneva, Switzerland 19 Jun 2002 - 21 Jun 2002. IEEE Computer Society, p. 215.

- Kluess, D., Zietz, C., Lindner, T., Mittelmeier, W., Schmitz, K.P. (2008). Limited range of motion of hip resurfacing arthroplasty due to unfavorable ratio of prosthetic head size and femoral neck diameter. *Acta Orthopaedica*, 79(6), pp.748-754.
- Kluge, W.H. (2009). Computer assisted hip resurfacing. *Orthopaedics and Trauma*, 23(3), pp.210-215.
- Köhnlein, W., Ganz, R., Impellizzeri, F.M., Leunig, M. (2009). Acetabular Morphology: Implications for Joint-preserving Surgery. *Clinical Orthopaedics and Related Research*, 467(3), pp.682-691.
- Krüger, S., Zambelli, P.Y., Leyvraz, P.F., Jolles, B.M. (2007). Computer-assisted placement technique in hip resurfacing arthroplasty: improvement in accuracy? *International Orthopaedics*, 33, pp.27-33.
- Langton, D.J., Jameson, S.S., Joyce, T.J., Webb, J., Nargol, A.V.F. (2008). The effect of component size and orientation on the concentrations of metal ions after resurfacing arthroplasty of the hip. *The Journal of Bone and Joint Surgery, British volume*, 90(9), p.1143.
- Lembeck, B., Mueller, O., Reize, P., Wuelker, N. (2005). Pelvic tilt makes acetabular cup navigation inaccurate. *Acta Orthopaedica*, 76(4), pp.517-523.
- Lewinnek, G.E., Lewis, J.L., Tarr, R., Compere, C.L., Zimmerman, J.R. (1978). Dislocations after total hip-replacement arthroplasties. *The Journal of Bone and Joint Surgery, American volume*, 60(2), p.217.
- Lubovsky, O., Peleg, E., Joskowicz, L., Liebergall, M., Khoury, A. (2010). Acetabular orientation variability and symmetry based on CT scans of adults. *International Journal of Computer Assisted Radiology and Surgery*, 5(5), pp.449-454.
- Malviya, A., Lingard, E.A., Malik, A., Bowman, R., Holland, J.P. (2010). Hip Flexion After Birmingham Hip Resurfacing: Role of Cup Anteversion, Anterior Femoral Head-Neck Offset, and Head-Neck Ratio. *The Journal of Arthroplasty*, 25(3), pp.387-391.
- Mardones, R.M., Gonzalez, C., Chen, Q., Zobitz, M., Kaufman, K.R., Trousdale, R.T. (2005). Surgical treatment of femoroacetabular impingement: evaluation of the effect of the size of the resection. *The Journal of Bone & Joint Surgery, American Volume*, 87(2), pp.273-279.
- Maruyama, M., Feinberg, J.R., Capello, W.N., D'Antonio, J.A. (2001). The Frank Stinchfield Award: Morphologic features of the acetabulum and femur: anteversion angle and implant positioning. *Clinical Orthopaedics and Related Research*, (393), pp.52-65.
- McGrory, B., Morrey, B.F., Cahalan, T.D., Cabanela, M.E. (1995). Effect of femoral offset on range of motion and abductor muscle strength after

- total hip arthroplasty. *The Journal of Bone and Joint Surgery, British volume*, 77-B(6), pp.865-869.
- McMinn, D., Treacy, R., Lin, K., Pynsent, P. (1996). Metal on metal surface replacement of the hip. Experience of the McMinn prosthesis. *Clinical Orthopaedics and Related Research*, (329 Supplement), pp.S89-98.
- Medical Arts Rehabilitation, (2011). *Determining the Q Angle*. [Online]. Available from: http://medicalartsrehab.com/images/q_angle.gif [Accessed on: 5 October 2011].
- Mizuno, Y., Kumagai, M., Mattessich, S.M., Elias, J.J., Ramrattan, N., Cosgarea, A.J., Chao, E.Y.S. (2001). Q-angle influences tibiofemoral and patellofemoral kinematics. *Journal of Orthopaedic Research*, 19(5), pp.834-840.
- Murphy, S.B., Simon, S.R., Kijewski, P.K., Wilkinson, R.H., Griscom, N.T. (1987). Femoral anteversion. *The Journal of Bone and Joint Surgery, American Volume*, 69(8), pp.1169-1176.
- Murray, D. (1993). The definition and measurement of acetabular orientation. *The Journal of Bone and Joint Surgery, British volume*, 75-B(2), pp.228-232.
- Murtha, P.E., Hafez, M.A., Jaramaz, B., DiGioia, A.M. (2008). Variations in acetabular anatomy with reference to total hip replacement. *The Journal of Bone and Joint Surgery, British volume*, 90-B(3), pp.308-313.
- Nagao, Y., Aoki, H., Ishii, S.J., Masuda, T., Beppu, M. (2008). Radiographic method to measure the inclination angle of the acetabulum. *Journal of orthopaedic science*, 13(1), p.62.
- Pandit, H., Glyn-Jones, S., McLardy-Smith, P., Gundle, R., Whitwell, D., Gibbons, C.L.M., Ostlere, S., Athanasou, N., Gill, H.S., Murray, D.W. (2008). Pseudotumours associated with metal-on-metal hip resurfacings. *The Journal of Bone and Joint Surgery, British volume*, 90-B(7), pp.847-851.
- Pauwels, F., (1980). *Biomechanics of the locomotor apparatus: contributions on the functional anatomy of the locomotor apparatus*, New York: Springer-Verlag.
- Perreira, A.C., Hunter, J.C., Laird, T., Jamali, A.A. (2010). Multilevel Measurement of Acetabular Version Using 3-D CT-generated Models: Implications for Hip Preservation Surgery. *Clinical Orthopaedics and Related Research*, 469(2), pp.552-561.
- Primal Pictures Ltd. (2011). *Anatomical Language*. [Online]. Available from: <http://www.anatomy.tv/StudyGuides/StudyGuide.aspx?guideid=9&NextID=0&customer=primal> [Accessed on: 25 October 2011].

- Romanowski, J.R. and Swank, M.L. (2008). Imageless Navigation in Hip Resurfacing: Avoiding Component Malposition During the Surgeon Learning Curve. *The Journal of Bone and Joint Surgery, American volume*, 90(Supplement_3), pp.65-70.
- Seyler, T.M., Lai, L.P., Sprinkle, D.I., Ward, W.G., Jinnah, R.H. (2008). Does Computer-Assisted Surgery Improve Accuracy and Decrease the Learning Curve in Hip Resurfacing? A Radiographic Analysis. *The Journal of Bone and Joint Surgery, American volume*, 90(Supplement_3), pp.71-80.
- Shimmin, A.J., Bare, J., Back, D.L. (2005a). Complications Associated with Hip Resurfacing Arthroplasty. *Orthopedic Clinics of North America*, 36(2), pp.187-193.
- Shimmin, A.J. and Back, D. (2005b). Femoral neck fractures following Birmingham hip resurfacing: a national review of 50 cases. *The Journal of Bone and Joint Surgery, British volume*, 87(4), pp.463-4.
- Smith & Nephew. (2007). *BHR FDA Surgical Technique* [Online]. Available from: http://global.smith-nephew.com/cps/rde/xbcr/smithnephew/BHR_FDA_Surgical_Technique_NEW_06-07.pdf [Accessed on: 10 October 2011].
- Su, E.P. (2011). *Hip Resurfacing Network*. [Online]. Available from: <http://www.hipresurfacingnewyork.com/hip-resurfacing.html> [Accessed on: 10 October 2011].
- United Kingdom. The National Health Service. (2007). *National Joint Registry for England and Wales, 4th Annual Report National Joint Registry*. The NJR Centre, Hemel Hempstead (ISSN 1753-9382).
- United Kingdom. The National Health Service. National Collaborating Centre for Chronic Conditions.(2008). *Osteoarthritis: national clinical guideline for care and management in adults.*, London: Royal College of Physicians.
- Vendittoli, P., Ganapathi, M., Nuno, N., Plamondon, D., Lavigne, M. (2007). Factors affecting hip range of motion in surface replacement arthroplasty. *Clinical Biomechanics*, 22(9), pp.1004-1012.
- Willert, H.G., Buchhorn, G.H., Fayyazi, A., Flury, R., Windler, M., Koster, G., Lohmann, C.H. (2005). Metal-on-Metal Bearings and Hypersensitivity in Patients with Artificial Hip Joints. A Clinical and Histomorphological Study. *The Journal of Bone and Joint Surgery, American volume*, 87(1), pp.28-36.
- Williams, D., Royle, M., Norton, M. (2009). Metal-on-Metal Hip Resurfacing: The Effect of Cup Position and Component Size on Range of Motion to Impingement. *The Journal of Arthroplasty*, 24(1), pp.144-151.

- Wheeless, C.R., (2011). Wheeless' Textbook of Orthopaedics [Online]. Available from: <http://www.wheelessonline.com/ortho/9738> [Accessed on: 6 October 2011].
- Wolf, A., DiGioia, A.M., Mor, A.B., Jaramaz, B. (2005). A kinematic model for calculating cup alignment error during total hip arthroplasty. *Journal of Biomechanics*, 38(11), pp.2257-2265.
- Yoon, Y.S., Hodgson, A.J., Tonetti, J., Masri, B.A., Duncan, C.P. (2008). Resolving inconsistencies in defining the target orientation for the acetabular cup angles in total hip arthroplasty. *Clinical Biomechanics*, 23(3), pp.253-259.
- Ziaee, H., Daniel, J., Datta, A.K., Blunt, S., McMinn, D.J.W. (2007). Transplacental transfer of cobalt and chromium in patients with metal-on-metal hip arthroplasty: a controlled study. *The Journal of Bone and Joint Surgery, British volume*, 89-B(3), pp.301-305.

University of Cape Town

8. Appendices

8.1. Appendix A

Equations used to convert inclination and anteversion angles.

- Anatomical angles to Operative angles:

$$\tan(OA) = \frac{\sin(AA) \sin(AI)}{\cos(AI)}$$

$$\tan(OI) = \tan(AI) \cos(AA) \cos(OA)$$

- Anatomical angles to Radiographic angles:

$$\tan(RI) = \tan(AI) \cos(AA)$$

$$\tan(RA) = \tan(AI) \sin(AA) \cos(RI)$$

- Operative angles to Radiographic angles:

$$\tan(RI) = \frac{\tan(OI)}{\cos(OA)}$$

$$\tan(RA) = \frac{\cos(OI) \sin(OA) \sin(RI)}{\sin(OI)}$$

- Operative angles to Anatomical angles:

$$\tan(AA) = \frac{\cos(OI) \sin(OA)}{\sin(OI)}$$

$$\tan(AI) = \frac{\tan(OI)}{\cos(AA) \cos(OA)}$$

- Radiographic angles to Operative angles:

$$\tan(OA) = \frac{\tan(RA)}{\cos(RI)}$$

$$\tan(OI) = \frac{\cos(RA) \sin(RI) \sin(OA)}{\sin(RA)}$$

- Radiographic angles to Anatomical angles:

$$\tan(AA) = \frac{\tan(RA)}{\sin(RI)}$$

$$\tan(AI) = \frac{\tan(RA)}{\sin(AA) \cos(RI)}$$

University of Cape Town

8.2. Appendix B

Radiographic anteversion (RA) and radiographic inclination (RI) in terms of the pelvic tilt angle (ϕ) according to Lembeck et al.(2005).

$$RA_{\phi} = \arcsin[(-\cos(RA_0) \cdot \cos(RI_0) \cdot \sin(\phi)) + (\sin(RA_0) \cdot \cos(\phi))]$$

$$RI_{\phi} = \operatorname{arccot} \left[(\cot(RI_0) \cdot \cos(\phi)) + \left(\frac{\tan RA_0}{\sin RI_0} \cdot \sin(\phi) \right) \right]$$

With: RA_0 = radiographic anteversion and RI_0 = radiographic inclination

University of Cape Town

8.3. Appendix C

Showing various input forms created in DriveWorks to generate the artificial femur and specify the location and orientation of the prosthetic acetabular cup.

Parameter	Value
Patient Name	Default
Femoral Length	80
Femoral Diameter	35
CCD angle	135
Q angle	12
Femoral neck to femoral head centre	60
Femoral neck diameter	35
Femoral head diameter	50
Resection level	0.0001
CCD to tip of greater trochanter	30
Femoral head offset angle	0
Femoral head offset distance	0.0001
Inclination Angle	45
Anteversion Angle	0

Figure C.1 – Illustrating the default input form used in DriveWorks to design the artificial femur, listing all the input fields.

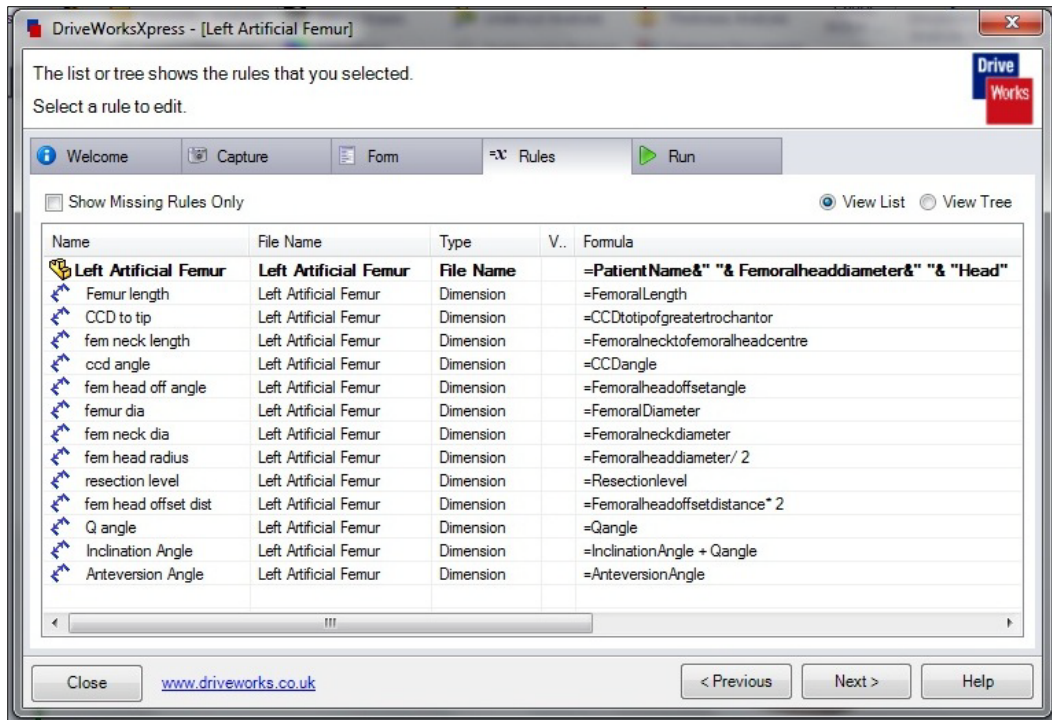


Figure C.2 – Showing how the the rules were created in DriveWorks for the left artificial femur. Rules included: File name, Femoral head diameter, Femoral head offset distance and Inclination angle.

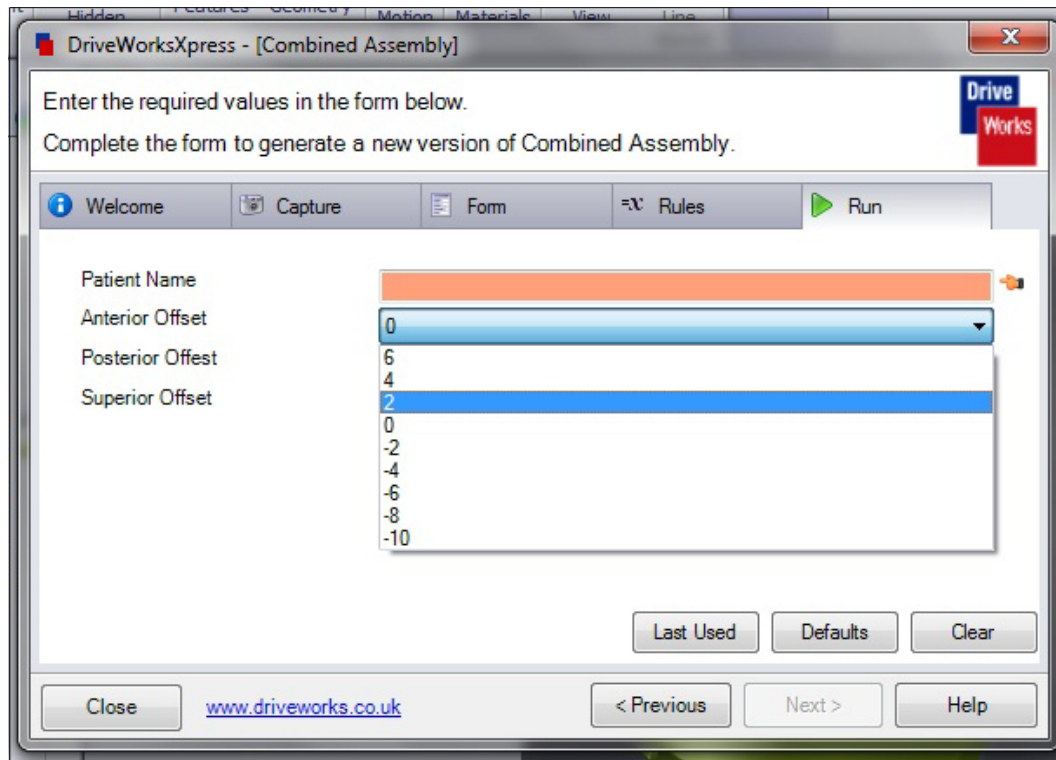


Figure C.3 – Showing the input form designed in DriveWorks to specify the location and orientation of the acetabular cup according to the offsets at each vertex point. Vertex 1 being the anterior offset, Vertex 2 being the posterior offset and Vertex 3 being the superior offset.